CLAASSEN, JOHANN OCKERT

PRODUCT QUALITY PARAMETERS IN THE REACTION CRYSTALLIZATION OF METASTABLE IRON PHASES FROM ZINC-RICH SOLUTIONS

Ph.D. (Metallurgical Engineering) **UP** **2005**

Product quality parameters in the reaction crystallization of metastable iron phases from zinc-rich solutions

by

Johann Ockert Claassen

Submitted in partial fulfillment of the requirements of the degree

Philosophiae Doctor in Metallurgical Engineering

in the
Department of Materials Science and Metallurgical Engineering,
University of Pretoria,
Pretoria, South Africa

November 2005

Product quality parameters in the reaction crystallization of metastable iron phases from zinc-rich solutions

by

Johann Ockert Claassen

Supervisor:
Prof. RF Sandenbergh
Faculty of Engineering, Built Environment and Information Technology, University of Pretoria, Pretoria

ACKNOWLEDGEMENTS

I would like to extend my gratitude to Kumba Base Metals Ltd. and Zincor Ltd. for the financial support received as well as the permission granted to publish the results of this study. I'm specifically indebted to our GM, Dr Willem van Niekerk, Zincor's Operations Manager, Oubaas Oosthuizen and my colleagues in the Zinc Plant who encouraged me along the way. I'm also grateful to Willem van der Merwe and his personnel at Kumba Research and Development who opened their doors for me to use their facilities.

With this work I want to acknowledge the role that Professor Roelf Sandenbergh has played in my academic and personal development since 1994. Prof., thank you for your kindness, the willingness to share your knowledge and experience and above all for helping me grow.

This study would not have materialized if it weren't for Ewald Meyer's insight in zinc processing, vision and encouragement. I salute you Ewald.

My dearest wife, Rika and loving boys Daniël, Pierre and Juan, thank you so much for your encouragement and unconditional love.

ABSTRACT

Iron is often present in leach liquors produced in chemical and hydrometallurgical processes. It is known that voluminous iron precipitates with high impurity values are formed if the conditions during its formation are not controlled well. These products are also often difficult to treat in downstream processes. This study therefore focused on the determination of product quality parameters for the production of good quality iron precipitates from zinc-rich solutions. Special attention was given to the quality of metastable phases such as ferrihydrite and schwertmannite formed at elevated temperatures and in the pH range 1.5 to 3.5 in a continuous crystallizer. These phases are produced over a range of supersaturation levels with the best quality products formed at lower supersaturation. It was shown that most industrial processes are operated well above the metastability limit at relatively high supersaturation. However, stagewise precipitation of iron, even above the metastability limit, yielded better quality products.

It was also shown that localized supersaturation levels could be controlled through changes in the micro and macromixing environments. The three-zone model approach was used to improve the quality of ferrihydrite and schwertmannite precipitates. Changes in the reactor design and the position of reagent feed points also impacted on the quality of the precipitates. Control over the localized supersaturation not only ensures the production of good quality nuclei, but also impacts on particle growth, which is required to make downstream processing of precipitates possible.

In precipitation processes, growth mainly takes place through agglomeration as the rate of molecular growth is generally low. The final quality of iron precipitates is greatly influenced by the quality of the agglomerates formed during iron precipitation. A Hadamard matrix was used to indicate the relative importance of the most relevant operating parameters for the formation of good quality iron precipitates.

Keywords iron, precipitation, reaction crystallization, product quality, metastability, supersaturation, ferrihydrite, schwertmannite, mixing, agglomeration

EXECUTIVE SUMMARY

Crystalline products are generally produced according to specifications that meet market requirements. The factors that influence the quality of these products have been studied extensively to allow industry to adhere to product specifications. However, the same cannot be said for precipitation systems. The lack of knowledge in this area probably stems from the fact that precipitation processes often produce low value products, are generally more complex and are difficult to control if compared with crystallization systems. This is specifically the case when a poorly crystalline phase, such as an iron hydroxide, is produced from ferric ion solution as big changes in supersaturation often occur. These changes in supersaturation typically result in the formation of a voluminous product with a high relative surface area that is difficult to treat in solid-liquid separation and storage steps. In zinc-rich solutions, a poor quality iron precipitate could result in high zinc losses, which include water soluble zinc that is difficult to remove through washing of the precipitate, adsorbed zinc, unleached ZnO and entrained $ZnSO_4$ solution. The production of a poor quality precipitate also very often increases the cost of the operation, i.e. more thickening, filtration and product drying or storage capacity are required.

In order to address the relatively high zinc losses associated with iron precipitates formed through the hydrolysis of ferric ions in zinc-rich solutions as well as the costs associated with the iron removal operation, the following steps were followed to improve iron precipitate quality:

- Identification of the iron phases present in a sulphate medium in the pH range 1.5 to 3.5 and the mechanisms involved in its formation. Initial work started in 2000 with the study of the Zincor iron removal process and its residues whereas this follow-up study mainly focused on the relative stability of the phases present.
- Determination of the influence of operating variables on the quality of these phases through its influence on supersaturation, which in turn affects the rate of the primary precipitation processes (nucleation and growth).
- Determination of the rate-limiting step and the factors that influence this step.

- Determination of the parameters that influence agglomeration of primary iron precipitates.

These steps covered the chemical, i.e. the specific phases formed and mechanisms involved, as well as the physical, i.e. the formation and growth of the solid phase, aspects of the precipitation of iron from ferric sulphate solution.

This approach was applied in a study of metastable iron phases, which include ferrihydrite and schwertmannite. Specific attention was given to the influence of operating parameters such as pH, temperature, seed addition and the mixing environment through its influence on supersaturation, on product quality parameters, which include the filterability of the precipitate, purity, particle size and density. The relative importance of the above-mentioned operating parameters in the agglomeration process was also addressed.

The hydrolysis of ferric iron, at temperatures ranging from 50 to 90°C, and pH values between 1.5 and 3.5, resulted in the formation of metastable iron phases with different morphologies and qualities. The changes in the morphology and product quality of ferrihydrite and schwertmannite were linked to changes in the relative supersaturation. These phases were precipitated over relative supersaturation levels ranging from about 1000 to 30,000. Ferrihydrite and schwertmannite precipitates formed at relative supersaturation levels below approximately 5000, contained lower impurity levels and were easier to filter.

The (meta)stability regions of these phases were also determined as a function of temperature and pH. A clear transition line between the stability regions of ferrihydrite and schwertmannite was determined following the change in their sulphate contents with a change in pH. This finding dispels the notion that schwertmannite is nothing else but ferrihydrite with high sulphate values. The solubility curve, on the other hand, was determined using a technique where the pH was cycled between predetermined values at different temperatures, noting the points where a sudden increase and decrease in the ferric iron concentration occurred. The solubility curve occurred at much higher pH values than the equilibrium solubility line, giving rise to a much narrower metastable zone of 0.2 to 0.3 pH units. Operating

within the metastable zone is therefore expected to be a difficult task. Nevertheless, it was shown that stagewise precipitation of iron, with controlled supersaturation above the metastable zone, increased the precipitate quality as defined by its purity.

Furthermore, since the nature of the iron precipitate formed is dependent on the degree of supersaturation, and as mixing may determine local supersaturation levels, the influence of the mixing environment on the quality of iron precipitates was investigated. In such processes the mixing rate is generally a few orders of magnitude slower than the rates of the chemical reaction and nucleation. Any change in the rate-limiting step is therefore expected to influence supersaturation, which in turn impacts on the nucleation and growth rates, which affect the final product quality. An effort should therefore be made to reduce supersaturation. In this study iron precipitate quality was improved by improving the mixing environment.

It is shown that the final product quality of iron precipitates formed through ferric iron hydrolysis is significantly improved by changes in the micro and macromixing environments. Results indicated that the specific filter resistance of the solids was improved by about 50% and the zinc content of the iron precipitates was reduced by about 75% and 14% for acid- and water soluble zinc, respectively using the three-zone model approach. The study also showed that product quality is more sensitive to cation (iron in solution) mass transfer than the mass transfer of the neutralizing agent in the region of the inlet points. As far as the influence of mixing time was concerned, it appears as though mixing times smaller than about 5 minutes should be avoided as it induced high supersaturation levels and fast nucleation rates.

Since product quality is more sensitive to changes in the macro- than the micromixing environment, the influence of reactor type and feed point position on product quality was also studied. The best results were achieved using a CSTR. The draft-tube-baffled (DTB) reactor, however, is expected to produce precipitates with superior quality when optimized. The study also indicated that feed points should be placed as far as possible from each other and in a position that gives adequate micro- and macro mixed fluids. The controlling mixing environment (micro or macromixing controlled) generally indicates where feed points should be located. In a well-mixed macrofluid, as found in a DTB reactor, feed points could be placed far away from the impeller.

When the macromixing environment is however less homogeneous such as in a CSTR, better results were obtained with the feed points placed closer to the impeller.

Lowering the supersaturation, through changes in the operating parameters and mixing environment, effectively reduce the nucleation rate to give more dense precipitates. However, even good quality nuclei formed in a well-controlled mixing environment are usually less than one micron in diameter. Unless these nuclei are allowed to grow, downstream processing of precipitates, such as liquid-solid separation and storage, could be difficult and costly. Low solute concentrations typically encountered in the formation of relatively insoluble phases during precipitation processes, however, do not support the desired molecular growth rates required to make these processes viable. Particle growth in precipitation systems rather takes place through agglomeration and was therefore studied in detail. The relative importance of some operating parameters was expressed in terms of the filterability of the solids formed, the change in the particle population density and iron removal efficiency, using the so-called Hadamard matrix. The effect of seed addition on the purity of agglomerates was also evaluated. It was found that specific attention should be given to pH control, seed addition, iron solution iron concentration and temperature control. Optimum agglomeration was found to occur at a pH of 3.0, 60°C, 15 to 35 g/L initial seed concentrations and initial seed sizes between 5 and 6μm. An initial seed concentration of 50g/L improved the filterability of the iron precipitate by about 80%.

LIST OF CONTENTS **PAGE**

1 BACKGROUND

1.1 Study of the Zincor iron removal process

Zincor Ltd. uses an integrated roast-leach-electrowinning circuit to produce high-grade zinc products as well as zinc-aluminium alloys from zinc sulphide concentrates [Meyer *et al.*, 1996]. Solution purification, specifically iron removal, forms an integral part of zinc refining circuits. Several processes, which include the hematite, jarosite, goethite and so-called para-goethite processes (ferrihydrite precipitation), have been developed to deal with iron in zinc-rich solutions, as discussed later.

At Zincor, iron is removed by means of the so-called Zincor Process, a process developed by Zincor over a period of nearly three decades. Most of the development work was done on a trial and error basis resulting in increased zinc losses, process disruptions and slow progress. However, early in 2000 a study of the Zincor process was initiated in order to speed up development work and minimise the impact of process changes on the circuit. This study by the authors aimed to characterise the Zincor Process and its residues and address soluble and insoluble zinc losses, which mainly result from the use of zinc calcine as a neutralising agent. In summary, it was found that [Claassen *et al.*, 2002; Claassen *et al.*, 2003(a)] the Zincor Process has a unique character and could be viewed as a process in its own right. This finding was based on the specific operating conditions employed in the process and the mineralogical composition of the residue produced (refer to section 1.2). Furthermore, soluble zinc losses could be reduced through improved pH and temperature control. The pH of the acid wash stage utilised in the process should be controlled at values between 2.7 and 2.9 due to silica gel formation at a pH below approximately 2.5 and to optimise particle growth. The study also indicated that the final pH of the iron removal step should be around 3.0.

It was also shown that insoluble zinc losses could be significantly reduced if a more reactive neutralising agent is used and/or a neutralising agent that contains no or little zinc. Finally, some basic work on the utilisation of seed material to improve the quality of the precipitated product also showed potential to reduce both soluble and insoluble zinc losses.

After completion of the study, several changes were made to the Zincor iron removal stage, such as changes to the operating set points, process controls and equipment. These changes assisted in stabilizing the process and reduced zinc losses associated with the iron residue. However, the inherent weakness of the Zincor Process, namely, the relatively high insoluble zinc loss associated with the final residue, was not adequately addressed. In order to reduce these losses, it was realized during the latter part of the study that more attention should be given to the factors that influence the two primary precipitation processes, nucleation and growth, i.e. a physical-chemical approach should be followed. It was proposed that the following important aspects should also be considered to improve the quality of iron precipitates:

- The rate-limiting step in the precipitation process.
- The influence of changes in the rate-limiting step on the quality of the precipitate.
- The impact of changes in the supersaturation level, which is the driving force for precipitation, on the quality of the precipitate.
- The influence and relative importance of operating parameters on the primary precipitation processes.
- Effective utilization of seed material to improve process stability and reduce zinc losses.
- The (meta)stability regions of the poorly crystalline phases present in the Zincor iron residue.

In an effort to address these aspects, a follow-up study, of which the detail is discussed in this document, was initiated early in 2003. The basis of this new study was the earlier work performed on the Zincor process since 2000. The determination of the mechanisms and phases formed during iron precipitation under the conditions specified by Claassen *et al.* [2002] is relevant to this follow-up study.

Since the speciation of phases involved in precipitation or crystallization processes could be seen as the first step to improve precipitate product quality, the process followed and findings of the earlier study on the characterization of the Zincor Process and its residues are discussed in more detail in section 1.2.

1.2 Speciation of iron phases

In precipitation systems, speciation of the phases present is done to determine the reaction mechanisms involved in the process, the relative stability of the phases present in the final product and the morphology of these phases.

Various analytical techniques were used to determine which phases are present in Zincor's iron residue. Firstly, results obtained from chemical and XRD analyses indicated that about 50% of the iron present in the residue could be associated with poorly crystalline phases. This was established by performing an elemental balance using the data obtained from these two techniques. The XRD study indicated the presence of crystalline iron-bearing phases, of which the most abundant were franklinite ($ZnO.Fe_2O_3$), plumbo jarosite ($Pb_{0.5}Fe_3(SO_4)_2(OH)_6$) and argento jarosite ($AgFe_3(SO_4)_2(OH)_6$).

A SEM-EDX study of the residue confirmed the presence of one or more poorly crystalline phase in the form of oxy-hydroxides and oxy-hydroxy sulphates. The difference in the morphology of the phases present was also indicated by the SEM backscattered images, i.e. dense crystalline particles and smaller poorly crystalline particles with relatively large surface areas. The images also clearly indicated that the poorly crystalline oxy hydroxide phase(s) contained significantly more zinc than the hydroxy salts, which include basic iron sulphates and jarosites.

To identify the poorly crystalline phases present was more difficult. Several techniques including FT-IR spectroscopy, Raman spectroscopy, X-ray Photoelectron spectroscopy (XPS) and Mössbauer effect spectroscopy (MES) were used. Of these techniques, MES gave the best results. Samples were analyzed at room (≈ 300 K), liquid nitrogen (≈ 77 K) and liquid helium temperature (≈ 5 K) as the different iron

phases expected to be present are magnetically ordered at different temperatures, giving the opportunity to identify phases through a process of elimination. The data obtained fitted the spectra of franklinite, jarosite, schwertmannite, a poorly crystalline oxy-hydroxy sulphate, and ferrihydrite, reasonably well.

Furthermore, MES indicated that neither goethite nor any of its polymorphs were present in the residue samples and it was therefore proposed that the oxy-hydroxide phase found during the SEM-EDX study, could be ferrihydrite. To confirm this, a number of synthetic samples were produced using the same conditions employed in Zincor's iron removal process. The simulation focused on the hydrolysis of ferric iron in the absence of alkali elements, i.e. no franklinite was present and no additional chemicals were added to simulate jarosite precipitation. MES, XRD and wet chemical analyses were again utilized to analyze the precipitates produced. The results obtained using these techniques all confirmed that schwertmannite and ferrihydrite should be present in the iron residue. The iron phases therefore proposed to be present in the Zincor iron residue and their abundances are shown in Table 1.

Table 1. Iron phases expected to be present in Zincor's iron residue [Claassen *et al.*, 2002].

Phase	Formula	Abundance (%)
Schwertmannite	$Fe_8O_8SO_4(OH)_6$	50
Ferrihydrite	$Fe_5O_7(OH).4H_2O$	
Jarosite(s)	$Pb[Fe_3(SO_4)_2(OH)_6]_2$, Plumbo jarosite and solid solution phases	20
Franklinite	$ZnO.Fe_2O_3$	25
Unknown	--	5

The reactions involved in the formation of these phases, were proposed to be:

$$4Fe_2(SO_4)_3 + ZnO(s) + 13H_2O = Fe_8O_8(OH)_6SO_4(s) + ZnSO_4 + 10H_2SO_4 \quad \ldots 1$$

$$3Fe_2(SO_4)_3 + PbSO_4(s) + ZnO(s) + 11H_2O = 2Pb_{0.5}Fe_3(SO_4)_2(OH)_6(s) + ZnSO_4 + 5H_2SO_4 \quad \ldots 2$$

$$5Fe_2(SO_4)_3 + ZnO(s) + 23H_2O = 2[Fe_5O_7(OH).\ 4H_2O](s) + ZnSO_4 + 14H_2SO_4 \quad \ldots 3$$

From this investigation, it should be highlighted that :

- 50% of the iron present in Zincor's iron residue is in the form of poorly crystalline ferrihydrite and schwertmannite, which are metastable towards goethite.
- Approximately 70% of the iron removed from the hot iron solution is in the form of these two phases. Any further study into the factors that influence the quality of iron precipitates should therefore focus on these phases.
- Ferrihydrite and schwertmannite form through a hydrolysis process in the absence of alkali and other elements. The iron and hydroxide concentrations are expected to play an important role in their formation as indicated in equations 1 and 3.
- Ferrihydrite and schwertmannite were found to have different morphologies and impurity levels. The relative stability and the factors that influence the stability and morphology of these phases should therefore be investigated.
- Due to their poor crystalline nature, these two phases contain high impurity levels as shown in the SEM-EDX study.
- Industrial processes where iron is removed at elevated temperatures, a pH range between about 2.5 and 3.5, and without significant amounts of alkali elements such as Na and K, probably all produce ferrihydrite and schwertmannite.

In previous paragraphs the need to determine the factors that influence the quality of poorly crystalline iron precipitates, such as ferrihydrite and schwertmannite, produced in the Zincor and probably other industrial processes where a sulphate leach medium is used under similar conditions, were indicated. In the present work the factors that

influence the quality of these poorly crystalline iron phases were studied. The steps used in this investigation could be summarized as follows:

- Speciation of the iron phases and the determination of the reaction mechanisms responsible for their formation. The initial work done on the Zincor iron removal process and its residues were used as basis, as summarized in sections 1.1 and 1.2.
- Study the differences in the morphology of the phases present.
- Determine the relative stability of ferrihydrite and schwertmannite.
- Study the role of supersaturation in the precipitation of ferrihydrite and schwertmannite.
- Determine the influence of typical operating conditions on the quality of ferrihydrite and schwertmannite precipitates.
- Determine the rate-limiting step in iron precipitation processes.
- Study the influence of changes in the mixing environment on precipitate quality.
- Study particle growth and specifically the factors that influence the agglomeration of iron precipitates.

2 INTRODUCTION

2.1 Precipitation in hydrometallurgy

Crystallization and precipitation are widely used industrial processes in the chemical and hydrometallurgical industries. Vast quantities of crystalline and poorly crystalline materials are manufactured commercially. These include the production of products such as pigments, dyestuffs, pharmaceuticals, fertilizers, plant protection agents and metallic products with varying metal contents and purities. All of these products are produced in one or more steps that include separation, purification, concentration and crystallization. The type of crystallization referred to here is generally known as "mass" or "bulk" crystallization where large numbers of particles are formed and grown at the same time in large industrial reactors. The specific method of crystallization employed to bring about the bulk removal of crystallites or precipitates from a solution or melt is a function of the properties of the solute. These include the sensitivity to thermal changes and the solubility of the crystallized product. Figure 1 indicates some criteria that could be used to choose the method of crystallization suitable for a specific application.

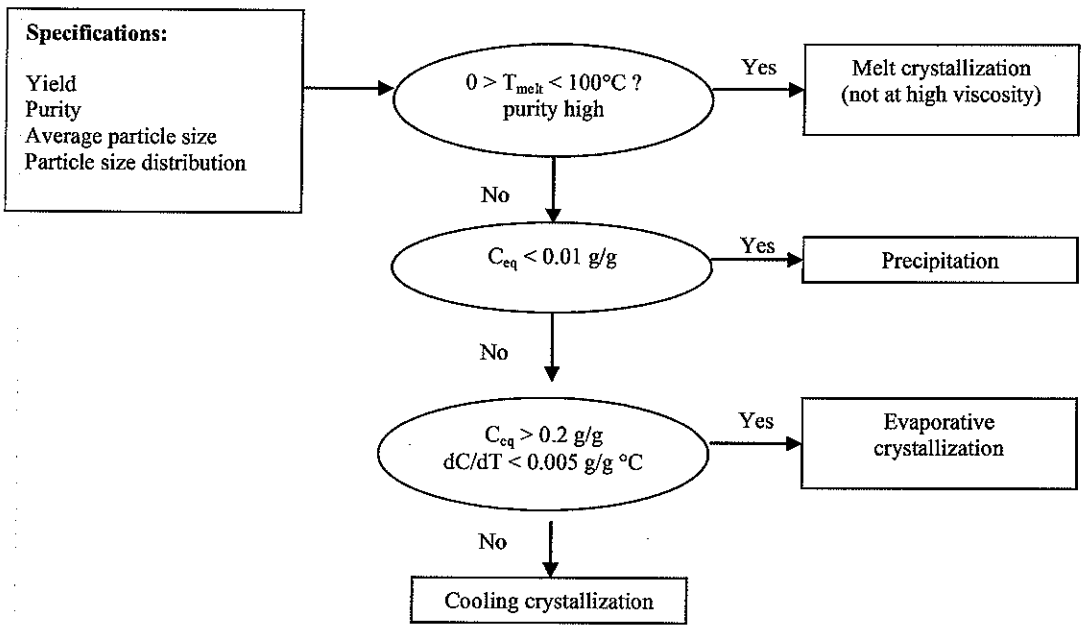

Figure 1: Decision diagram to choose the method of crystallization [After Rosmalen Van and Kramer, 1998]. C_{eq} = equilibrium solution concentration of element being removed.

In precipitation processes, the driving force, i.e. the change in the supersaturation level, for the phase change is provided by a chemical reaction. Under these conditions a solid with a relatively low solubility of ca. 1% is formed compared to ca. 20% for solids formed in crystallization processes, i.e. the equilibrium concentration in solution of the element being precipitated is low (Refer to Figure 1). This indicates that a relatively high supersaturation is present during precipitation processes. Despite this fact and the impact the high driving force has on product quality, precipitation, or reactive crystallization is widely used in the minerals and metals industry. Reactive crystallization is used to produce metal sulphides, phosphates, hydroxides and carbonates, to name a few. Table 2 gives a summary of some compounds produced from precipitation processes.

Table 2. Summary of ionic and hydrolytic precipitation methods [Habashi, 1999].

Precipitate	Precipitating agent	Example
Oxides, hydrated oxides and hydroxides	H_2O OH^-	TiO_2, $Al(OH)_3$, $Be(OH)_2$ Cu_2O, $Mg(OH)_2$, $Co(OH)_2$
Hydroxy salts	OH^- + Anion	$Cu(OH)_2.CuCO_3$, Jarosites, Iron hydroxy sulphates
Polyacids and their salts:		
Vanadates	H^+	$Na_4V_6O_{17}$, $(NH_4)_4[V_4O_{12}]$
Molybdates	H^+	$(NH_4)_4[H_2MO_6O_{21}].3H_2O$
Tungstates	H^+	$Na_2W_{12}O_{41}.28H_2O$
Uranates	OH^-, MgO	$(NH_4)_2U_2O_7$, $Na_2U_2O_7$, MgU_2O_7
Dialuminates	OH^- + Cation	$LiAl_2(OH)_7.2H_2O$
Sulfides	S^{2-}	CuS, NiS, CoS, ZnS
Carbonates	CO_3^{2-}	Li_2CO_3
Chlorides	Cl^-	CuCl, $(NH_4)_2PtCl_6$, K_2TiCl_6
Cyanides	CN^-	CuCN
Fluorides	F^-	PuF_3, $UF_4.nH_2O$
Oxalates	$(C_2O_4)^{2-}$	$Th(C_2O_4)_2$, $Li_2(C_2O_4)_3$
Peroxides	O_2^{2-}	$UO_4.2H_2O$, PuO_4
Sulfites	$(NH_4)_2SO_3$	Copper ammonium sulfites
Metalloids	H^+	Se from selenosulfate solution

Most of the compounds listed in Table 2 contains the sought after element whereas an element such as iron is in most cases precipitated as part of a purification step, i.e. it is treated as an impurity. Iron, one of the most abundant elements on earth, mostly ends up in leach solutions and typically needs to be eliminated prior to the final product removal step.

This is also true for the hydrometallurgical processing of zinc concentrates. These concentrates generally contain between 1% and 10% iron with some concentrates that can contain up to 18% [Chen and Cabri, 1986]. Initial attempts to remove iron from leach solutions as a hydroxide resulted in poorly filterable, voluminous and gelatinous precipitates [Tainton and Leyson, 1924]. This was a direct result of the high supersaturation levels present during the precipitation of iron from ferric ion solutions. Later attempts focused on the establishment of processes where precipitates can be formed using more dilute solutions, i.e. the level of supersaturation is kept low to improve the quality of nucleates and promote particle growth rather than nucleation.

This principle is used in two of the precipitation processes developed to control and remove iron from zinc-rich process solutions, *i.e.* the goethite (FeOOH) and the so-called para-goethite processes [Gordon and Pickering, 1975]. During more or less the same period, the hematite (Fe_2O_3) process [Tsunoda *et al.*, 1973; Onozaki et al., 1986] was developed and implemented at the Iijima Zinc Refinery in Akita, Japan. It was also recently shown [Claassen *et al.*, 2002] that the Zincor Process discussed earlier, which is similar to the para-goethite process [Patrizi *et al.*, 1985; Cubeddu *et al.*, 1996; McCristal and Manning, 1998], produces mainly iron hydroxy sulphates in the form of schwertmannite ($Fe_8O_8SO_4(OH)_6$) and plumbo-jarosite ($Pb_{0.5}Fe_3(SO_4)_2(OH)_6$). The establishment of these processes in the zinc industry was preceded by the development of the jarosite process ($AFe_3(SO_4)_2(OH)_6$) where A is typically Na^+, K^+ or NH^+. These processes, excluding the Zincor Process, are shown in Figure 2.

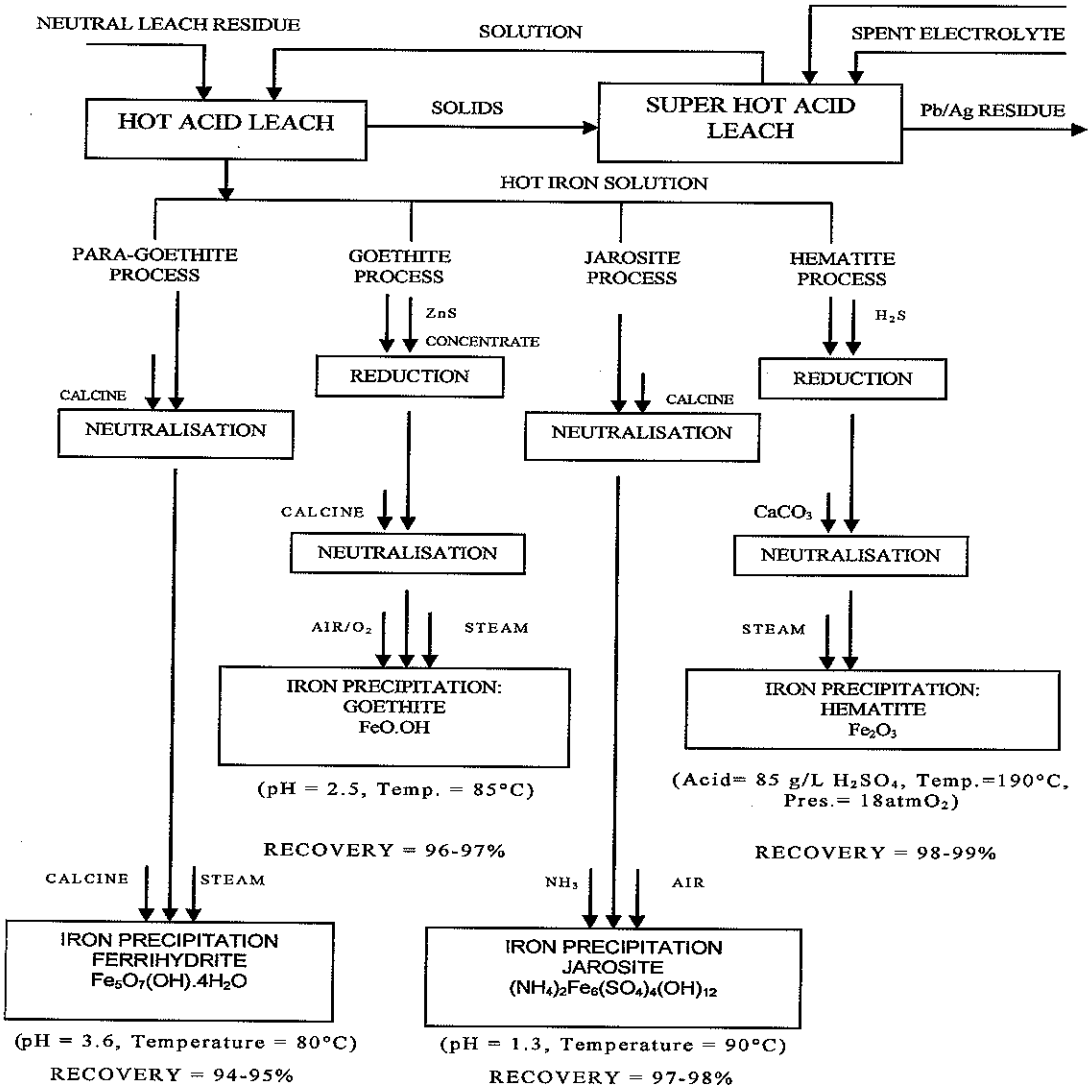

Figure 2. Iron removal processes used in the zinc industry to purify zinc-rich process solutions [After Claassen *et al.*, 2003(b)].

The advent of the jarosite process reduced the complexity of the early treatment of the zinc containing neutral leach residues dramatically. It was the first iron removal process that allowed the production of a filterable residue on a commercial scale and is still the most widely used iron precipitation process used in the zinc industry today [Pammenter *et al.*, 1986; Uusipaavalniemi and Karlman, 1996]. A simplified flowsheet of the jarosite process is shown in Figure 3.

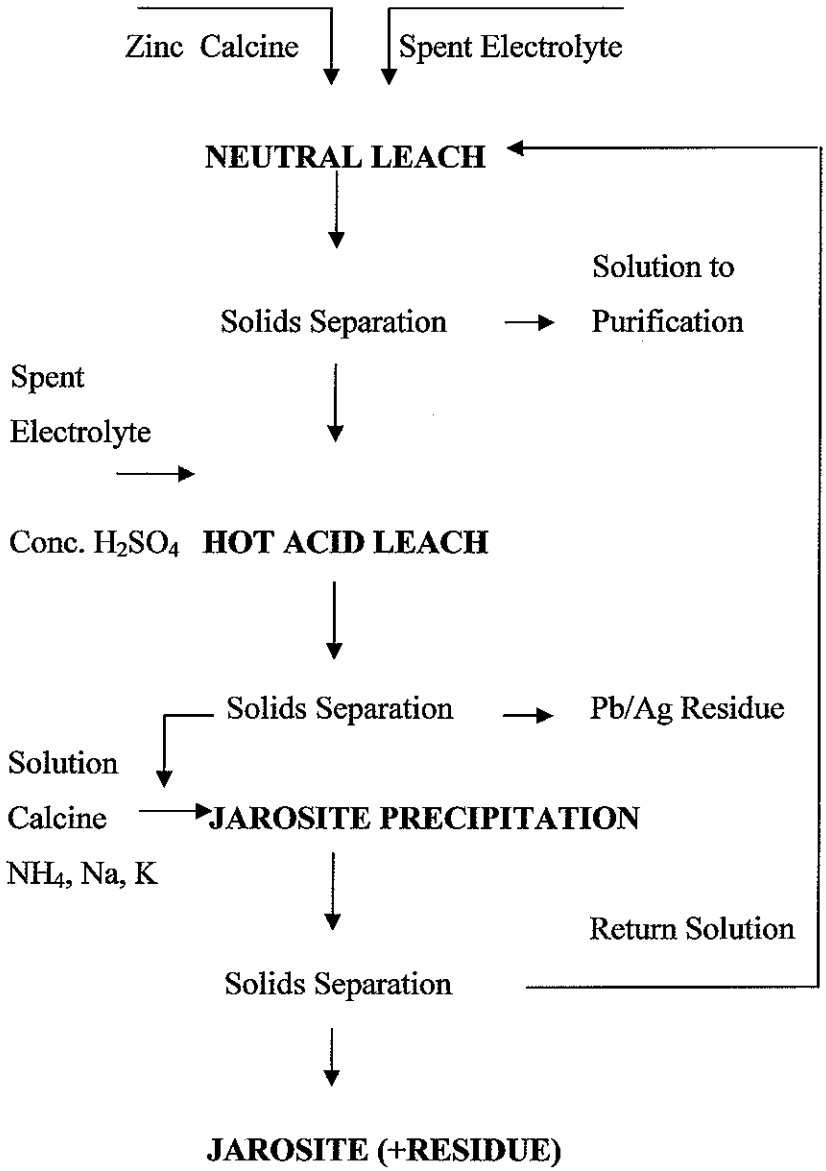

Figure 3: Simplified jarosite precipitation flowsheet [Arregui *et al.*, 1980].

Whereas volumes have been published on the jarosite and goethite processes, little is known about the para-goethite and Zincor processes, that mainly produce ferrihydrite [Loan *et al.*, 2001] and schwertmannite [Claassen *et al.*, 2002] respectively. These phases were reported to be poorly crystalline with high surface areas and are metastable towards goethite [Bigham *et al.*, 1990, 1994, 1996; Cornell and Schwertmann, 1996; Jambor and Dutrizac, 1998; Dutrizac, 1999]. As such, the iron-bearing residues produced in the para-goethite and Zincor Processes is less filterable, more voluminous and contains more zinc than goethite, jarosite and hematite residues

[Dutrizac, 1985]. Even though the para-goethite and Zincor Processes are relatively simple and easy to operate, higher zinc recoveries than what these processes can achieve are required in an extremely competitive industry.

However, precipitation of sparingly soluble substances from solution, such as iron, has not been studied to the same extent as most crystallization processes. This probably indicates that these processes are difficult to study as reaction crystallization (precipitation) generally involves the simultaneous and rapid occurrence of primary processes in the presence of secondary processes [Söhnel and Garside, 1992]. The primary processes involve mixing on macro, micro and molecular scale, the chemical reaction (sometimes with a complex mechanism), nucleation and growth of the particles. Secondary processes playing a role during reactive crystallization include agglomeration, ageing and ripening of the precipitates. As a result very little information is available in the literature on reaction crystallization. The general approach in studying these systems is therefore to apply classical crystallization theory to a specific system and make adjustments where necessary through empirical observations.

The main drive for studying crystallization and precipitation processes is to enable the engineer to design and control these processes with the emphasis on the production of a suitable quality product, i.e. optimum recovery and materials handling properties, at the required rates and as economical as possible. However, if precipitation processes are not well understood and controlled, gelatinous phases could form which would severely hamper downstream processes such as liquid-solid separation, which include filtration, thickening and bulk storage.

2.2 Precipitate product quality

In general the type of precipitate, the purity of the precipitate, density of the particles, particle size and size distribution influence the economics of a precipitation process. These factors are all strongly influenced by the primary and secondary precipitation processes mentioned earlier. This is discussed in detail for crystallization systems by Nielsen [1964, 1967], Walton [1967, 1969], Nyvlt [1971, 1982], Nyvlt *et al.* [1985], Mullin [1972, 1976], Pamplin [1975], Garside [1977], Söhnel and Garside [1992], Mersmann [2001] and David and Klein [2001].

However, as far as product quality of iron precipitates is concerned, very little information is available. Reference is made in the literature to iron precipitate product quality parameters, such as particle size, size distribution and porosity [Cornell and Schwertmann, 1996], but little attention is paid to the factors that influence product quality and the importance of controlling the supersaturation to obtain the desired product [Demopoulos, 1993].

A proper understanding of the stability of iron phases formed in the precipitation process as well as the kinetics of precipitation (nucleation and growth) and all the factors, such as hydrodynamics, temperature, supersaturation/pH, and seeding, that impact on iron precipitate product quality, are therefore required. In order to address all these issues, the results obtained from the study were summarized in three sections. In the first chapter, the chemical aspects of iron precipitation is addressed, with the results obtained from the earlier study of the Zincor iron removal process and its residues as basis, by studying the influence of typical operating parameters on the stability of poorly crystalline phases as well as the influence of supersaturation, which is the chemical driving force for precipitation, on the quality of these precipitates. In the next two chapters attention is given to factors that influence the nucleation and growth processes with the emphasis on controlling the local supersaturation levels. This was done by studying, firstly, the impact of changes in the mixing environment on the quality of schwertmannite and ferrihydrite precipitates and secondly, the influence of operating parameters on agglomeration growth.

3. IRON PHASE (META)STABILITY

3.1 Introduction

Bulk crystallization processes are widely used in the chemical industry to remove wanted and unwanted elements from leach solutions. In hydrometallurgical zinc circuits for example, elements such as iron, cobalt, cadmium, nickel, calcium, copper and lead are all removed in a series of complex precipitation (reaction crystallization), cementation (reduction crystallization) and crystallization processes (cooling crystallization). Even the electroplating process in these zinc-refining circuits can be regarded as a crystallization process, since it requires the same primary and secondary crystallization steps than those encountered in other crystallization processes.

The precipitate quality, expressed in terms of particle size and size distribution, impurity content and solids density, generally influences the economics of an operation as it directly impacts on the cost of down stream processing, loss of pay metals in residue streams and the production of a final product that meets client expectations. Gösele *et al.* [1990] indicated that if crystallization processes are not well controlled, gelatinous and voluminous products are formed which typically have a detrimental effect on down stream processes, such as liquid-solid separation processes, as illustrated in Figure 4.

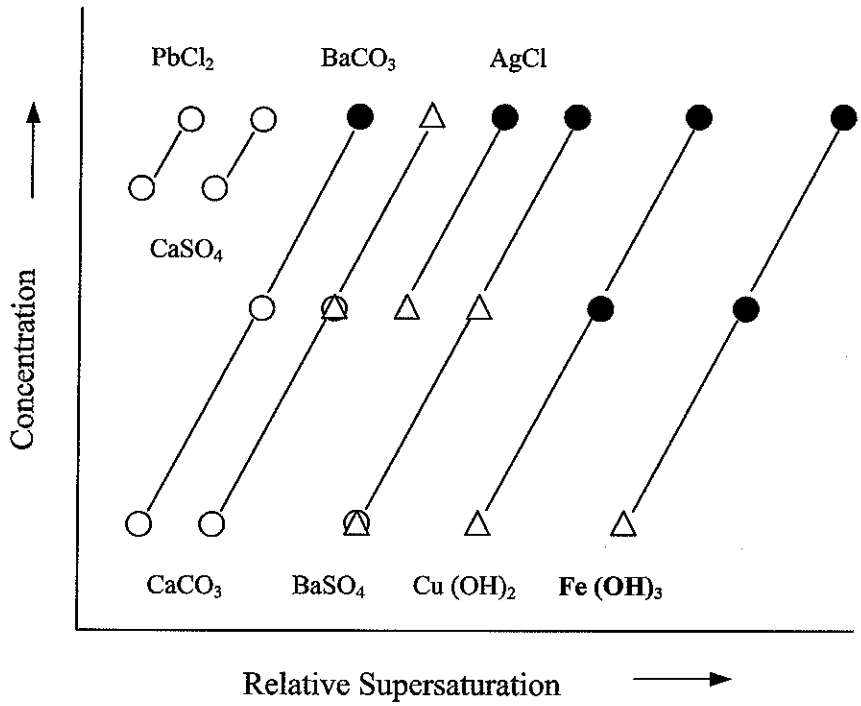

Figure 4. Simplified diagram of precipitation characteristics of various inorganic salts [After Gösele *et al.* 1990]. O = crystalline product, Δ = temporary gelatinous , ● = permanent gelatinous.

It follows from Figure 4 that control over the supersaturation and solute concentration is required to ensure the production of a product with adequate down stream processing potential. This is not a straightforward task, especially when poorly soluble phases, such as ferric iron hydroxides, are produced. Changes in the operating variables, which include temperature, pH and reduction-oxidation potential, supply the driving force, in the form of supersaturation, to crystallization processes and control the solute concentration. These changes not only influence the rate of the primary crystallization steps, i.e. nucleation and growth, but in some instances, such as for example reaction crystallization processes, it also influences the type of mineralogical phase that is produced and its stability. This is specifically the case when iron is precipitated from hot, dilute solutions where dilution is required to lower the solute iron concentration to improve cristallinity of the final product. By varying the pH and temperature, a series of products in the form of different mineralogical phases with different morphologies, particle sizes, size distributions and densities are

produced. The different iron phases that could be produced in a sulphate-containing environment as a function of pH and temperature, as suggested by Babcan [1971], are shown in Figure 5.

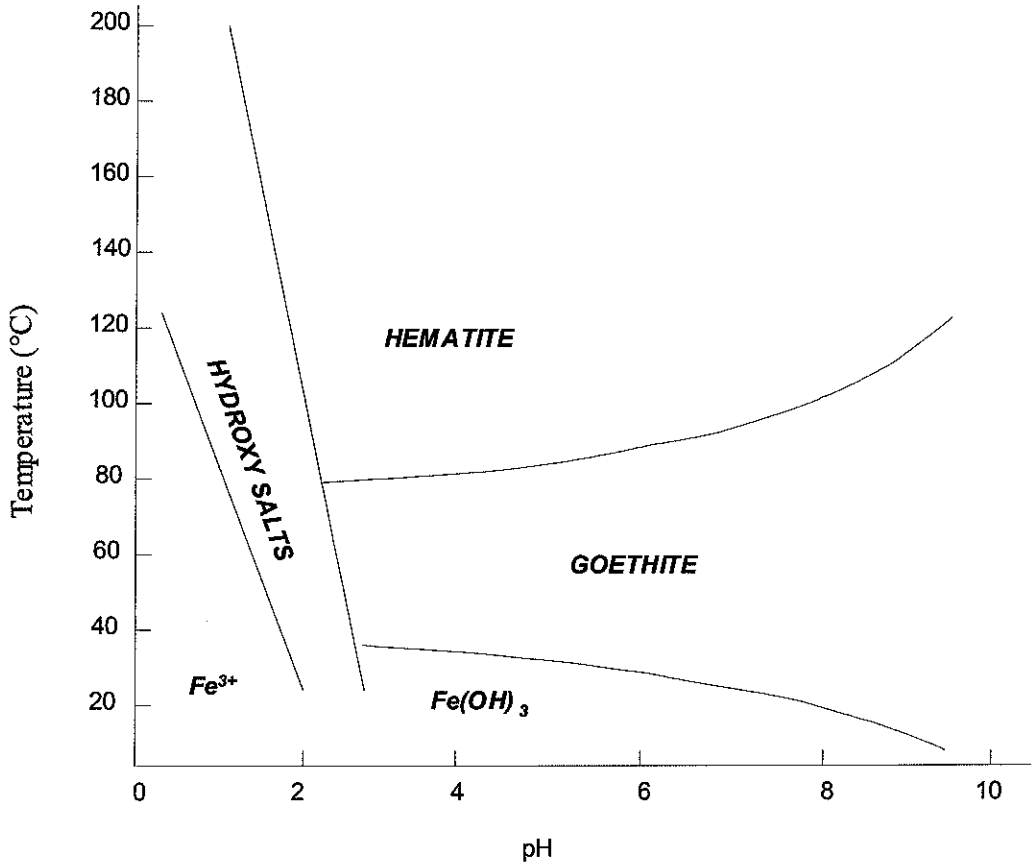

Figure 5. Stability diagram showing the conditions for the precipitation of different iron phases from 0.5 M ferric sulphate solutions [Babcan, 1971]. Hydroxy salts = basic iron sulphates.

The iron phases shown in Figure 5 are all equilibrium phases and therefore do not include metastable or intermediate phases. The equilibrium phases, however, are not always present in industrial iron residues or residues that contain significant amounts of iron. In some environments, it was shown that phases such as ferrihydrite [Jambor and Dutrizac, 1998; Loan *et al.*, 2001] and schwertmannite [Claassen *et al.*, 2002], which are metastable towards goethite, are produced, as discussed earlier.

As was mentioned earlier, temperature and pH not only define the stability of iron phases, as illustrated in Figure 5, but also impact on the kinetics of the precipitation process, due to their influence on supersaturation. The level of supersaturation, and

specifically the critical supersaturation, is described by the so-called metastability curve or metastability limit. The metastable zone, which is the region between the solubility curve and the metastability limit, exists due to the activation energy required to form new particles and defines the supersaturation that might be present when no new nuclei are formed. Within this zone, particle growth in the form of molecular growth is favoured. This results in fewer, bigger and denser particles of a uniform size, whereas above the metastability limit, nucleation and agglomeration growth are the dominant processes [Dirksen and Ring, 1991; Kind, 2002]. This also influences the final product quality since agglomerated particles tend to have much larger surface areas.

Therefore, in order to optimize product quality, specifically in reaction crystallization processes, not only the type of species formed and its stability need to be considered, but also the role that supersaturation plays due to its effect on the primary crystallization processes. In the case of iron precipitates, variables such as pH and temperature determine both the supersaturation and the stability of the species precipitated.

Experimental work was done to establish the influence of temperature and pH on the stability of ferrihydrite and schwertmannite, the range of the metastable zone in a seeded environment, product quality parameters and the relative supersaturation.

3.2 Experimental

The experimental work performed comprised three parts. The first part of the study focused on the determination of the metastable zone and the relative supersaturation levels, followed by an investigation into the benefits of stagewise precipitation. Lastly, information was gathered on the influence of specifically temperature and pH on some product quality parameters.

3.2.1 Determination of the metastable zone and supersaturation levels

The experimental arrangement consisted of a sealed, flat-bottomed stirred tank reactor with a diameter (D) of 120mm and working volume of 2L, equipped with four outer baffles. It was stirred with a three-blade marine-type impeller with diameter d $\simeq$ D/2 rotating at 1000 rpm. The temperature was controlled within 1°C of the setpoint using a heating mantle and controller.

Experiments were conducted at temperatures of 50, 70 and 90°C and at pH values ranging from 1.5 to 3.5. For each experiment, a solution containing 5 g/L sulphuric acid and about 11.5 g/L Fe as $Fe_2(SO_4)_3$ was prepared. The pH was raised manually at a rate of approximately 0.5 units every 20 minutes on the forward cycle using $Ca(OH)_2$ powder (pH range 1.5 to 2.5) and ZnO powder (pH range 2.5 to 3.5). On the reverse cycle (pH 3.5 to pH 1.5), 98% sulphuric acid was added drop wise to lower the pH at the same rate mentioned above. Each experiment was repeated at least three times. Samples were taken at regular pH intervals, except over the critical pH range, where the critical supersaturation level was exceeded, where samples were taken more frequently. Approximately 10 mL solution was extracted during the sampling process. Each sample was immediately filtered and the extracted solution was analysed for ferric iron concentration and pH. Distilled water and chemicals of CP grade were used in all experiments.

3.2.2 Stagewise precipitation

The experimental setup used comprised three crystallizers in series, each with an active volume of 3.96L and an inside diameter of 16cm. Each reactor was equipped with four outer baffles fixed to the wall of the vessel, a riser box and overflow launder, as shown in Figure 6.

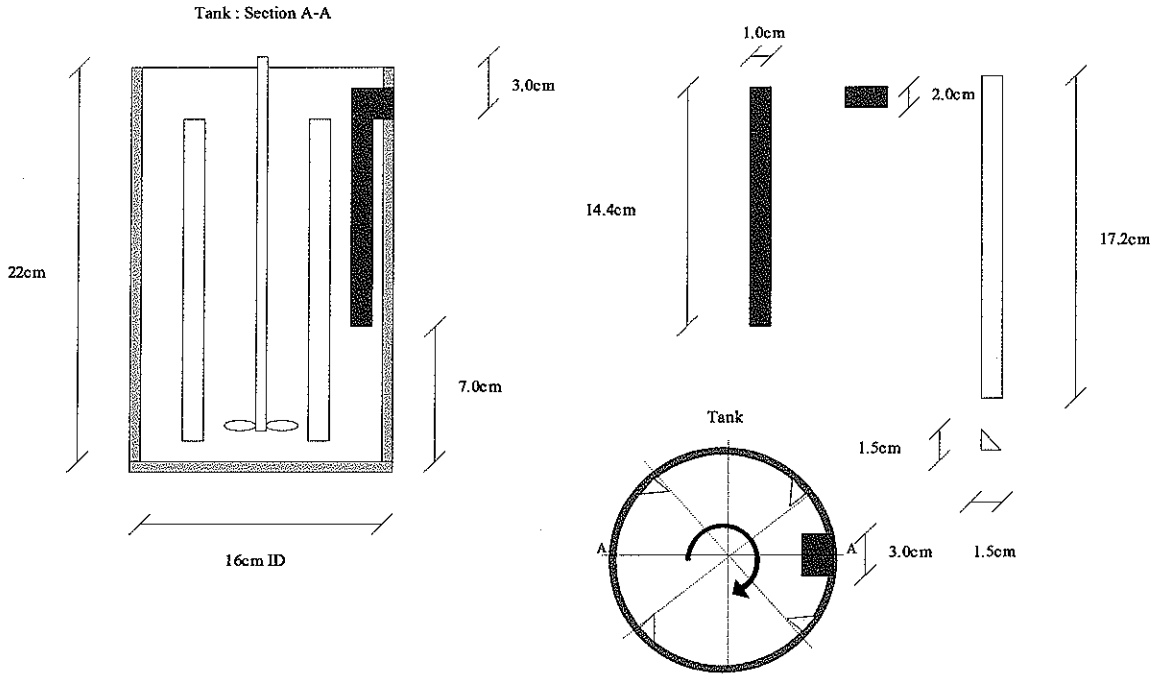

Figure 6. Dimensions of the crystallizer used to determine the influence of stagewise precipitation on product quality.

Three-blade marine type impellers, with diameters d ≃ D/2.5, were used at a stirring rate of 600 rpm to keep the solids in suspension. Table 3 gives a summary of the experimental conditions used to determine the influence of stagewise precipitation on product quality parameters.

Table 3. Experimental conditions used to determine the influence of stagewise precipitation on product quality.

	Parameter		Flow	
Experiment	Temperature (°C)	pH profile	Iron solution (mL/min)	Calcine slurry (mL/min)
Base case	65	3.20	26.9	41.1
		3.31	***	***
		3.39	***	***
1	65	3.20	26.9	41.1
		2.80	1.33	***
		2.94	***	***
2	65	2.50	29.0	36.1
		3.00	***	2.5
		3.09	***	***
3	65	2.50	26.9	45.0
		2.74	***	***
		3.01	***	0.8

The hot iron solution contained 5 g/L free acid and 15 g/L iron, added as $Fe_2(SO_4)_3$. Roasted zinc calcine, in the form of a 7.5% calcine slurry prepared with distilled water, was used as neutralising agent. The calcine used had a d_{50} value of about 38μm and ZnO content of approximately 70%. In all experiments the calcine slurry and hot iron solution were pumped continuously to the first of three reactors in series to control the pH at the predetermined setpoints. The two streams were placed on opposite sides of the reactor with the outlet points positioned just below the agitator blades. Hot iron solution and ZnO slurry were also pumped on separate lines to

reactors 2 (Experiments 1 and 2) and 3 (Experiment 3), respectively, to adjust the pH values as indicated in Table 3.

Samples of 250 mL each were taken from reactor 3 at the end of each experiment, which lasted for about three hours, and immediately filtered. The solution samples were analysed for pH and ferric iron concentration. The filter cakes were weighed and dried to determine the moisture content and analysed for zinc and iron. The dry solids density of each sample was also determined. Wet filter cake samples were taken and mixed with distilled water to determine particle size and size distribution using a Malvern particle size analyser.

3.2.3 Determination of the influence of temperature and pH on product quality

In order to determine the influence of pH and temperature on product quality parameters such as cake moisture content, particle solids density, particle impurity content (zinc and sulphate) and particle size, the sealed glass precipitator with an active volume of 2L, mentioned earlier, was used in a continuous mode. Hot iron solution containing 5 g/L free acid and 10 g/L iron, added as $Fe_2(SO_4)_3$, as well as a 2.5% ZnO slurry were continuously pumped to the reactor using peristaltic pumps. All the reagents used were of CP grade.

The outlet points of the reactant streams were placed just below the agitator blades on opposite sides of the vessel. The level in the reactor was controlled with another peristaltic pump. The flow rate of ZnO slurry varied with a change in the pH setpoint as summarised in Table 4.

Table 4. Average hot iron solution (HIS) and ZnO slurry flow rates used to precipitate iron at different pH setpoints.

pH	HIS flow rate (mL/min)	ZnO slurry flow rate (mL/min)
1.8	21.1	< 1
2.2	21.1	10
2.6	21.1	14
3.0	21.1	16
3.4	21.1	17

Experiments were performed at temperatures of 50, 60, 70 and 80°C. Each experiment ran for three hours and was repeated at least three times. At the end of each experiment, two 250 mL samples were taken. The first sample was filtered and dried at 120°C for one hour to determine the cake moisture content. The other sample was filtered and the cake washed with 1 L of hot water. The filtrate extracted prior to the hot water wash, was analysed for ferric iron and pH. The washed filter cake was again dried at 120°C for one hour, analysed for zinc and sulphate and the dry solids density determined.

Wet filter cake samples of about 5 mL each were also taken and mixed with distilled water at ambient temperature to determine the product mean particle size and size distribution using a Malvern particle size analyser.

XRD analyses were also performed on the dried, washed filter cake. Cu-Kα radiation at a wavelength of approximately 0.154 nm was used.

3.3 Results and discussion

3.3.1 Iron phase (meta)stability and the role of the supersaturation level in iron precipitate product quality

3.3.1.1 Determination of the metastable zone

In order to develop a (meta)stability diagram for iron precipitated from a ferric iron solution under industrial conditions and to calculate typical supersaturation levels present during this process, the metastability zone for iron precipitation had to be determined first. This was done using a method of cycling the pH between a lower and higher limit at different temperatures. The ferric iron concentration as a function of pH at a specific temperature was then plotted, as shown in Figures 7 to 9 (also see Appendix 1). The critical pH values for nucleation (A) and solubilisation (B) were then determined by extrapolation of the slope of the ferric concentration versus pH line to the initial ferric concentration.

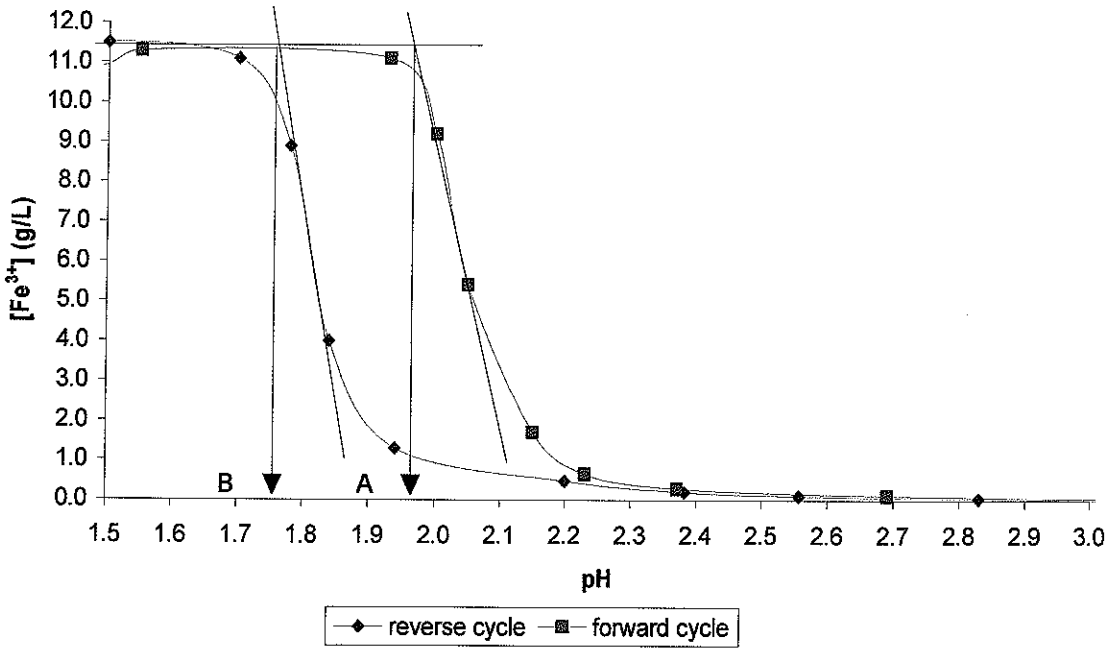

Figure 7. Average ferric iron concentration as a function of pH determined at 50°C. The pH was changed stepwise in increments of 0.5 pH units every 20 minutes. The pH was increased by adding $Ca(OH)_2$ and ZnO powder and decreased by adding 98% H_2SO_4. The total sulphate concentration varied between 0.2 and 0.25 moles/L.

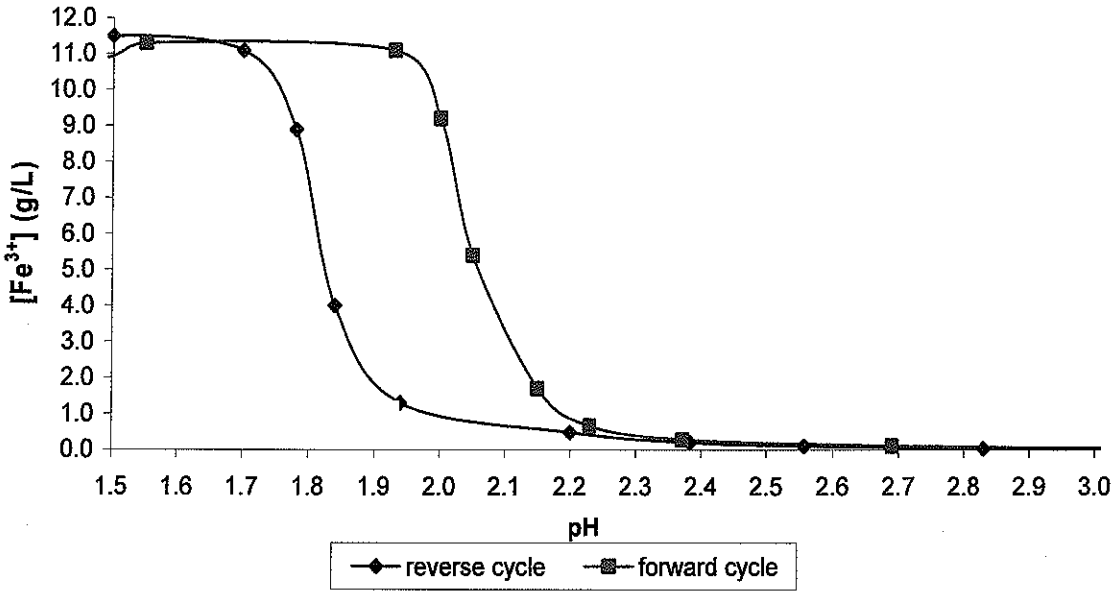

Figure 8. Average ferric iron concentration as a function of pH determined at 70°C. The pH was changed stepwise in increments of 0.5 pH units every 20 minutes. The pH was increased by adding $Ca(OH)_2$ and ZnO powder and decreased by adding 98% H_2SO_4.

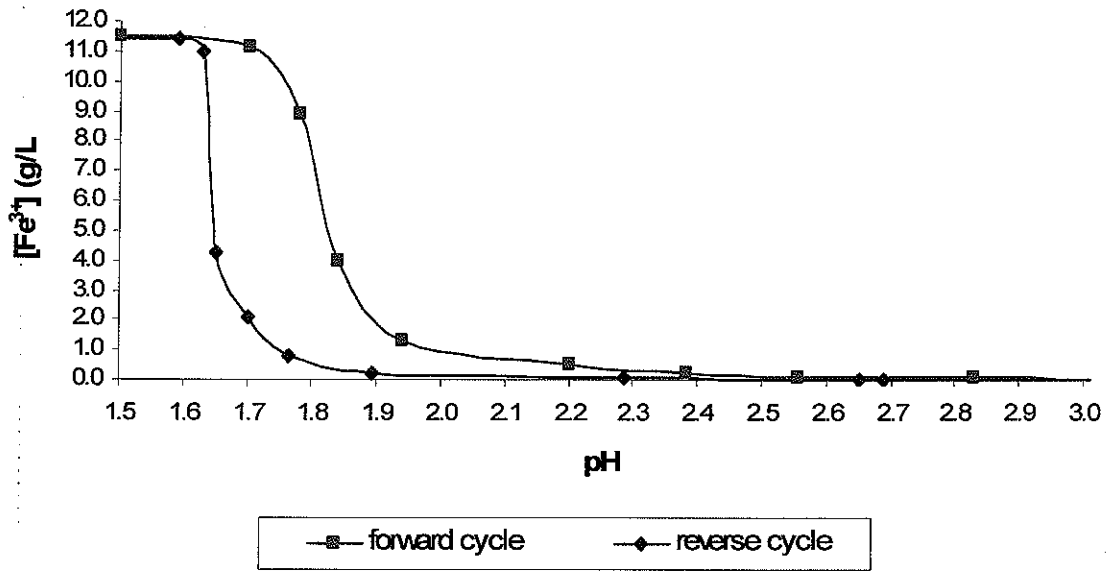

Figure 9. Average ferric iron concentration as a function of pH determined at 90°C. The pH was changed stepwise in increments of 0.5 pH units every 20 minutes. The pH was increased by adding $Ca(OH)_2$ and ZnO powder and decreased by adding 98% H_2SO_4.

From the data presented in Figures 7 to 9, the critical pH values of nucleation (e.g. point A, pH ≈ 1.97, Fig. 7) and solubilisation (point B, pH ≈ 1.76, Fig. 7) were determined. The critical pH values for nucleation and solubilisation, defining the boundaries of the metastable zone as a function of temperature, are shown in Figure 10.

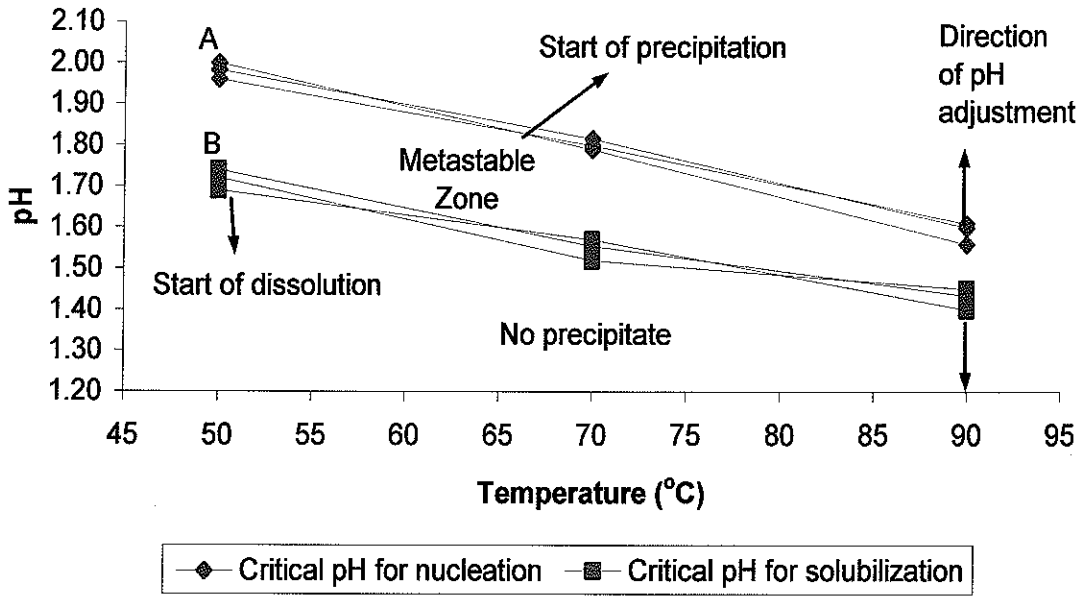

Figure 10. Illustration of the metastable zone determined for the precipitation of iron from a ferric iron solution containing approximately 11.5 g/L Fe as $Fe_2(SO_4)_3$ and 5 g/L H_2SO_4. The pH was varied using $Ca(OH)_2$ and ZnO powder, and 98% H_2SO_4 .

According to the definition of the metastable zone, the equilibrium solubility limit forms the lower boundary of the metastable region. However, the width of the metastable region may be reduced by an increase in temperature, the presence of isomorphic and anisomorphic material [Garside *et al.*, 1972 and Mullin and Ang, 1976] and a mixing intensity such as the 1000 rpm used. When the solubility limit determined in this study (Figure 10) is compared with the equilibrium solubility limit, the reduction in the width of the metastable zone is evident, as shown in Figure 11. STABCAL™ software with the available NBS-database was used to calculate the equilibrium [Fe^{3+}] solubility line X (refer to Appendix 2) and the data for line Y was taken from the literature [Cornell and Schwertmann, 1996]. Lines X and Y show the equilibrium solubility of goethite, which is the equilibrium phase for ferrihydrite and

schwertmannite, as a function of pH. It is clear from Figure 11 that there is reasonable agreement between the two lines for pH values smaller than about 3.0. In this study iron concentrations reflected by line X was used for the calculation of the relative supersaturation, as will be shown later.

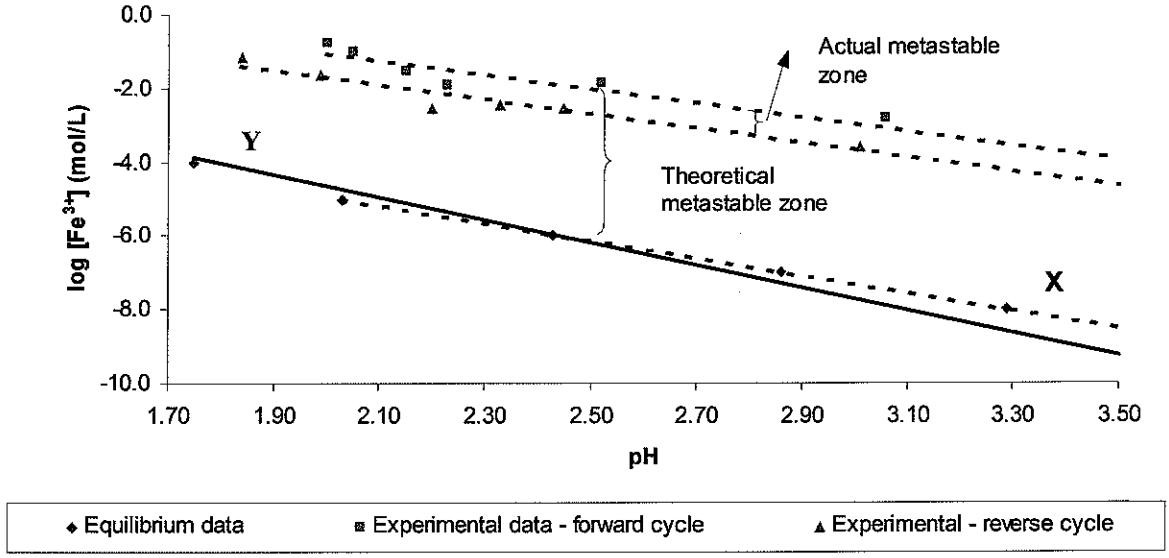

Figure 11. Ferric concentration as a function of pH for the precipitation of iron at 50°C from a ferric iron solution containing approximately 11.5 g/L Fe as $Fe_2(SO_4)_3$ and 5 g/L H_2SO_4. The pH was varied using $Ca(OH)_2$ and ZnO powders, and 98% H_2SO_4. The experimental reverse cycle line forms the new solubility limit.

It follows from Figure 11 that a high degree of supersaturation is required to initiate precipitation and that the relatively small metastable zone of between 0.2 and 0.3 pH units (from Figure 10), would require precise control to achieve good precipitate properties. Claassen *et al.* [2003(b)] have shown that iron removal processes are frequently operated at pH values above the metastability limit. This results in an increase in the supersaturation levels, which in turn leads to an increase in the nucleation rates with resultant finely divided, poorly crystalline particles, which tend to agglomerate [Dirksen and Ring, 1991] to give a final product with relatively high impurity levels. Furthermore, the choice to utilise the metastability limit to improve product quality is influenced by factors such as the co-precipitation of other phases, i.e. phases resulting from the presence of silica in some industrial hot iron solutions,

the value of the product being removed, as recycling has a cost implication, the reduction in the concentration of oxygen or gaseous reagents at low pH values (goethite iron removal process) and the need to precipitate a specific iron phase, such as ferrihydrite, that is stable only at higher pH values.

Therefore, although the metastable zone might be useful in the chemical industry, i.e. in the production of pigments, the factors mentioned above need to be considered in metallurgical processes. It nonetheless, provides useful information that could be used to improve product quality in some iron removal processes. Firstly, it could act as a control reference point to lower supersaturation in an iron precipitation process, and/or it could be used to calculate typical supersaturation levels in a specific application, as illustrated in the following paragraphs. Secondly, it could be used to illustrate why stagewise precipitation [Demopoulos, 2003] could improve iron precipitate product quality. Generally, the solute concentration changes stepwise with a step change in temperature (cooling crystallization) or pH (reaction crystallization) within the metastable region. By using the same principle, even at conditions outside the metastable zone, it was shown that product quality could be improved as discussed later.

3.3.1.2 Determination of supersaturation and the (meta)stability diagram

The relative supersaturation present during a precipitation process typically determines the quality of the precipitate, with poorer quality precipitates being formed at high levels of supersaturation. The relative supersaturation (σ) present during the precipitation experiments were calculated using the minimum concentration required to initiate precipitation substituted in equation 4, and shown in Figure 12 as a function of pH and temperature.

$$\sigma = (c - c_{eq})/c_{eq} = \Delta c/c_{eq} \qquad .....4$$

Where: c = actual solute concentration (mol/L)

c_{eq} = equilibrium solute concentration (mol/L)

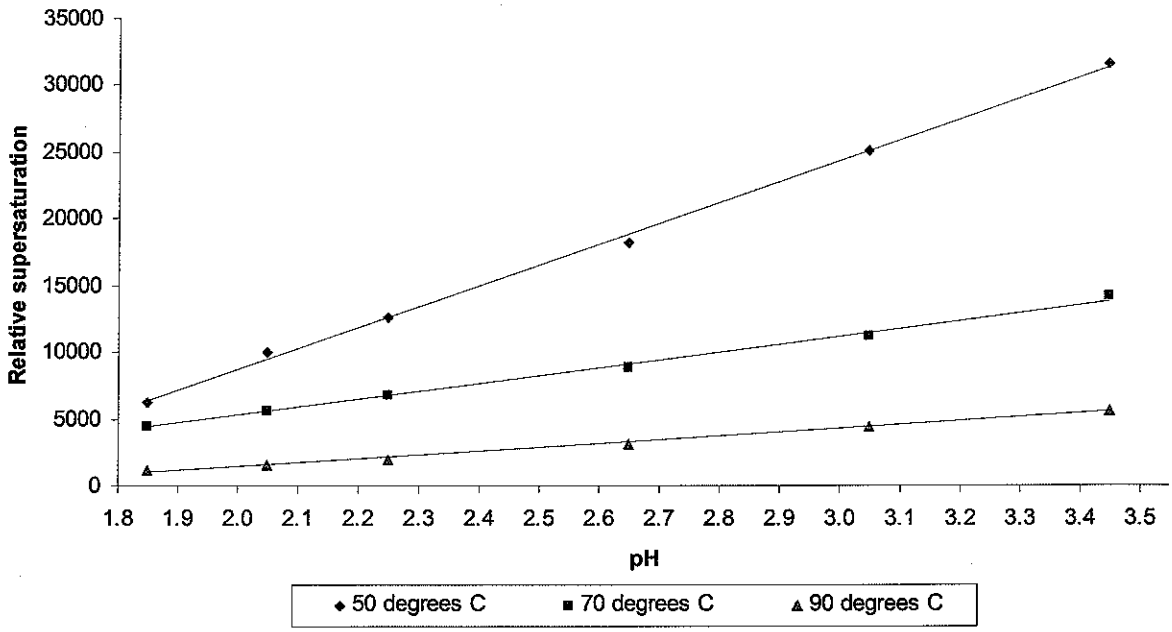

Figure 12. Relative supersaturation required as a function of pH at different temperatures for the hydrolysis of ferric iron from iron solutions containing approximately 11.5 g/L Fe added as $Fe_2(SO_4)_3$ using $Ca(OH)_2$- and ZnO powder to control the pH.

From Figure 12 it is clear that lower degrees of supersaturation are required for precipitation of iron at higher temperatures and lower pH values. Better quality precipitates could thus be expected for such conditions. This was indeed found to be the case in previous work [Claassen *et al.*, 2002] where open structured ferrihydrite was produced at a temperature of 65ºC and a pH of 3.2, compared to more dense schwertmannite, obtained at 65ºC and a pH of 2.7, as shown in Figure 13.

Figure 13. SEM backscattered image of an iron bearing particle, showing open structured ferrihydrite particles (Particles A) covered with a more dense structured schwertmannite layer (Portion B) [Claassen *et al*., 2002].

The zones for metastable iron precipitates may be defined in terms of temperature and pH by considering the chemical analyses, in the case of the hydroxy salts, and XRD analyses, in the case of ferrihydrites, and are shown as Figure 14.

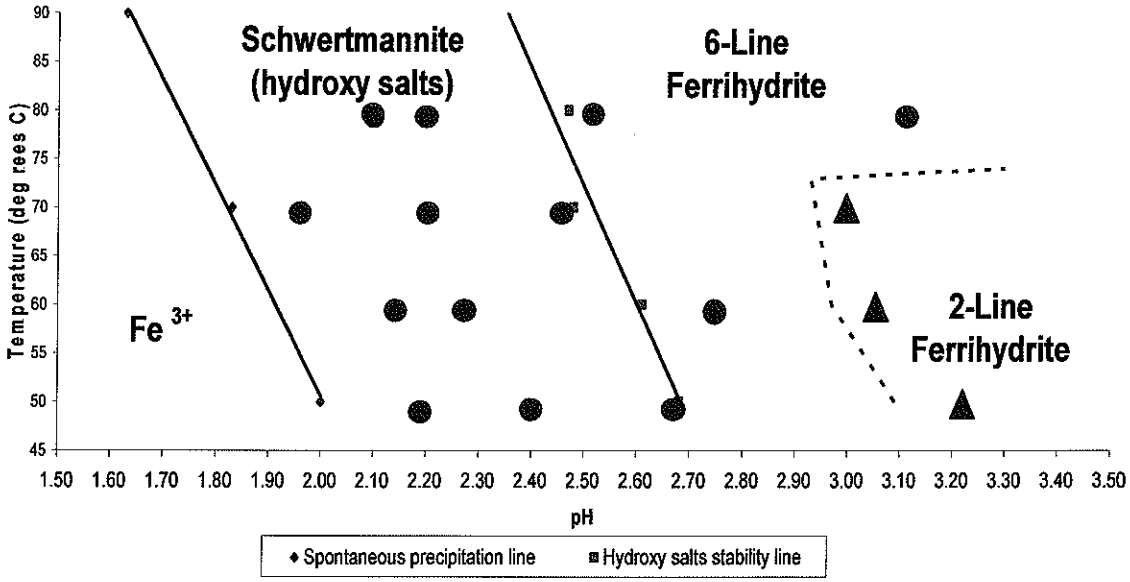

Figure 14. Metastability diagram for ferric iron hydrolysis from a 10 g/L Fe (added as $Fe_2(SO_4)_3$ solution) using ZnO powder to control the pH. ●= 6-line ferrihydrite and schwertmannite and ▲ = 2-line ferrihydrite obtained from XRD analyses. The total sulphate concentration varied between 0.2 and 0.25 moles/L during all experiments.

In Figure 14, the boundary between the hydroxy salts (schwertmannite) and ferrihydrite was obtained by washing the precipitates produced in the continuous reactor with hot water, and noting the conditions where the sulphate content started to rise, as indicated in Figure 15.

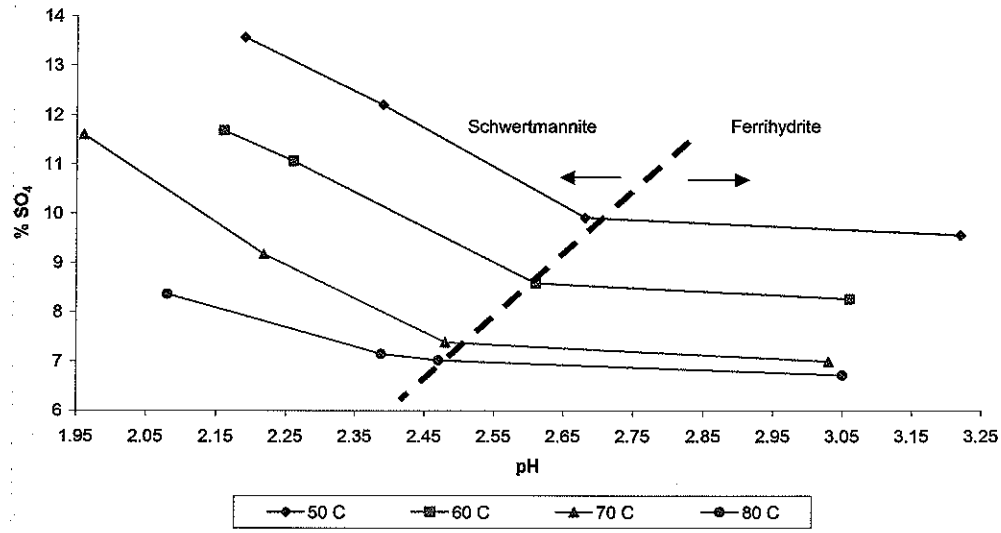

Figure 15. Influence of pH and temperature on the sulphate content of iron precipitated from a hot iron solution containing 10 g/L Fe (as $Fe_2(SO_4)_3$) using ZnO powder to control the pH in a continouos reactor.

The different iron phases and their crystallinity were identified using XRD analyses. The data obtained for the 60°C isoterm are summarized in Table 5.

Table 5. X-ray diffraction results obtained from synthetic iron precipitate samples produced in a continuous reactor at 60°C.

pH	d-values (nm)		
	Schwertmannite	2-line ferrihydrite	6-line ferrihydrite
3.06		Uncertain	
		Uncertain	
		0.2561	
		Very weak	
		Very weak	
		0.1506	
		Very weak	
2.75			0.5033*
			0.3323*
			0.2554
			0.2219
			0.1927
			0.1702
			0.1510
			Very weak
2.16	0.4895		
	0.3423		
	0.2526		
	0.2214		
	0.1940		
	0.1648		
	0.1517		
	Very weak		

* Indicate presence of schwertmannite

The data obtained in Table 5 is in good agreement with work done by Bigham *et al.* [1990], Jambor and Dutrizac [1998] and Claassen *et al.* [2002].

The determination of the schwertmannite (meta)stability region at elevated temperatures is unique as it has previously only been identified in natural environments [Bigham *et al.*, 1990, 1994, 1996]. It also appears from Figure 15, as if there is a definite hydroxy salt/schwertmannite phase transition line, as indicated in Figure 14, which supports the notion of schwertmannite as a separate phase, rather than being ferrihydrite with adsorbed sulphate. In the temperature range 50°C to 90°C, this transition line is between 0.1 and 0.2 pH units above the line reported by Babcan [1971] who worked at 0.5 M $Fe_2(SO_4)_3$ (refer to Figure 5). It is known that the stability regions for iron oxide and oxy-hydroxide phases are extended to lower pH values due to the presence of high sulphate levels. This is a result of the formation of iron sulphate complexes and buffering of the pH. The latter is caused by the combination of free H^+ ions with bisulphate ions. The net effect is that oxide and oxy-hydroxide iron phases are stable at higher free acid concentrations.

It appears from Figure 15 rather as if both ferrihydrite and schwertmannite contain variable amounts of sulphate, which probably result from a change in morphology, with a change in pH and temperature, and the increased stability of ferrihydrite with an increase in pH and temperature, above the hydroxy salt stability line. If the data in Table 5 is considered, it appears as though schwertmannite is also present at pH values above the hydroxy salt stability line (6-line ferrihydrite region), as indicated by the presence of peaks at approximately 17 and 27 2θ, which are not well defined in the case of ferrihydrite, as shown in Figure 16.

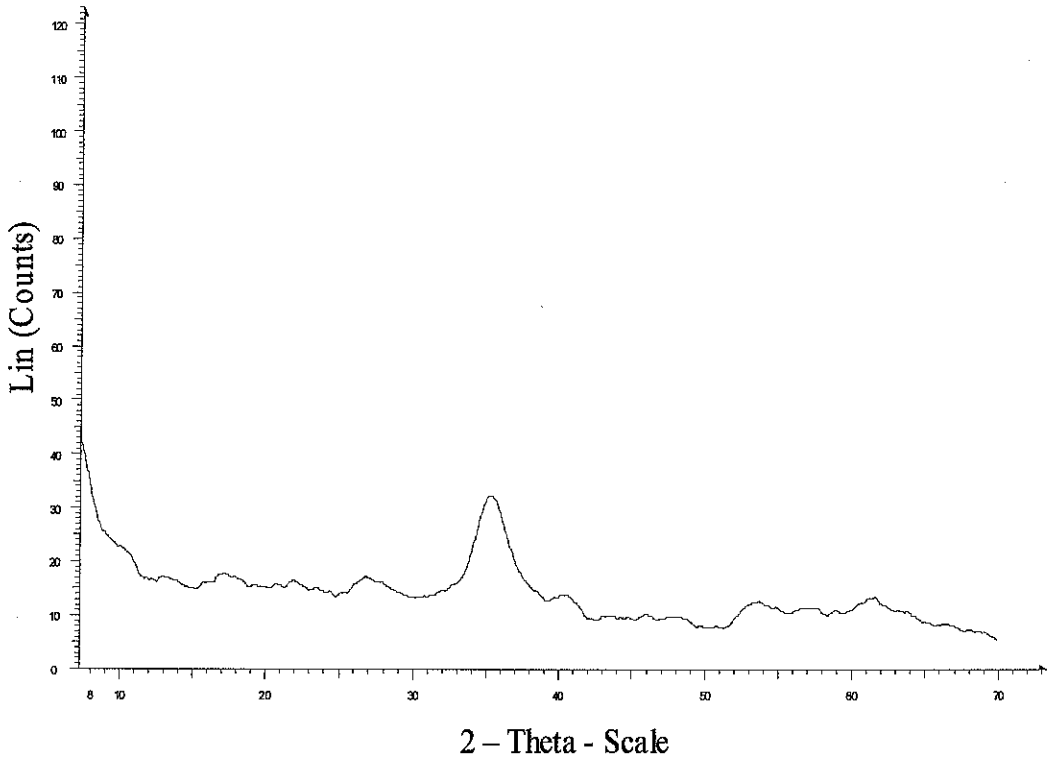

Figure 16. X-ray diffractogram of a poorly crystalline synthetic iron precipitate produce at 60°C and a pH of 2.75 in a continuous crystallizer.

The stability of iron hydroxy sulphates in the acidic pH region stems from the presence of species such as $FeSO_4^+$ in iron sulphate media, that is believed to play an important role in the formation of these phases [Ashurst and Hancock, 1977]. Species such as $Fe_2(OH)_2(SO_4)_2$ were also found in sulphate solutions, which is believed to be the precurcers of iron hydroxysulphate precipitates [Yakovlev *et al.*, 1977].

Finally, the influence of supersaturation on the cristallinity and product quality of iron phases produced at temperatures between 50 and 90°C and pH values between about 1.5 and 3.5, can be summarized by combining the data presented in Figures 12 and 14, as shown in Figure 17. Although the different precipitates may be formed over a range of supersaturations, it can be expected that the best quality precipitates would be formed at lower degrees of supersaturation.

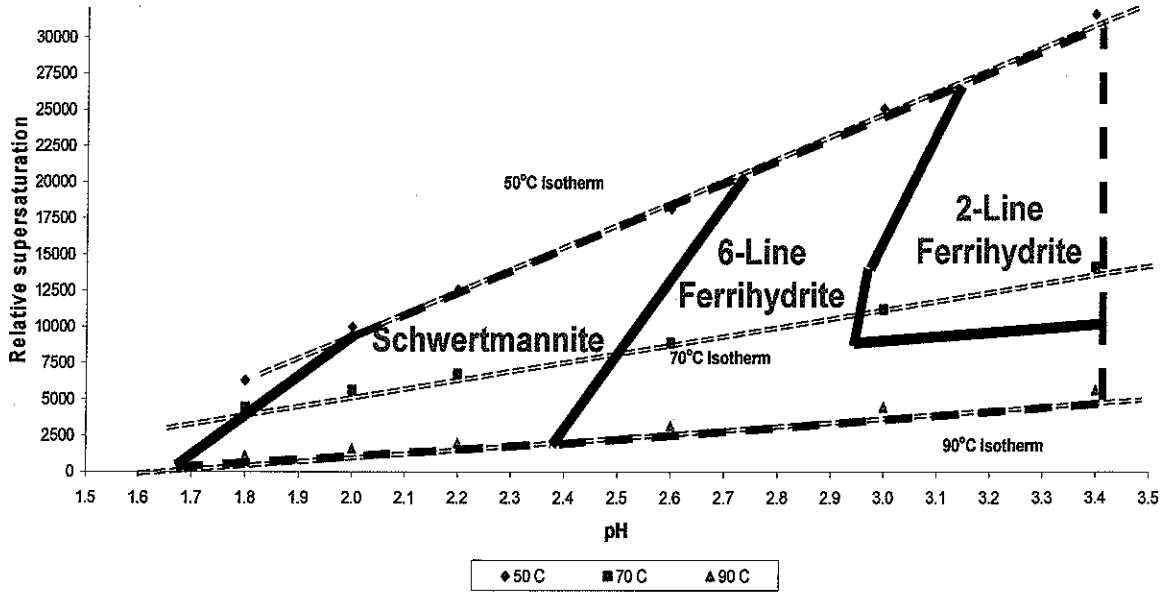

Figure 17. Phase stability of iron precipitates in terms of relative supersaturation and pH .

3.3.1.3 Stagewise precipitation

Stagewise precipitation is done by operating within the metastable zone to improve product quality. The applicability of this approach to a process operated above the metastable region was evaluated. Table 6 summarises the results obtained when iron was removed stagewise using three continuous crystallizers in series.

Table 6. Results obtained from stagewise iron removal experiments performed at 65°C.

Experiment	pH profile	Moisture (%)	Water soluble Zn* (%)	Weak acid soluble Zn** (%)
Base case	3.20 3.31 3.39	57	2.86	5.41
1	3.20 2.80 2.94	54	1.57	3.83
% Improvement		**5.3**	**45.1**	**29.2**
2	2.50 3.00 3.09	43	1.18	3.65
% Improvement		**24.6**	**58.7**	**32.5**
3	2.50 2.74 3.01	46	1.22	4.02
% Improvement		**19.3**	**57.3**	**25.7**

* Filter cake washed with hot water only to remove water soluble zinc

** Filter cake washed with a pH = 1.5 solution to remove entrapped zinc

In the base case experiments, hot iron solution was contacted with calcine slurry at a pH of 3.2 in the first of three reactors in series, where after the pH increased without further additions to about 3.4 in the last reactor. According to Figures 14 and 17, 2-line ferrihydrite was probably produced at a relatively high relative supersaturation level of about 17000 in this process. Particles with a high surface area were probably formed, which would explain the relatively high moisture and impurity content in

terms of water soluble and weak acid soluble zinc values of the precipitate summarized in Table 6.

In Experiment 1, a leach/acidification step was performed at pH 2.80 in the second reactor. This mode of operation is utilised in the Zincor roast-leach-electrowinning zinc refinery [Claassen et al., 2003(b)] to remove iron from zinc-rich process solutions. During the acid wash step, some 2-line ferrihydrite particles were probably dissolved and reprecipitated as 6-line ferrihydrite and schwertmannite (refer to Figure 14 and Table 5) at relative supersaturation levels around 15000. This leaching step resulted in a reduction in the relative particle surface area as well as the zinc content of the solids formed, as shown in Table 6.

Experiments 2 and 3 were used to investigate the influence of stagewise precipitation on some product quality parameters, i.e. the pH was incrementally increased to remove iron to the desired levels. In Experiment 2, the pH in the first reactor was controlled at 2.5, followed by an increase in pH, through the addition of calcine slurry into the second reactor to raise the pH to 3.0, where after it increased to about 3.1 in the last vessel. In the first reactor schwertmannite, which has a more dense structure than ferrihydrite, was probably produced at relative supersaturation of about 12000. The lower nucleation rates, at lower supersaturation, and improved leaching of the ZnO neutralising agent probably resulted in a significant reduction in the impurity levels of the final product, as is evident from the data presented in Table 6. The remaining supersaturation was then used in the second reactor to probably agglomerate the particles. In Experiment 3, the pH in the first reactor was again controlled at 2.5, and then left to increase to about 2.75 in the second reactor. Calcine was added to the third reactor to increase the pH to 3.00 to ensure adequate iron removal, which could explain the slight increase in the zinc values of the final product. These results indicate that the stagewise precipitation of iron, even above the metastability limit, could significantly improve product quality.

3.3.2 Influence of temperature and pH on final product quality

3.3.2.1 Solids moisture content

The moisture content of a precipitated product can be used to indicate its downstream processing potential in terms of its drying requirements and ease of handling, as it gives an indication of the relative surface area of the precipitates. Figure 18 shows how the iron precipitate moisture content is influenced by pH and temperature.

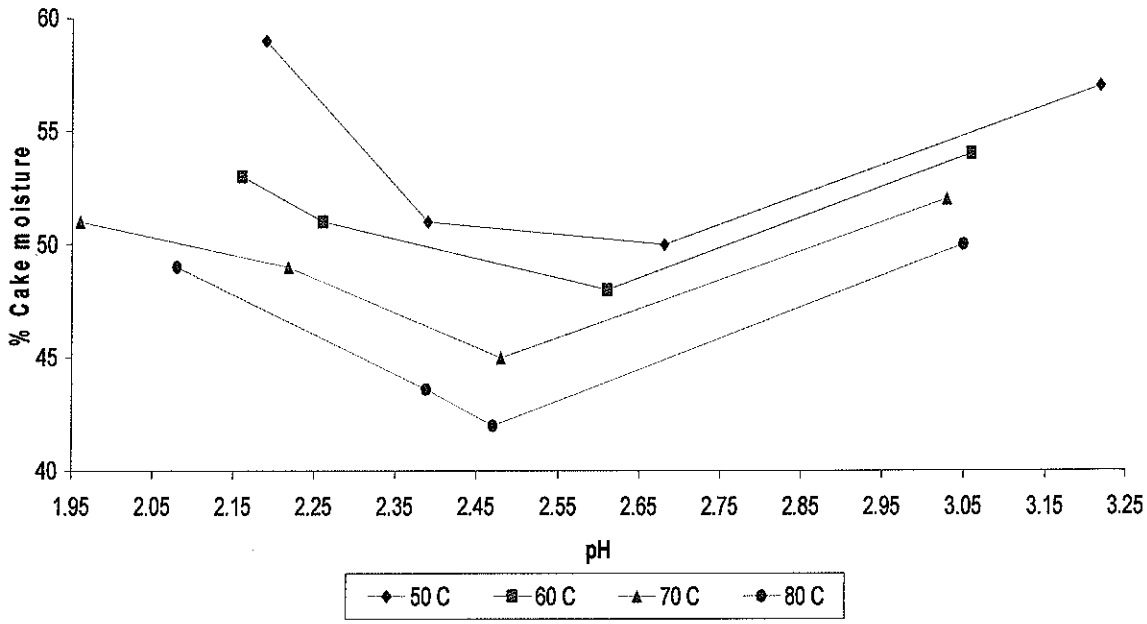

Figure 18. Filter cake moisture content for iron precipitates produced in a continous crystallizer from a hot iron solution containing 5 g/L H_2SO_4 and 10 g/L Fe (as $Fe_2(SO_4)_3$) using ZnO powder as neutralising agent as a function of pH and temperature.

The precipitate moisture content is significantly influenced by pH and temperature as indicated in Figure 18. Cake moisture decreases with an increase in temperature and reaches a minimum at pH values between 2.45 (80°C) and about 2.68 (50°C). The effect of temperature on precipitate moisture content is probably the result of the formation of more dense particles at higher temperatures as indicated by the results shown in Figure 19.

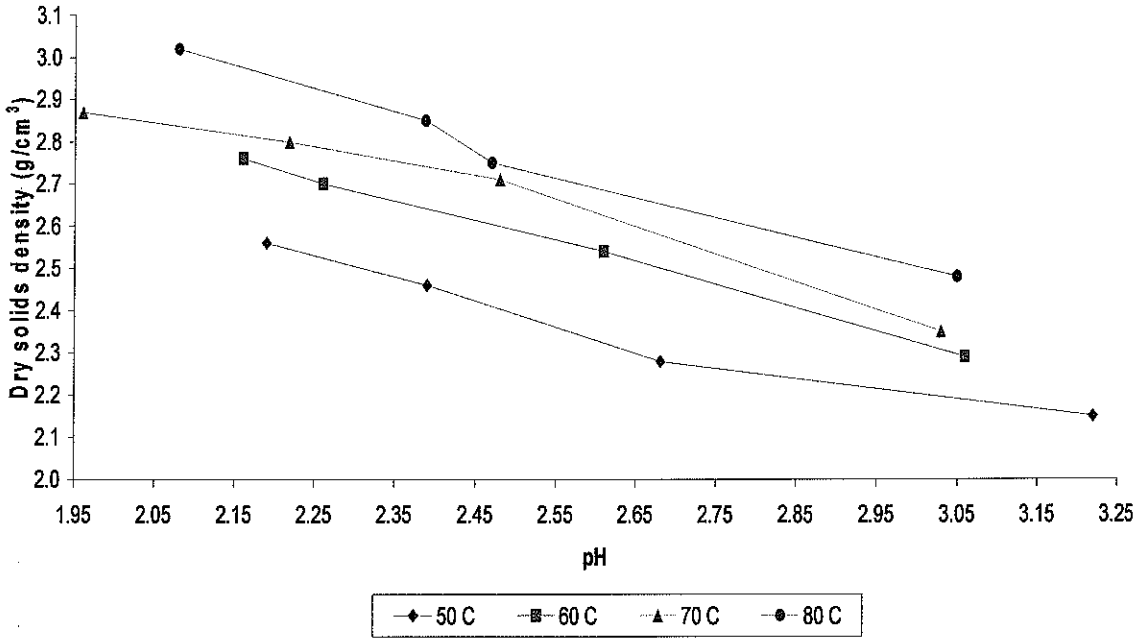

Figure 19. Influence of pH and temperature on precipitate solids density for iron precipitates produced in a continous crystallizer from a hot iron solution containing 5 g/L H_2SO_4 and 10 g/L Fe (as $Fe_2(SO_4)_3$) using ZnO powder as neutralising agent.

It is known that better quality precipitates are formed at higher temperatures as a result of the lower supersaturation levels required, as indicated in Figure 17. The increase in moisture content at lower and higher pH values is probably a result of a reduction in the mean particle size (increase in relative surface area) at lower pH and the formation of more voluminous particles at higher pH values. The high supersaturation levels generated at high pH values also supports fast nucleation rates and an increase in population density and surface area. Both the mean precipitate particle size and population density increase with increasing pH, as shown in Figures 20 and 21. The increase in size of the particles is most probably caused by agglomeration.

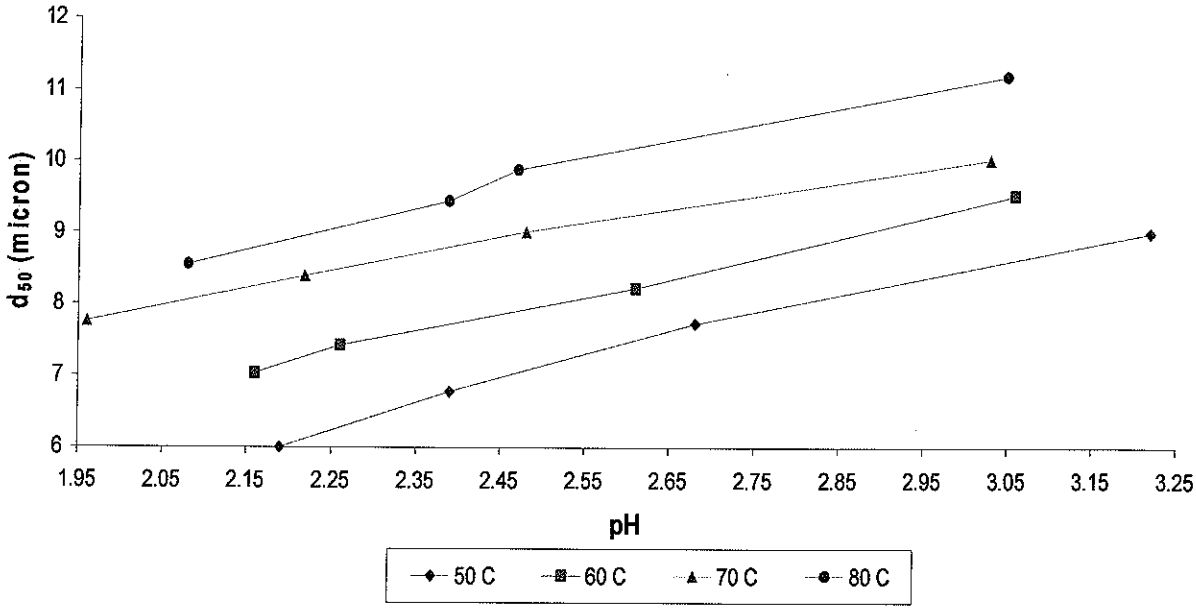

Figure 20. Influence of pH and temperature on precipitate mean particle size for iron precipitates produced in a continous crystallizer from a hot iron solution containing 5 g/L H_2SO_4 and 10 g/L Fe (as $Fe_2(SO_4)_3$) using ZnO powder as neutralising agent.

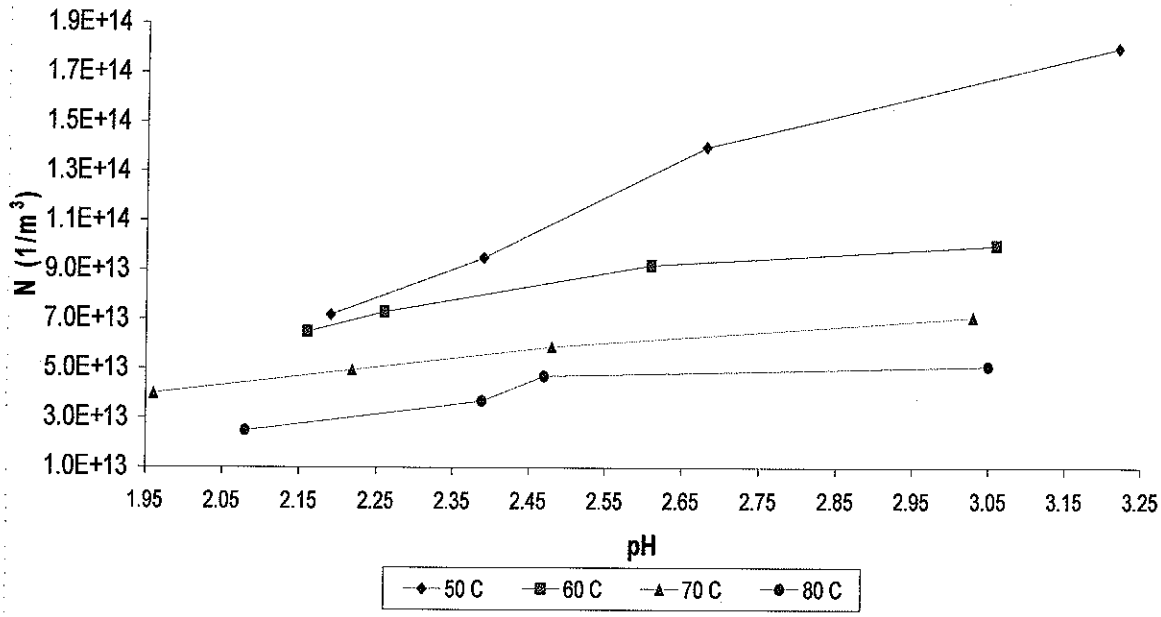

Figure 21. Influence of pH and temperature on precipitate population density obtained from Malvern particle anlyses for iron precipitates produced in a continous crystallizer from a hot iron solution containing 5 g/L H_2SO_4 and 10 g/L Fe (as $Fe_2(SO_4)_3$) using ZnO powder as neutralising agent.

3.3.2.2 Solids zinc content

Reaction crystallization requires a reagent to generate the necessary chemical driving force for solids formation from leach solutions. In the zinc industry, ferric iron is often removed through hydrolysis by contacting hot iron solution with zinc calcine containing approximately 70% ZnO, as summarized by Claassen *et al.* [2003(b)]. The use of a zinc containing neutralizing agent typically results in high zinc losses and often the production of iron residues with high sulphate loadings. Figure 20 shows the influence of pH and temperature on the zinc content of ferric iron precipitated through hydrolysis using ZnO as the neutralizing agent. The zinc content of iron precipitates increased significantly with an increase in pH and temperature as shown in Figure 22. This is probably a result of a combination of high supersaturation (at higher pH values) and faster diffusion of iron species to the growth points [Sakamoto, *et al.*, 1976 and Yamada, 1980], which could entrain unleached ZnO or zinc sulphate solution. The reduction in the reactivity of ZnO with an increase in pH, probably exacerbated the problem.

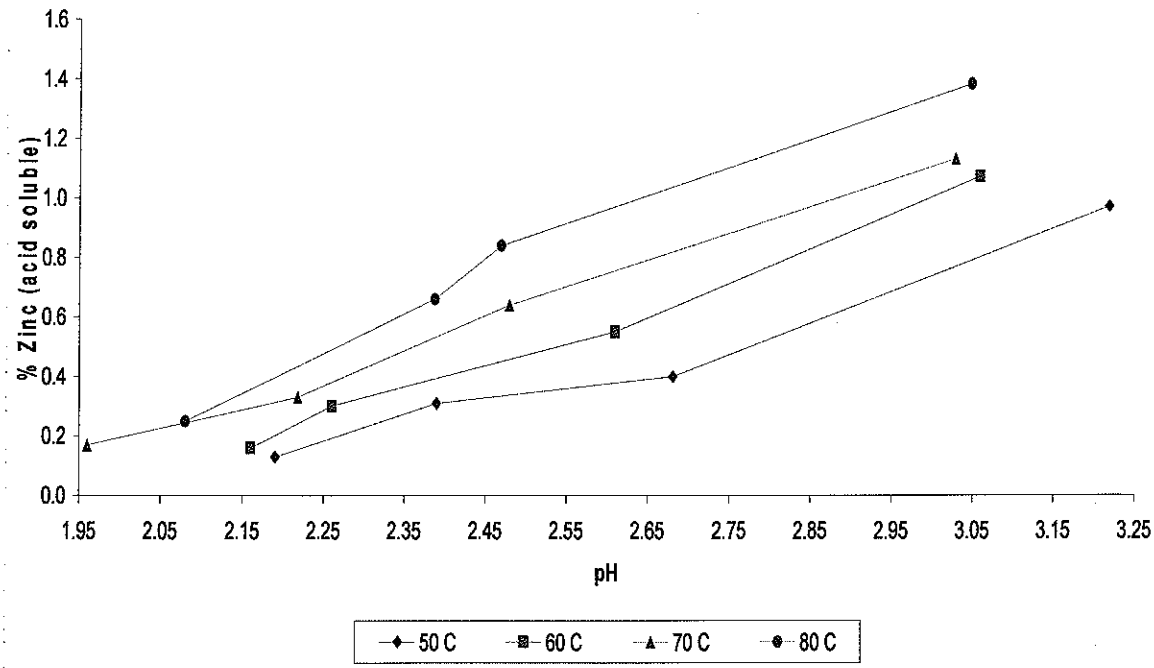

Figure 22. Influence of pH and temperature on the zinc content of iron precipitates produced in a continous crystallizer from a hot iron solution containing 5 g/L H_2SO_4 and 10 g/L Fe (as $Fe_2(SO_4)_3$) using ZnO powder as neutralising agent.

3.4 Conclusions

Control over the factors that influence product quality in crystallization processes is of utmost importance as it affects the economics and ease of handling in down stream processes. It was shown that the type of phase produced and the supersaturation influenced final product quality. Hydrolysis of ferric iron in the temperature range 50°C to 90°C and at pH values between about 1.5 and 3.5, as typically used in many industrial processes, result in the formation of poorly crystalline, metastable iron phases such as ferrihydrite (2-line and 6-line) and schwertmannite. In this study, the stability regions of these phases were determined as a function of easily controllable parameters such as pH and temperature. Typical relative supersaturation levels required for the precipitation of ferrihydrite and schwertmannite were also calculated from data defining the metastable zone for ferric iron hydrolysis. It was shown that ferrihydrite and schwertmannite are formed over a range of supersaturation levels. Since supersaturation determines the rate of the primary crystallization processes, i.e. nucleation and growth, the morphology and product quality of these phases varied with changes in the parameters that influence supersaturation. It also appears as though hydroxy salts, which include schwertmannite, are generally of a better quality as indicated by a higher solids density and lower zinc content than oxy hydroxides, which include ferrihydrite, that were formed at higher relative supersaturation.

The study showed that even though poorly crystalline iron phases, such as schwertmannite and ferrihydrite, were produced, the quality of these phases could be improved by controlling the supersaturation. This could be done through careful selection of control parameters such as pH and temperature and using a stagewise precipitation process.

In addition to the role that pH and temperature play in determining supersaturation, the influence of changes to the mixing environment on supersaturation was studied. In the next chapter, special attention is given to the influence of changes in the macro and micromixing environments, reactor design and feed point location on precipitate product quality.

4. MIXING AND PRECIPITATION

4.1 Introduction

Precipitation of poorly soluble phases such as iron hydroxides is generally associated with fast reaction kinetics resulting in rapid nucleation. High nucleation rates in turn are known to have a detrimental effect on product quality. The product quality can therefore be greatly influenced by mixing efficiency if the process is mixing controlled. The importance of controlling the mixing environment during precipitation processes stems from a difference in the timescales of the various mixing environments (macro-, meso- and micro mixing environments) compared to the timescales of the precipitation processes present in a typical precipitator as summarised in Figure 23.

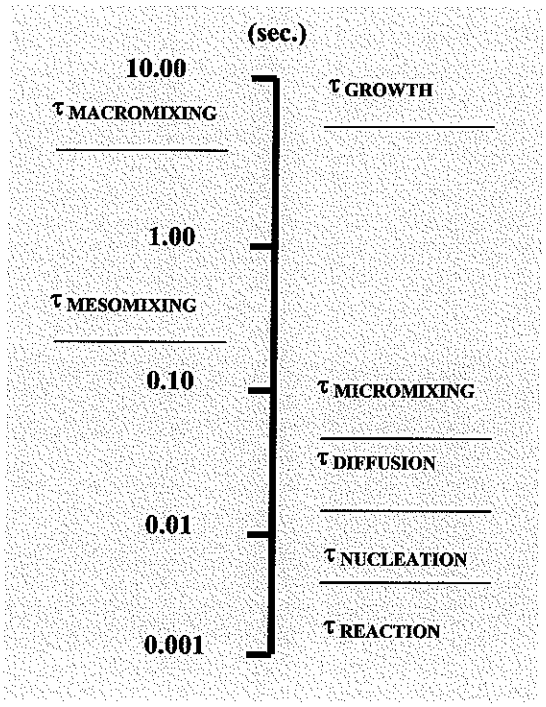

Figure 23. Illustration of the difference between mixing and precipitation (nucleation and growth) time scales [Adapted from Vicum *et al.*, 2004].

In Figure 23 macromixing refers to fluctuations in concentration on the scale of the reactor diameter and the characteristic time for this level of mixing is the reactor circulation time. Mesomixing refers to mixing at the scale of the reactant inlet tubes,

with the tube diameter and the inlet flow rate that influence the mixing time. On the micro scale (vortex scale), micromixing describes the segregation state of a fluid element in terms of its volume and homogeneity. The timescale of micromixing is influenced by the amount of energy dissipated in a system and the properties of the fluid. Since the reaction and nucleation rates in precipitation processes could be orders of magnitude faster than the mixing times, as illustrated in Figure 23, inhomogeneities in species concentration throughout the reactor are expected to occur. This in turn influences the supersaturation, which determines the rates of nucleation and growth. The fact that all the processes shown in Figure 23 occur simultaneously in a precipitator, as well as the difficulties associated with scaling up laboratory scale experiments to plant scale processes, make the study of the mixing environment in precipitation processes and the prediction of the range and distribution of supersaturation relatively difficult.

Different mixing strategies have therefore been investigated in an effort to improve product quality in precipitation processes [Gösele and Kind, 1991; Franke and Mersmann, 1995; Van Leeuwen *et al.*, 1996 (a); Van Leeuwen *et al.*, 1996 (b); Baldyga and Orciuch, 2001]. These and other studies focussed on the influence of the type of process (batch, semi-batch or continuous), location of the feed points, type of mixing (mechanical, jet, etc.), micromixing effects (energy input), mesomixing effects (nozzle design) and macromixing effects (reactor design and type of impeller) on product quality in precipitation processes. Of particular interest is the work done by Gösele and Kind [1991] and later Van Leeuwen *et al.* [1996 (b)] on the so-called three-zone approach for precipitation processes. The three-zone model, illustrated in Figure 24, represents the three main mixing environments found in a mixed reactor, namely the macromixing (pumping action of the impeller/ recirculation time), mesomixing (mixing intensity at the reactant inlets) and micromixing (mixing intensity at the impeller tip/stirring rate) regions.

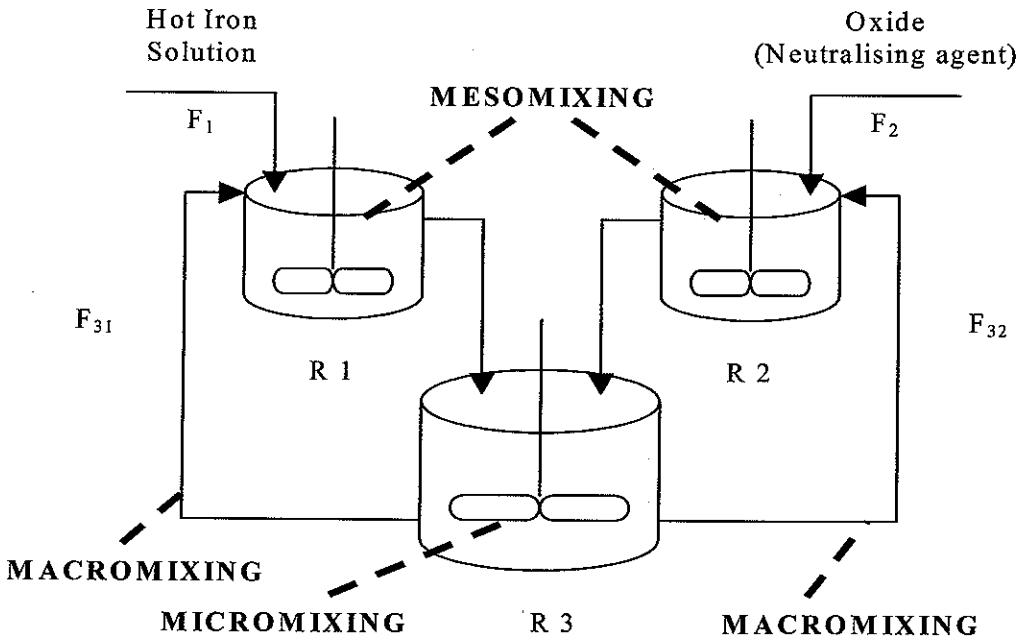

Figure 24. Three-zone model used to study the influence of mixing on iron precipitate product quality [Adapted from Gösele and Kind, 1991].

From Figure 24 it is clear that the influence of the three mixing regimes on product quality can be studied in isolation by varying the recirculation flow rates (F_{31} and F_{32}), the total residence time (mixing time) and the mixing rates in R1, R2 and R3. The three-zone model, as well as different reactor designs and variations in the feed point locations, were used in this study to determine whether the quality of iron precipitates can be improved when the mixing regime is changed. The need to investigate the influence of changes in the mixing environment on iron precipitate quality arise from the fact that it has received relatively little attention compared to the other factors used to control supersaturation during iron precipitation. In the zinc industry, for example, the jarosite process was developed [Patents, 1964; 1965(a); 1965(b)] to produce a crystalline product with the addition of an alkali element at high temperatures and pH values below 2 (refer to Figure 3). These conditions force the supersaturation down as it increases ferric iron solubility. Furthermore, in the goethite iron removal process developed later [Patents, 1966; 1972], supersaturation is effectively controlled by the rate of ferrous iron oxidation using air, which is relatively slow at high temperatures and pH values of around 2.5. But, it is when

ferric iron solution is neutralized at pH values greater than about 3.0, as is the case in the so-called para-goethite process [Loan *et al.*, 2002] and similar Zincor process [Claassen *et al.*, 2002] as well as many other industrial processes, that a more voluminous product containing higher impurity values is produced. If conditions are not well controlled in these processes, a product that is difficult to treat in down stream processes, such as gelatinous precipitates, can be produced, as illustrated earlier in Figure 4. Figure 4 also indicates that crystalline products can be produced from dilute solutions at low relative supersaturation levels. Improved control over the range and distribution of supersaturation during ferric iron precipitation is required in many industrial processes, as the morphology and high impurity content of the products typically produced in this manner, have a detrimental effect on the economics of the operations, as it increases the cost of down stream processes (solid-liquid separation processes and residue storage), and in some cases contributes to the loss of valuable metals [Claassen, 2002].

In this section the influence of changes in the macro, meso and micromixing environments on iron precipitate quality was studied by giving attention to mainly the following areas:

- The mean residence times were calculated from residence time distribution (RTD) data obtained for a CSTR and a draft tube baffled reactor [Fogler, 1999]. This was done to evaluate the impact of changes in the type of impeller, mixing rate, reactor design, feed point location and type of pre-mixer on the mixing efficiency, i.e. to evaluate the influence of changes in the macro and micromixing environments on the residence time of a species. Furthermore, since efficient mixing is required in precipitation systems, as alluded to in previous paragraphs, the use of the mean residence time to indicate optimal mixing conditions were evaluated.
- The three-zone model approach was used to isolate the effect of macro, meso and micromixing on iron precipitate quality.
- The influence of changes in the reactor geometry and feed point location on product quality was studied.

4.2 Experimental

4.2.1 Residence time distribution and the mean residence time

The mean residence times were calculated from the distribution of residence times for a CSTR and a draft tube baffled (DTB) reactor. The dimensions of these reactors are shown in Figures 6 and 25, respectively. 10 mL of a 20% NaCl solution was pulse injected into the inlet to the reactor at the start of each experiment. The change in the NaCl concentration in the outlet of the different reactors evaluated was then measured with a conductivity meter. Each experiment was terminated after 35 minutes. Experiments were conducted in triplicate. The variables and their ranges used to determine the RTD and mean residence times in a CSTR and DTB reactor are summarized in Table 7.

Table 7. Variables and their ranges used to determine the RTD and mean residence times in a CSTR and DTB reactor.

Experiment	Variable	Range		
1	Reactor type	CSTR	____	DTB reactor
2	Stirrer speed (rpm)	200	400	600
3	Type of agitator	Flat, 2-blade	Pitched, 3-blade	Pitched, 4-blade
4	Feed point position	Near the agitator	____	At the solution interface
5	Type of pre-mixer	Y-mixer	____	T-mixer

The pre-mixers used were pipe mixers with an inside diameter of 3mm. The outlets of these mixers were placed near the agitator blades in each experiment.

In all experiments, distilled water was fed at a constant rate of 440mL/min to the CSTR and 435mL/min to the DTB reactor. The water inlet point was placed near the agitator blades. The NaCl used was of CP grade.

For the calculation of the mean residence times, the concentration curve (C(t)) was first constructed from the conductivity measurement data. The accuracy of the data captured was checked by performing a mass balance at the end of each experiment. The residence time distribution function was then calculated using equation 5, followed by equation 6 for the calculation of the mean residence time t_m.

$$E(t) = C(t)/{}_0\int^{\infty} C(t)dt \qquad \ldots.5$$

$$t_m = {}_0\int^{\infty} t \times E(t)dt \qquad \ldots.6$$

The so-called five-point quadrature formula [Fogler, 1999] was used to calculate the areas underneath the concentration and distribution function curves.

4.2.2 Three-zone model approach to improve iron precipitate product quality

The experimental arrangement used in this part of the study is shown in Figure 22. All the reactors (R1-R3) were sealed and baffled vessels. The dimensions of reactor 3 (R3) were shown in Figure 6. In the case of R1 and R2, four 5mm wide baffles were used in each vessel to assist mixing. Reactors with volumes of 600mL, 1000mL, 1500mL and 2500mL were fabricated and used in positions R1 and R2 (refer to Table 8). To determine the influence of the macromixing environment on product quality, a parameter called the Exchange Rate Ratio (Er) was defined as follows (refer to Figure 22):

$$Er = F_{31}/[F_{31} + F_{32}] \qquad \ldots.7$$

In order to eliminate the effects of a change in the total residence time (total mixing time remained constant at about 1 hour) with changes in Er, the volumes of R1 and R2 were changed by means of using different reactor sizes. The levels in R1 and R2 were controlled at preset values with peristaltic pumps. Changes made to the volumes

of these vessels also necessitated adjustments to the energy input (stirring rate) to these reactors to eliminate the effect of changes in the mesomixing environment. The Er was calculated with respect to low and high values of F_{32}. The experimental parameters used to determine the influence of changes in the Exchange Rate Ratio on iron precipitate product quality are summarised in Table 8.

Table 8. Experimental parameters used to determine the influence of solution exchange rates on iron precipitate product quality using the three-zone model approach.

Er	Reactor volume (mL)			Flow (mL/min)				Stirring rate (rpm)		
	R1	R2	R3	F_1	F_2	F_{31}	F_{32}	R1	R2	R3
0	0	0	4010	38.7	28.2	0.0	0.0	0	0	600
0	0	480	4010	38.7	28.2	0.0	7.1	0	210	600
0	0	820	4010	38.7	28.2	0.0	12.7	0	270	600
0	0	1150	4010	38.7	28.2	0.0	18.3	0	310	600
0.15	589	3335	4010	38.7	28.2	9.7	54.8	230	530	600
0.15	202	1140	4010	38.7	28.2	3.2	18.3	180	300	600
0.35	1070	1980	4010	38.7	28.2	17.4	32.3	310	410	600
0.35	610	1140	4010	38.7	28.2	9.9	18.3	240	320	600
0.45	1070	1310	4010	38.7	28.2	17.4	21.3	310	330	600
0.45	920	1140	4010	38.7	28.2	15.0	18.3	280	320	600
0.55	1070	880	4010	38.7	28.2	17.4	14.2	310	280	600
0.55	1370	1140	4010	38.7	28.2	22.4	18.3	330	320	600
1.00	640	0	4010	38.7	28.2	9.7	0.0	240	0	600
1.00	1100	0	4010	38.7	28.2	17.4	0.0	310	0	600
1.00	1450	0	4010	38.7	28.2	23.2	0.0	350	0	600
1.00	2380	0	4010	38.7	28.2	38.7	0.0	440	0	600

In these experiments CP grade ZnO powder was used as neutralising agent. Experiments were also conducted using roasted zinc calcine instead of the CP grade ZnO powder. The zinc content and some of the main impurity values of the calcine used, are shown in Table 9.

Table 9. Chemical composition of the calcine used to precipitate iron using the three-zone model approach.

Zn (%)	Fe (%)	Pb (%)	SiO_2 (%)	Cu (%)	Mn (%)
55.70	5.18	3.00	2.86	1.00	0.92

The calcine used had a d_{50} of about 18μm. It was added as a 15% (mass/mass) slurry prepared with distilled water. 10 g/L initial seed with a d_{50} of about 6μm was also used. The experimental parameters used to determine the influence of changes in the macromixing environment on iron precipitate quality for the case where industrial zinc calcine is used as neutralising agent, is summarized in Table 10.

Table 10. Experimental parameters used to determine the influence of solution exchange rates on iron precipitate product quality using the three-zone model approach and industrial zinc calcine as neutralising agent.

Experiment	Reactor volume (mL)			Flow (mL/min)				Stirring rate (rpm)		
	R1	R2	R3	F_1	F_2	F_{31}	F_{32}	R1	R2	R3
Base case			4010	30.1	38.9					600
HIS recirculation	600		4010	30.1	38.9	13.6		240		600
Calcine slurry recirculation		1150	4010	30.1	38.9		38.9		320	600
HIS and calcine slurry recirculation	600	1150	4010	30.1	38.9	13.6	38.9	240	320	600

The effect of mixing time on iron precipitate product quality was investigated by changing the recirculation flow rates at an Er of 0.5. The mixing time was defined as follows:

$$M_t = Volume_{TOTAL} / [F_{31} + F_{32}] \quad \ldots.8$$

Where: $Volume_{TOTAL} = Vol_{R1} + Vol_{R2} + Vol_{R3}$

The experimental parameters used to determine the influence of changes in the mixing time (macromixing) on iron precipitate product quality are summarised in Table 11.

Table 11. Experimental parameters used to determine the influence of mixing time on iron precipitate product quality using the three-zone model approach.

Mt (min)	Reactor volume (mL)			Flow (mL/min)				Stirring rate (rpm)		
	R1	R2	R3	F_1	F_2	F_{31}	F_{32}	R1	R2	R3
0	350	350	750	7.3	5.3	0	0	200	200	260
3	350	350	750	7.3	5.3	242	242	200	200	260
6	350	350	750	7.3	5.3	121	121	200	200	260
15	350	350	750	7.3	5.3	48	48	200	200	260
30	350	350	750	7.3	5.3	24	24	200	200	260
60	350	350	750	7.3	5.3	12	12	200	200	260

To determine the influence of micromixing on iron precipitate product quality, the agitator speed in reactor 3 (R3) was varied at a fixed Er and Mt. The experimental parameters used to determine the influence of changes in the energy dissipation in R3 on iron precipitate product quality are summarised in Table 12.

Table 12. Experimental parameters used to determine the influence of micromixing on iron precipitate product quality using the three-zone model approach.

Er	Mt (min)	Reactor volume (mL)			Flow (mL/min)				Stirring rate (rpm)		
		R1	R2	R3	F_1	F_2	F_{31}	F_{32}	R1	R2	R3
0.35	6	600	1100	4010	38.7	28.2	9.9	18.3	240	310	200
0.35	6	600	1100	4010	38.7	28.2	9.9	18.3	240	310	400
0.35	6	600	1100	4010	38.7	28.2	9.9	18.3	240	310	600
0.35	6	600	1100	4010	38.7	28.2	9.9	18.3	240	310	800

4.2.3 Influence of reactor design and feed point location on iron precipitate quality

4.2.3.1 Reactor design

The crystallizers used to precipitate iron included an open baffled reactor, shown in Figure 6, a draft tube reactor with dimensions shown in Figure 25, a fluidised bed reactor shown in Figure 26 and a pipe mixer with inside diameter of 5mm in the form of a Y-piece combined (upstream of) with the baffled reactor, shown in Figure 6.

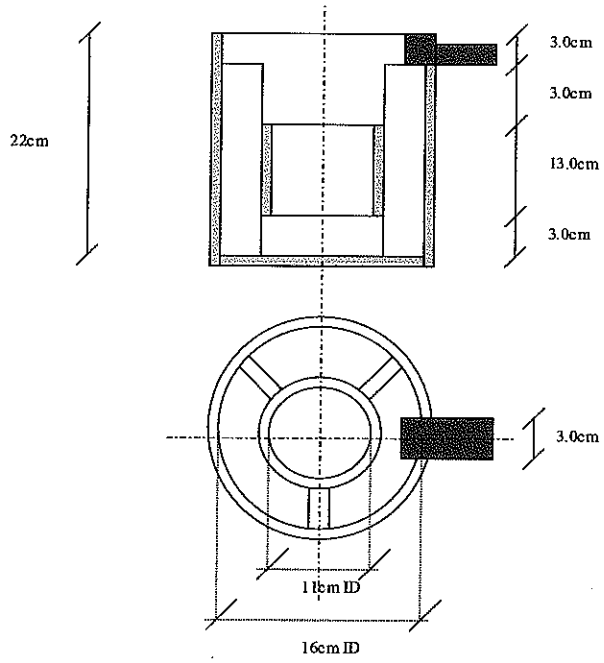

Figure 25. Dimensions of the draft tube reactor used to precipitate iron from a hot iron solution.

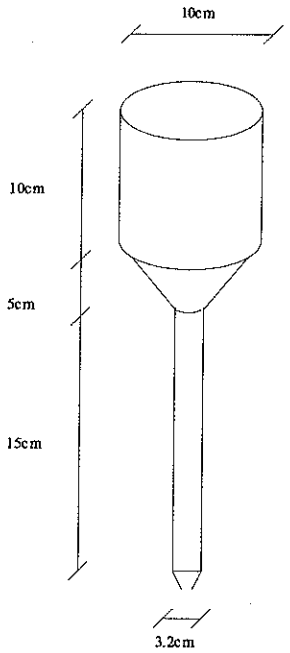

Figure 26. Dimensions of the fluidised bed reactor used to precipitate iron from a hot iron solution.

The experimental parameters used to investigate the influence of reactor design on iron precipitate product quality are summarised in Table 13.

Table 13. Experimental parameters used to determine the influence of reactor design on iron precipitate quality.

Reactor	Active reactor volume (mL)	Flow (mL/min)		Stirring rate (rpm)
		Iron solution	Oxide slurry	
Open baffled	4010	38.2	27.8	400
Draft tube	3970	38.2	27.8	390
Fluidised bed (air agitation)	1300	9.6	7.0	≈3500 mL/min
Pipe - open baffled reactor combination	4020	38.2	27.8	400

In these experiments, the hot iron solution and ZnO slurry feed points were placed on opposite sides of the reactors with the outlets positioned beneath the agitator blades.

4.2.3.2 Role of feed point location

In this part of the study the open baffled (see Figure 6) and draft tube (see Figure 25) reactors were used. The details of the experiments conducted are summarised in Table 14.

Table 14. Experimental parameters used to determine the influence of feed point location on iron precipitate quality.

Reactor	Feed point location	Total reactor volume (mL)	Flows (mL/min)		Stirring rate (rpm)
			Iron solution	Oxide slurry	
Open baffled reactor	Distant, at surface	4010	38.2	27.8	400
Open baffled reactor	Distant, beneath stirrer	4010	38.2	27.8	400
Open baffled reactor	Side by side, at surface	4010	38.2	27.8	400
Open baffled reactor	Side by side, beneath stirrer	4010	38.2	27.8	400
Draft tube reactor	Distant, at surface	3970	38.2	27.8	390
Draft tube reactor	Distant, beneath stirrer	3970	38.2	27.8	390

Note: 'Distant' means diametrically opposed

In all the experiments three-blade marine type impellers were used as mixers. The pH and temperature in reactor 3 (R3) were controlled at 3.2 $\pm$ 0.1 and 60°C $\pm$ 1°C, respectively. Each of the experiments referred to in Tables 8, 11 and 12 was terminated after two hours whereas the rest of the experiments were stopped after one

hour. At the end of each experiment, 250 mL slurry was extracted from reactor 3 (R3). The slurry was filtered in a Buchner funnel with a surface area of 50 cm^2. 10 mL of a 0.1% non-ionic flocculant was added to aid filtration. The filterability of the precipitates was then determined using equation 9.

$$\alpha\eta = (2\ t\ \Delta p\ A)/VH \qquad \ldots.9$$

Where:

$\alpha\eta$	=	specific filter resistance of the filter cake [Pa. $s.m^{-2}$]
t	=	filtration time [s]
Δp	=	differential pressure [Pa]
A	=	filtration area [m^2]
V	=	filtrate volume [m^3]
H	=	filter cake thickness [m]

The filtered solids were dried to determine the moisture content and analysed to obtain the dry solids density, zinc content (water soluble and acid soluble zinc), iron content and the total sulphates present.

The hot iron solutions used were made up with distilled water and contained 5 g/L H_2SO_4 and 10 g/L Fe added as $Fe_2(SO_4)_3$. ZnO powder slurried to a concentration of 5% (mass/mass) with distilled water was used as neutralising agent. Chemicals used were of CP grade.

4.3 Results and discussion

The performance of crystallization processes is dependent on the ability to predict and control the range and distribution of supersaturation. Whereas this is relatively easy to do, for example, in cooling and evaporative crystallisation processes, the same cannot be said for precipitation processes (e.g. for reaction and reductive crystallization). The introduction of reagents with their own chemical and physical properties, especially if solid phase reagent(s) are used, the formation of another poorly soluble solid phase with its own characteristics and the interaction between these phases and their environments contribute, amongst other things, towards the difficulties typically experienced to control and model supersaturation.

In order to improve control over supersaturation in iron precipitation processes, an attempt was made in this study to first of all determine how sensitive iron precipitate product quality is to changes in the mixing environment, and secondly to determine means of improving product quality through focusing on the macro-, meso- and micromixing regimes. Lastly, the influence of changes in the macro and micromixing environments on the mean residence time for two reactor types was also determined, since mixing efficiency is often expressed in terms of the mean residence time.

4.3.1 Three-zone model approach to improve iron precipitate product quality

4.3.1.1 Role of macromixing

As far as the influence of the Exchange Rate Ratio (Er) on precipitate quality is concerned, the influence of ferric iron solution recirculation (Er = 1), oxide recirculation (Er = 0) and a combination of the two (0 > Er < 1) on the specific filter resistance and purity of the precipitate were specifically studied at a fixed mixing time (Mt). Figure 27 shows the effect of neutralizing agent and iron solution recirculation on specific filter resistance. The flow ratios used in these experiments were calculated as follows:

Iron solution recirculation flow ratio = F_{31} / F_1 10

Oxide recirculation flow ratio = F_{32} / F_2 11

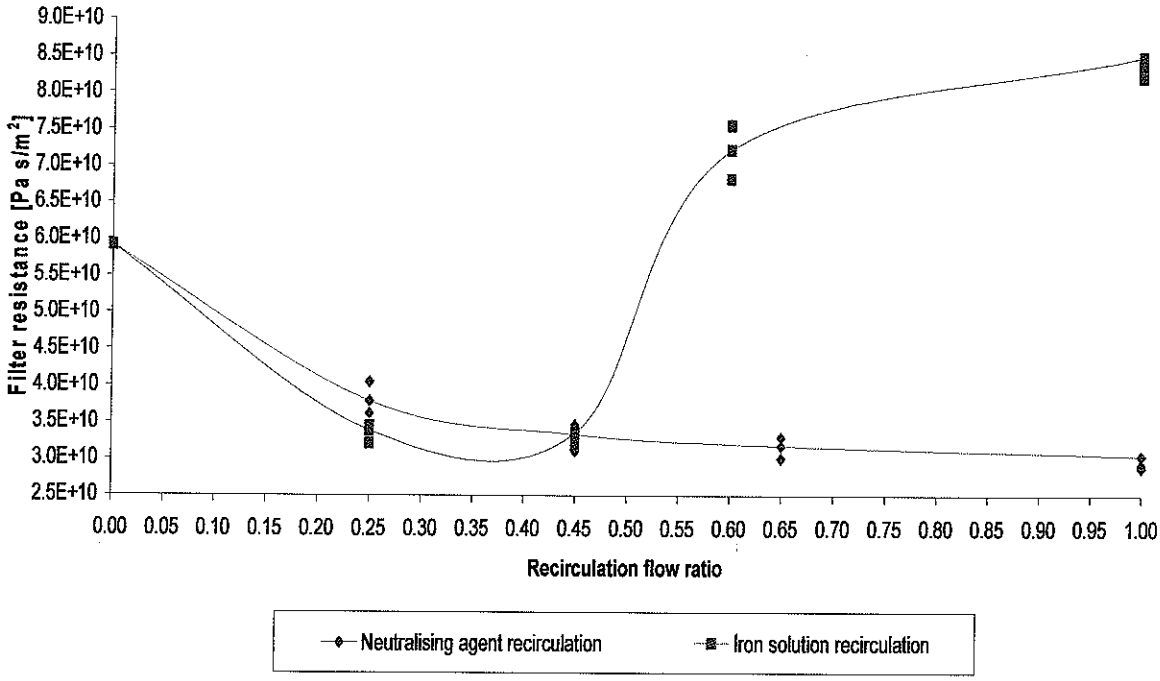

Figure 27. Effect of iron solution and oxide slurry recirculation on specific filter resistance for iron precipitated from an iron solution containing 5 g/L H_2SO_4 and 10 g/L Fe, added as $Fe_2(SO_4)_3$, using a 5% ZnO slurry as neutralising agent.

When the two recirculation flows were combined to give Er values between zero and one, a similar graph than for iron solution recirculation was obtained as illustrated in Figure 28.

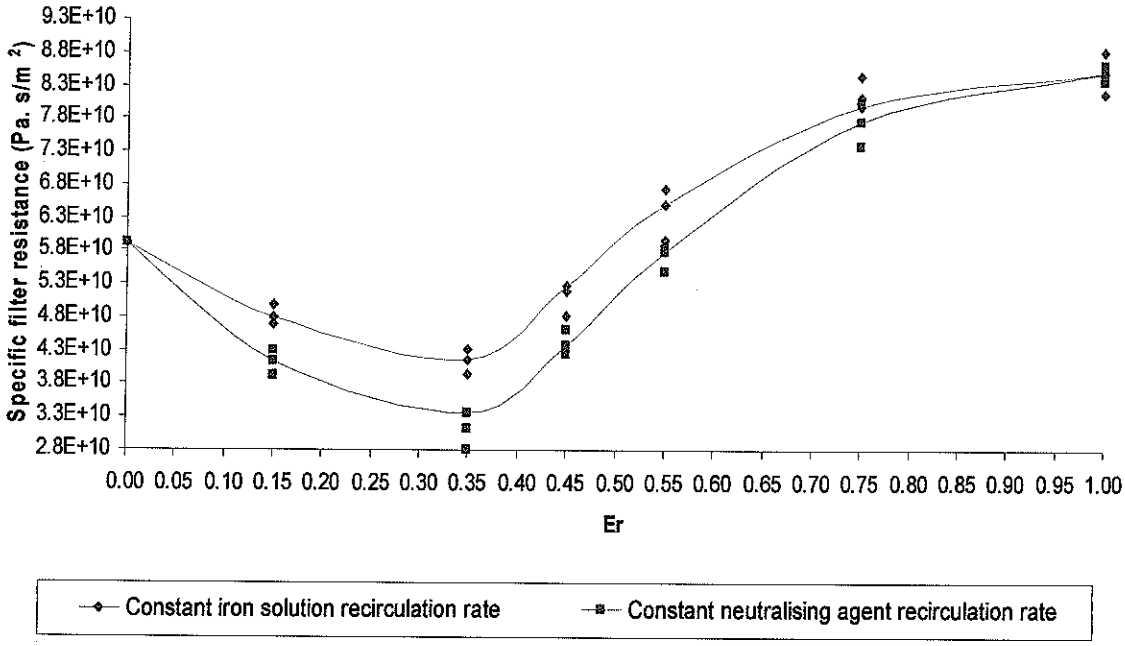

Figure 28. Effect of iron solution and oxide slurry recirculation on specific filter resistance for iron precipitated from an iron solution containing 5 g/L H_2SO_4 and 10 g/L Fe, added as $Fe_2(SO_4)_3$, using a 5% ZnO slurry as neutralising agent.

Figures 27 and 28 indicate that iron precipitate product quality is relatively sensitive towards mass transfer in the inlet regions (inlet regions represented by reactors R1 and R2) as precipitate filterability improved by about 50%. An optimum was achieved at Er values around 0.35. The graphs also indicate that the filterability of the precipitate is more sensitive towards changes in the iron solution recirculation flow rates (cation mass transfer). The reduction in the filter resistance of the material obtained through these experiments was also accompanied by improvements in the purity of the precipitate as shown in Figures 29 and 30.

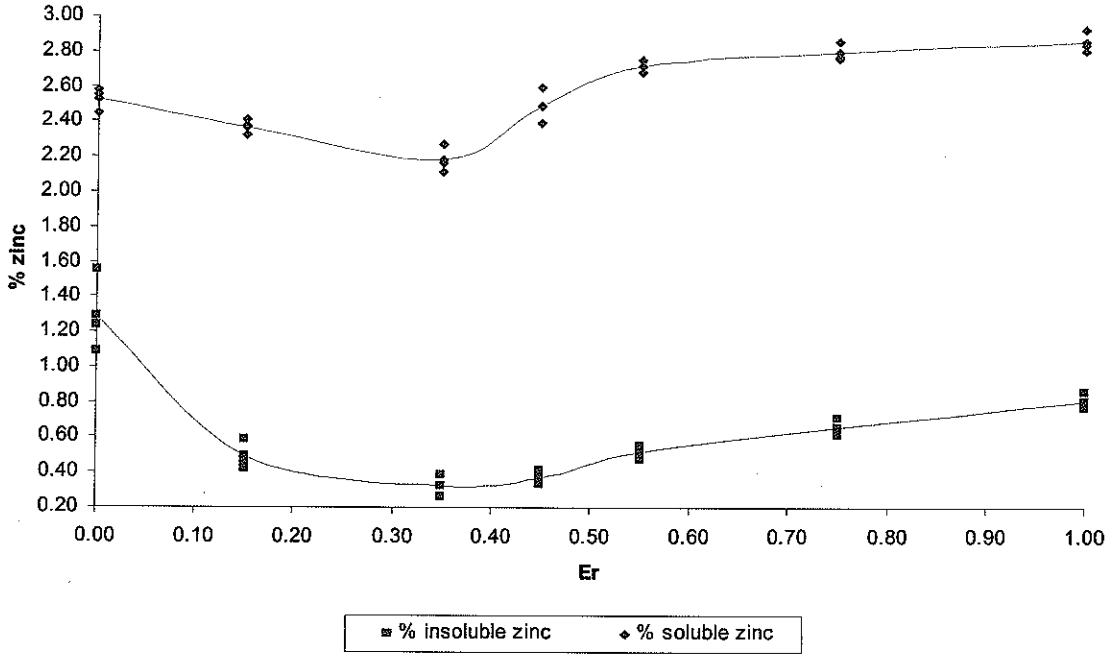

Figure 29. Effect of solution recirculation on the zinc content of iron precipitated from an iron solution containing 5 g/L H_2SO_4 and 10 g/L Fe, added as $Fe_2(SO_4)_3$, using a 5% ZnO slurry as neutralising agent.

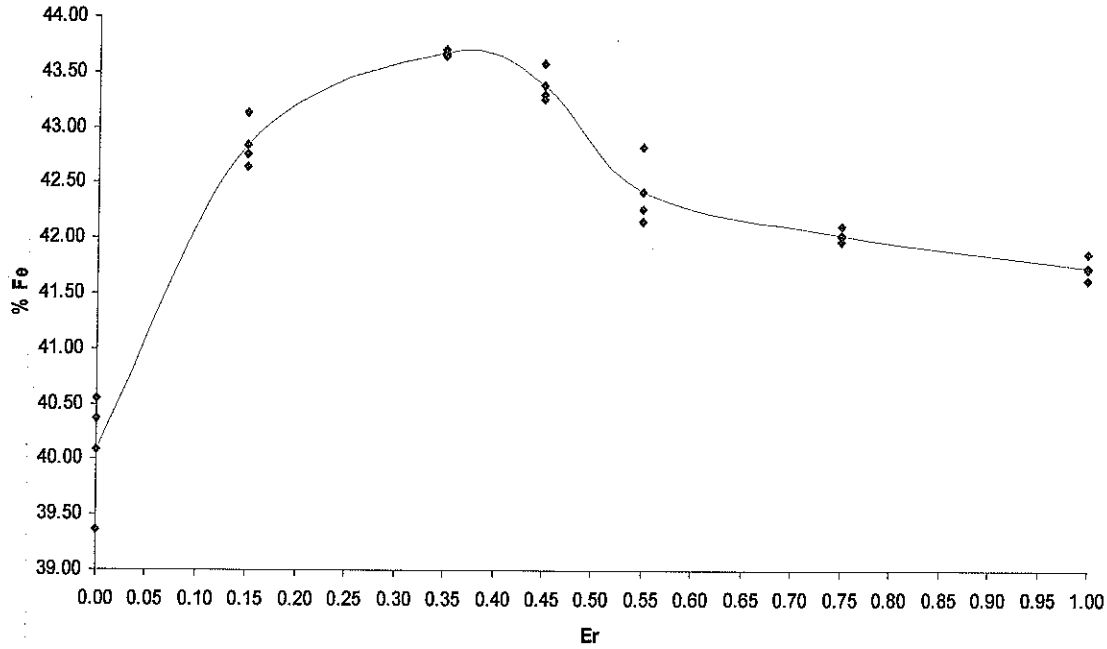

Figure 30. Effect of solution recirculation on the iron content of iron precipitated from an iron solution containing 5 g/L H_2SO_4 and 10 g/L Fe, added as $Fe_2(SO_4)_3$, using a 5% ZnO slurry as neutralising agent.

Figure 29 shows an almost 75% average reduction in the acid soluble zinc concentration (represents entrained $ZnSO_4$ solution and unleached ZnO) and a 14% average reduction in the water soluble zinc content (represents relative surface area of the particulates formed) of the iron precipitated at an Er of about 0.35. The iron content of the precipitate was also raised by almost 9%, as illustrated in Figure 30.

Although the data obtained clearly reflects the importance of effective mixing of the reagent streams with the bulk of the solution in reactor 3, the exact mechanisms involved are not fully understood. From Figure 27 it appears as though recirculation of bulk solution through reactor 2 (R2) resulted in a more dilute environment, which probably led to a reduction in supersaturation in the area around the oxide inlet point in R3. In the case of iron solution recirculation, it is proposed that the positive effect of initial dilution, up to Er values around 0.35, was probably overshadowed by an increase in supersaturation at higher Er levels, due to an increase in the iron concentration in reactor 1, caused by the redissolution of recycled solids in this vessel, which operated at pH values between about 1.45 and 1.80.

For the case where industrial zinc calcine was used as neutralising agent, the reduction in the insoluble zinc loss values was less than indicated in previous paragraphs for CP grade ZnO powder, as shown in Table 15.

Table 15. The effect of applying the three-zone model approach on iron precipitate quality when industrial zinc calcine was used as neutralising agent.

Experiment	Weak acid soluble Zn (%)	Average specific filter resistance (Pa s/m^2)
Base case (no recirculation)	6.85	4.55×10^{10}
HIS recirculation	5.92	3.91×10^{10}
% Improvement	**13.6**	**14.1**
Calcine recirculation	5.08	3.24×10^{10}
% Improvement	**25.8**	**28.8**
HIS and calcine recirculation	5.39	3.54×10^{10}
% Improvement	**21.3**	**22.2**

The lower than expected improvements in the zinc content of the iron precipitates produced using calcine with a d_{50}-value of 18μm, as neutralising agent, could probably be attributed to its lower reactivity, as defined by its mean particle size, compared to the ZnO powder, which had a d_{50}-value of 2μm. A reduction in the mean particle size of the calcine is expected to yield better results. The introduction of more fines, in the form of refractory materials, when calcine is used, could also have contributed to slightly lower filtration rates shown in Table 15 compared to the results shown in Figure 27. Furthermore, the reasons for the lower than expected improvement in the zinc content and filterability of the iron precipitate, in the case where only HIS was circulated ($F_{31}/F_1 \approx 0.45$), is not clear. It is possible that silica gel formation in R1 might have contributed to the slightly lower filterability of the precipitate [Claassen, 2002]. Calcine also contains refractory zinc, in the form of zinc ferrite and zinc silicates (excluding willemite) that cannot be leached at the conditions prevailing in R1. Nonetheless, the improvements of nearly 26% and 29% in the weak

acid soluble zinc value and filterability of the precipitate, respectively, when only the neutralising agent is circulated, is noteworthy as it would significantly reduce water and weak acid soluble zinc losses associated with iron precipitates.

Regarding the influence of the mixing time on precipitate quality, it was found that an increase in mixing time resulted in an improvement in the filterability of the solids formed as shown in Figure 31. The high filter resistance at short mixing times probably resulted from increased nucleation rates that promoted colloid formation, as suggested by Nielsen [1964].

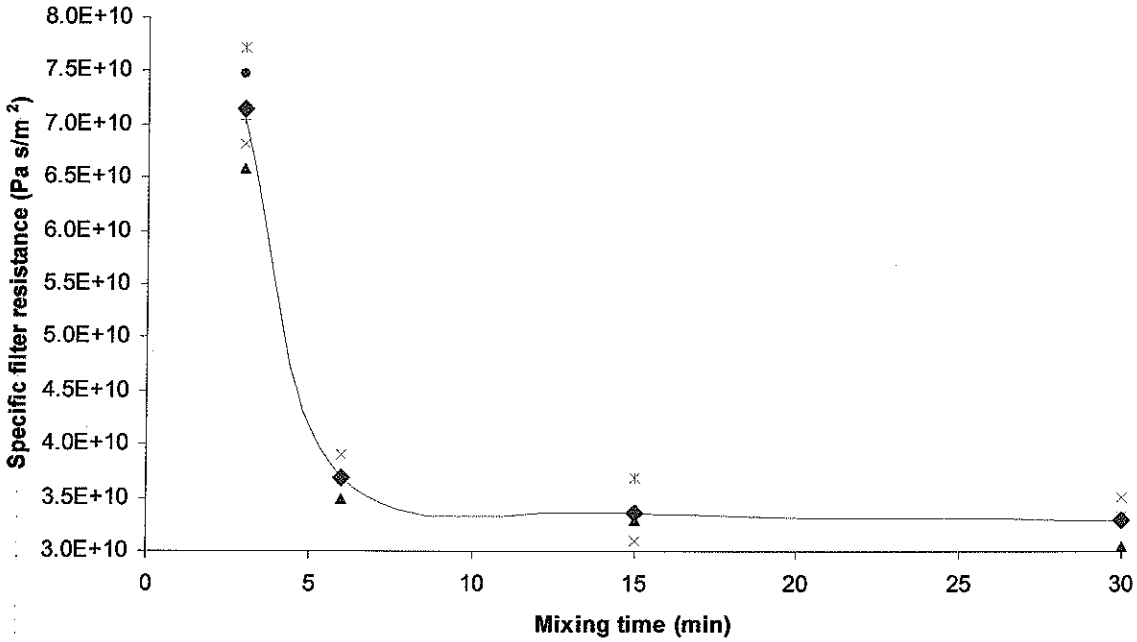

Figure 31. Effect of mixing time on the specific filter resistance of iron precipitated from an iron solution containing 5 g/L H_2SO_4 and 10 g/L Fe, added as $Fe_2(SO_4)_3$, using a 5% ZnO slurry as neutralising agent.

4.3.1.2 Role of mesomixing

Changes in the mesomixing environment (stirring rates in reactors 1 and 2) had very little effect on the final iron precipitate product quality, as supersaturation in R1 and R2 was not altered during the process. The specific filter resistance of solids produced when the mixing rates in R1 and R2 was changed independently from 200rpm to 600rpm, changed by less than 10%.

4.3.1.3 Role of micromixing

Increased micromixing, as indicated by increased stirring in reactor R3, increased the specific filter resistance, as shown in Figure 32. This is probably due to the short micromixing times at the stirrer outlet giving rise to supersaturation peaks causing increased nucleation rates [Franke and Mersmann, 1995]. Higher energy inputs in precipitation systems are also known to break up precipitates due to their relatively low strength.

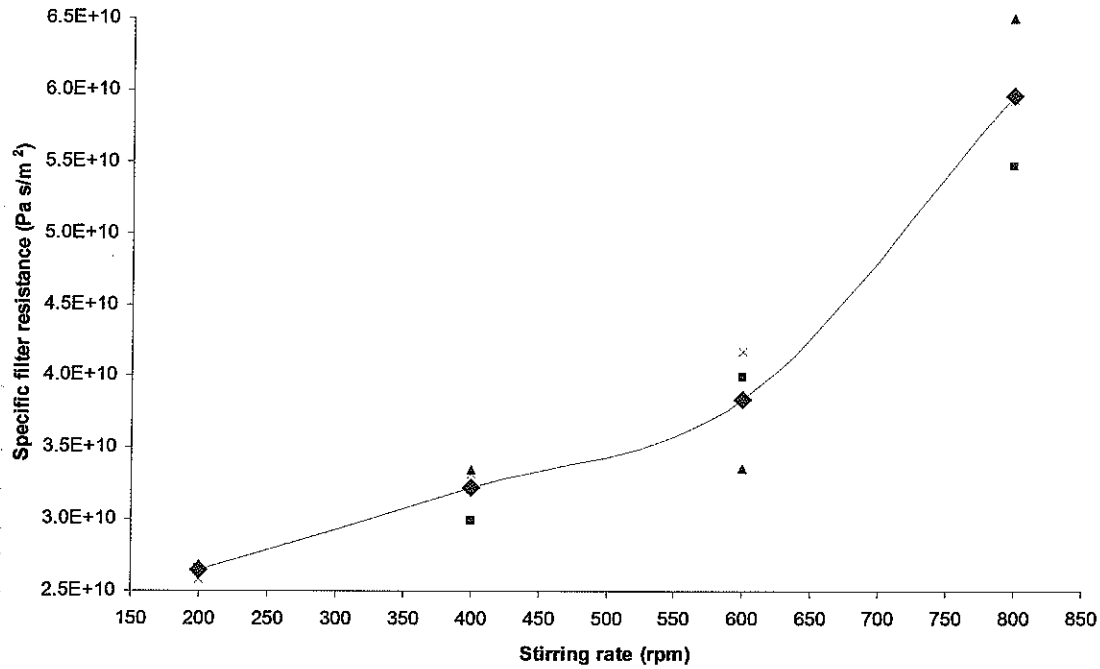

Figure 32. Effect of stirring rate, i.e. micromixing, on specific filter resistance of iron precipitated from an iron solution containing 5 g/L H_2SO_4 and 10 g/L Fe, added as $Fe_2(SO_4)_3$, using a 5% ZnO slurry as neutralising agent.

4.3.2 Influence of reactor design and feed point location on iron precipitate quality

In the case of precipitation processes, the chemical reaction and nucleation take place mainly in the contact zones around the reactant inlet points leading to high local supersaturation. The extent and distribution of supersaturation is influenced by the time it takes to disperse the reactants and blend it over the entire volume of the reactor. This in turn is influenced by, amongst other things, the design of the precipitator and the position of the feed points.

Furthermore, from the above paragraphs it appears as though product quality (specific filter resistance in this case) is more sensitive towards changes in the macro- than the micromixing environment, in the range between 200 and 600rpm, where the influence if macromixing was studied. If this is the case, the influence of reactor type and feed point position on product quality should be considered [Franke and Mersmann, 1995].

4.3.2.1 Role of reactor design

The reactors evaluated included a CSTR, a DTB reactor, a fluidised bed reactor and a pipe reactor. The stirring rate (refer to Table 13) for the mechanically stirred vessels was the same and selected to keep precipitated solids in suspension throughout each experiment. The average specific filter resistance of the solids produced in each of these reactors is summarised in Table 16.

Table 16. Average specific filter resistance of iron precipitates produced in different continuous reactors.

No.	Reactor type	Average specific filter resistance
		(Pa s/m^2)
1	Baffled reactor (CSTR)	3.66×10^{10}
2	Draft tube baffled reactor (DTB reactor)	6.34×10^{10}
3	Fluidised bed reactor	8.99×10^{10}
4	Pipe reactor – baffled reactor combination	1.01×10^{11}

Note: For 1, 2 and 4, reactant inlets beneath impeller. For reactor 3, inlets placed at opposite sides of the reactor at the bottom of the cylindrical section.

From Table 16 it appears as though improved mixing (macromixing) obtained with the DTB reactor (improved circulation flow around the draft tube) and the pipe reactor resulted in higher specific filter resistance values. This was probably due to shorter micromixing times achieved (faster macromixing rates give shorter micromixing times). The compartmentalisation (reduced mixing volumes) of the draft tube reactor and the small mixing volume (less dilution) of the pipe reactor, contributed towards higher nucleation rates and poor filterability. In both these reactors a well-mixed macrofluid was observed. This implies that the reactors were operated in the region of micromixing control. Franke and Mersmann [1995] showed that a macromixing-controlled environment is entered at lower mean specific power input values (lower stirring rates) for a DTB reactor, giving improved product quality (increased particle size). However, the product quality was shown to be sensitive towards feed point location when the mixing environment is macromixing controlled (lower stirring rates). At lower stirring rates solids might start building up in the reactor. If solids build up in a DTB reactor could be controlled and the optimum feed point location is found, a precipitate with superior qualities could probably be

produced. On the other hand, a pipe reactor (T-piece or Y-piece) or specially designed mixing nozzles, should probably only be used in cases where solids are precipitated from very dilute solutions or where the solubility of the solid phase formed is in the g/L range.

The air mixed fluidised bed reactor also gave high filter resistance values, probably due to the presence of a poorly mixed macrofluid, resulting in an inhomogeneous mixing environment with high supersaturation levels and nucleation rates. Adequate dispersal of air in the fluidised bed proved to be essential to improve the filterability of the precipitate produced in this type of reactor. The main benefit of air mixing or jet mixing is that it eliminates the contact between particles and the blades to minimise particle breakage. This type of reactor should therefore be useful when the shear strength of precipitates is lower.

As far as the CSTR (open baffled reactor) is concerned, it appears as though adequate micro- and macromixing times were achieved. This allowed fairly good dilution of the reagents in the bulk, which lowered the supersaturation and nucleation rates. The reactor was therefore probably operated within the transition zone between the macro- and micromixing controlled environments. This type of reactor is the most commonly used reactor in the chemicals and metallurgical industries. It, however, leaves little scope to improve precipitate product quality compared to the DTB and fluidised bed reactors, i.e. limited particle breakage and well-mixed macrofluid conditions could be obtained simultaneously in these reactors, when optimized.

The influence of reactor type on other product quality parameters studied followed the same trend as the specific filter resistance data shown in Table 16. Table 17 indicates the impact that the type of reactor had on iron precipitate purity, mean particle size and dry solids density.

Table 17. Influence of the type of reactor used for iron precipitation on the quality of the final product.

Reactor type	Average sulphate content (%)	Average dry solids density (g/cm^3)	Average mean particle size (μm)
Baffled reactor (CSTR)	9.13	2.91	14.10
Draft tube baffled reactor (DTB reactor)	9.64	2.55	13.58
Fluidised bed reactor	10.04	2.21	9.63
Pipe reactor – baffled reactor combination	14.01	2.03	6.09

From the data presented in Tables 16 and 17, it is clear that the type of reactor used to precipitate iron needs to be considered when the final product quality is of importance. It could also be argued that any change to the mixing environment (impeller dimensions and shape, geometry of the reactor and reactor type) needs to be carefully studied to ensure that it doesn't have a detrimental effect on product quality.

Other factors to consider include the concentration of the element to be removed, the specific energy input (influenced by the shape and size of the mixer), the properties of the precipitate (size and shear strength) and the feed point location. The latter is discussed in more detail in the following paragraphs.

4.3.2.2 Role of feed point location

The influence of feed point location on product quality in CSTR and DTB reactors are summarized in Table 18.

Table 18. Influence of feed point location on iron precipitate quality.

Reactor	Feed point location	Specific filter resistance (Pa s/m^2)	Sulphate content (%)	Dry solids density (g/cm^3)	Mean particle size (μm)
Open baffled reactor	Distant, at surface	4.72×10^{10}	9.81	2.89	13.46
Open baffled reactor	Distant, beneath stirrer	3.66×10^{10}	9.13	2.91	14.10
Open baffled reactor	Side by side, at surface	6.20×10^{10}	10.54	2.22	12.15
Open baffled reactor	Side by side, beneath stirrer	5.25×10^{10}	10.04	2.35	12.79
Draft tube reactor	Distant, at surface	6.84×10^{10}	9.70	2.51	13.16
Draft tube reactor	Distant, beneath stirrer	6.34×10^{10}	9.64	2.55	13.58

Note: 'At surface' means just above the solution interface; 'distant' means on the opposite side of the reactor

The data in Table 18 indicates that improved product quality is achieved when the feed points are placed on opposite sides of the reactor and near the agitator blades. Product quality in the DTB reactor is less sensitive towards feed point location because the micromixing process controls the precipitation process with a bigger

difference expected at lower energy inputs. The CSTR is more sensitive towards feed point location indicating that the process is macromixing controlled as discussed earlier. More dilution is achieved when the inlet points are placed far away from each other and near the impeller. Mixing would probably have been better with the inlets placed below the solution surface compared to just above the solution interface, where dilution takes longer to occur.

4.3.3 Residence time distribution and mean residence time

In paragraphs 4.3.1 and 4.3.2 it was shown that iron precipitate quality is sensitive towards changes mainly in the macro and micromixing environments, as the precipitation process is mixing controlled. Optimal mixing conditions for every application therefore needs to be found, i.e. for new and existing equipment where precipitation is mixing controlled. One way of doing this is through the determination of the distribution of residence times for different reactors, mixing rates, impeller types and feed point location. The mean residence times obtained for these scenarios are summarized in Table 19.

Table 19. Average mean residence times calculated for different mixing regimes using residence time distribution data.

Experiment	Variable	Mean residence time (seconds)	
		CSTR	DTB reactor
1	Reactor type	471	463
2	Stirrer speed (rpm)		
	200	458	453
	400	465	459
	600	471	463
3	Type of agitator		
	Flat 2-blade	453	449
	Pitched 3-blade	456	450
	Pitched 4-blade	461	452
4	Feed point position		
	At the solution interface	465	459
	At the agitator blades	461	452
5	Type of pre-mixer		
	Y-mixer	458	445
	T-mixer	456	444

difference expected at lower energy inputs. The CSTR is more sensitive towards feed point location indicating that the process is macromixing controlled as discussed earlier. More dilution is achieved when the inlet points are placed far away from each other and near the impeller. Mixing would probably have been better with the inlets placed below the solution surface compared to just above the solution interface, where dilution takes longer to occur.

4.3.3 Residence time distribution and mean residence time

In paragraphs 4.3.1 and 4.3.2 it was shown that iron precipitate quality is sensitive towards changes mainly in the macro and micromixing environments, as the precipitation process is mixing controlled. Optimal mixing conditions for every application therefore needs to be found, i.e. for new and existing equipment where precipitation is mixing controlled. One way of doing this is through the determination of the distribution of residence times for different reactors, mixing rates, impeller types and feed point location. The mean residence times obtained for these scenarios are summarized in Table 19.

Table 19. Average mean residence times calculated for different mixing regimes using residence time distribution data.

Experiment	Variable	Mean residence time (seconds)	
		CSTR	DTB reactor
1	Reactor type	471	463
2	Stirrer speed (rpm)		
	200	458	453
	400	465	459
	600	471	463
3	Type of agitator		
	Flat 2-blade	453	449
	Pitched 3-blade	456	450
	Pitched 4-blade	461	452
4	Feed point position		
	At the solution interface	465	459
	At the agitator blades	461	452
5	Type of pre-mixer		
	Y-mixer	458	445
	T-mixer	456	444

From Table 19 it is evident that, for the range of the different variables chosen, the changes in the macro and micromixing environments had little effect on the mean residence times. This confirms that:

- Mixing efficiency expressed in terms of the mean residence time cannot be used as an indicator of the influence of changes in the macro and micromixing environments on product quality.
- The use of the mean residence time is probably limited to specifying total residence time/reactor volume required to allow particle growth in a precipitation system, since the chemical reaction and nucleation requires very little time to take place.
- The localized supersaturation, as determined by chemical and physical variables, has the biggest impact on product quality.
- It is better to use parameters, such as the filterability and purity of the precipitate, to evaluate the influence of changes in the mixing environment on product quality, as illustrated in previous paragraphs.

4.4 Conclusions

The study showed that iron precipitate product quality is sensitive to changes in the mixing environment. Of specific importance are changes in the micro- and macromixing environments. The three-zone model approach was used to separate the effects of macro- and micromixing on precipitate quality. It was shown that product quality was more sensitive to changes in the macromixing regime. Data obtained suggested that optimum product quality, expressed in terms of the specific filter resistance and solids purity, could be achieved at Er values around 0.35. The specific filter resistance of the solids was improved by about 50%, and the zinc content of the iron precipitates was reduced by about 75% and 14% for acid- and water soluble zinc, respectively. The results also showed that product quality is more sensitive to cation (iron in solution) mass transfer than to the mass transfer of the neutralizing agent in the region of the inlet points. In the case where zinc calcine was used as a neutralising agent, improvements of about 26% and 29% for weak acid soluble zinc losses and the filterability, respectively, were achieved. The smaller improvements were probably a

result of the presence of refractory zinc in the calcine, silica gel formation and the introduction of more fines into the system.

As far as the influence of mixing time was concerned, it appears as though mixing times smaller than about 5 minutes should be avoided as it induced high supersaturation levels and fast nucleation rates.

Furthermore, when product quality is more sensitive to changes in the macro- than the micromixing environment, the influence of reactor type and feed point position on product quality should also be considered. It was shown that the best results were achieved using a CSTR. The DTB reactor, however, is expected to produce precipitates with superior quality when optimised. The study also indicated that feed points should be placed as far as possible from each other and in a position that gives adequate micro- and macro mixed fluids. The controlling mixing environment (micro- or macromixing controlled) generally indicates where feed points should be located. In a well-mixed macrofluid (DTB reactor), feed points could be placed far away from the impeller. When the macromixing environment is, however, less homogeneous (CSTR), better results were obtained with the feed points placed closer to the impeller.

The changes in the micro and macromixing environments, as discussed in this section, had little impact on the mean residence times calculated from residence time distribution data, obtained for the CSTR and DTB reactor. It is therefore recommended that parameters such as the filterability and purity of precipitates are rather used to indicate the influence of changes in the mixing environment on precipitate product quality. Due to the sensitivity of product quality towards the mixing environment, a proper understanding of the precipitation system is required before changes are made to the mixing system, reactor geometry and feed point locations.

Whereas the aim of this chapter was to ensure the production of good quality nuclei by controlling supersaturation through changes in the mixing environment, the following section focuses on growing these nuclei into particles with a relatively low surface area and good liquid-solid separation properties.

5. AGGLOMERATION

5.1 Introduction

Precipitation processes are characterized by high supersaturation levels and fast nucleation rates. If it is assumed that the range and distribution of supersaturation in a crystallizer is controlled reasonably well, dense nuclei with a relatively low surface area can be formed. However, even good quality nuclei formed in a well-controlled environment are usually less than one micron in diameter. Unless these nuclei are allowed to grow, downstream processing of precipitates, such as liquid-solid separation and storage, could be difficult and costly. Low solute concentrations typically required for the formation of relatively insoluble phases during precipitation processes, however, do not support the desired molecular growth rates required to make these processes viable. Particle growth in precipitation systems rather takes place through agglomeration, as indicated in Table 20.

Table 20. Different nucleation and growth mechanisms encountered in crystallization and precipitation processes [After Dirksen and Ring, 1991].

Initial Supersaturation	Colloid stability	Nucleation	Atomistic growth	Morphology
1-2	High	None	None	____
	Low	Heterogeneous	Slow, predominantly screw dislocation	Discrete well-formed crystals, no agglomeration
2-5	High	Heterogeneous	Slow, predominantly surface nucleation	Discrete well-formed crystals, no agglomeration
	Low	Heterogeneous	Dendritic	Poorly formed or dendritic crystals, no agglomeration
10-50	High	Heterogeneous	Dendritic	Poorly formed or dendritic crystals, no agglomeration
	Low	Homogeneous	Diffusion-limited	Colloid stability dependent, agglomerated
>1000	High	Homogeneous	Diffusion-limited	Colloid stability dependent, agglomerated

In precipitation processes, agglomeration growth (the process where stable nuclei and clusters are cemented together by isomorphic material) occurs at a much faster rate than molecular growth. Nuclei could grow to particulates as big as 100μm in diameter within a reasonable time period (< 5 hours). Even though agglomeration growth makes down stream processing in most precipitation processes possible, it generally results in the formation of particles with a high relative surface area and high impurity values. Optimisation in terms of product quality improvement of the agglomeration growth process is therefore required. In order to improve precipitate product quality, a good understanding of the impact of the different parameters on agglomeration is required. When agglomeration growth is broken down in stages, the various factors that influence the process become clearer. The three main steps include the following:

- Particles collide as a result of their properties and the hydrodynamic environment. This step is governed by the probability of collisions and/or the collision frequency.
- Next, the particles need to stay together for a period of time to allow interparticle bridges to be formed; this is influenced by interparticle forces/interactions.
- A step of consolidation where nuclei, clusters and particulates are cemented together through molecular growth.

Considering these steps, it follows that the properties of the particles, interparticle forces, fluid dynamics and properties of the solution might influence the agglomeration process and therefore the quality of the final product. It was found [Dirksen and Ring, 1991] that interparticle forces were affected by the addition of adsorptives, with agglomeration favoured by the addition of hydrophobic adsorptives. In terms of the effect of solution variables, it was also shown that agglomeration was generally supported by high temperature, high diffusivity, small particles, high particle number density, low viscosity, high supersaturation and strong bonding forces. The impact of changes in the hydrodynamic environment proved to be more complex, as the above-mentioned factors could promote agglomeration up to a point, after which disruption prevents agglomeration.

In industrial environments, however, not all these parameters are easily controllable. Furthermore, the quality of the solution to be treated is influenced by concentrate composition and the efficiency of upstream processes, which typically could vary considerably with time. A better understanding of the effect of easily controllable operating parameters such as pH, temperature, solute concentration, recycling of seed material and stirring rate on agglomeration would be useful. In addition, since it is not expected that all these parameters have an equally important role to play in the agglomeration process, their relative importance also need to be determined. This would enable the engineer and operator to focus on the specific variables that have the biggest influence on growth and final product quality.

In this study, the effect of the above-mentioned easily controllable operating parameters and their relative importance on the agglomeration of metastable iron phases such as ferrihydrite and schwertmannite were investigated. Since, most iron phases are relatively stable (poorly soluble), high relative supersaturation levels are encountered in iron precipitation processes, as indicated earlier. The high supersaturation levels in turn support agglomeration growth in these processes as indicated in Table 20. In a study of the Zincor iron removal process, Claassen [2002] identified the presence of agglomerates in the final precipitate as shown in Figure 33.

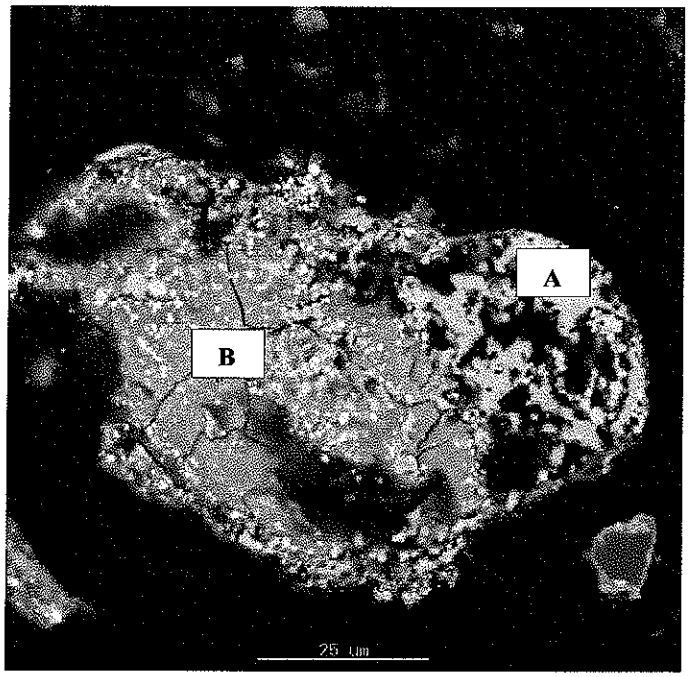

Figure 33. SEM image of agglomerated iron particles A (ferrihydrite) and B (schwertmannite) found in an industrial iron residue produced in the Zincor iron removal process. It also appears as though particle B consists of agglomerated primary particles and clusters of primary particles [Claassen, 2002].

The agglomerated particles, shown in Figure 33, also supports the point previously raised, that even though agglomeration growth gives precipitates that could be effectively handled in down stream processes, an increase in the relative surface area of the particles usually result in increased losses of valuable metals, such as zinc. An attempt was therefore made in this study to find means to reduce the zinc losses associated with metastable iron phases present in many iron residues in the zinc industry.

5.2 Materials and methods

In an earlier investigation into the factors that influence the filterability of metastable iron phases, Claassen *et al.* [2003(a)] showed that pH, temperature and seed addition had a positive impact on the growth rate as well as the final particle size. For reasons highlighted in previous paragraphs, it was decided to also determine the relative importance of these and other operating parameters on agglomeration. The relative

importance of the variables was studied using an algorithm, the so-called Hadamard matrix [Seyssiecq *et al*, 1998], combined with product quality parameters, such as the specific filter resistance and the degree of agglomeration, as characterized by the change in particle population density. Lastly, the specific influence of seed material on product quality parameters, such as the filterability, final particle size and precipitate purity, was studied in more detail.

5.2.1 Experimental setup and procedures

A continuous reactor with four baffles and a riser box was used in all experiments. The dimensions of the reactor are shown in Figure 6.

A hot iron solution made up with distilled water, $Fe_2(SO_4)_3$ and 5 g/L H_2SO_4 was continuously fed to the reactor in order to maintain a constant supersaturation level at a given set of conditions, details of which are shown in Table 21. The iron was precipitated with ZnO powder slurried to a consistency of 2.5% (mass/mass) using distilled water. The chemicals used were of CP grade. Both the reactant streams were fed at a rate of approximately 33 $\pm$ 4mL/min to the reactor. The outlet points of both streams were positioned just underneath the agitator blades on opposite sides of the reactor. Each experiment was terminated after one hour. At the end of each experiment, 250 mL slurry was extracted from the reactor. The slurry was filtered in a Buchner funnel with a surface area of 50 cm^2. 5 mL of a 0.1% non-ionic flocculant was added to aid filtration. The filtered solids were dried at 120°C for one hour to determine the moisture content and analysed to obtain the zinc content, as water soluble and acid soluble zinc, and the total sulphates present.

Samples of 10 mL each were also taken from the reactor at the beginning and end of each experiment to determine particle size and size distribution using the Malvern Mastersizer particle analyzer.

The experimental setup and procedures followed to determine the influence of pH and temperature on the degree of agglomeration were discussed elsewhere [Claassen *et al*., 2003(a)].

5.2.2 Relative importance of the operating variables

A Hadamard matrix was used to determine the relative importance of each operating parameter on the agglomeration process. A Hadamard matrix is a n × n matrix with all the elements presented as +1 or –1. The first row and column can be arranged in such a manner that their elements are all +1. The matrix only exists if n = 2 or if n is divisible by 4. Furthermore, all parameters used in the matrix need to be independent from each other. The properties and uses of a Hadamard matrix are discussed in detail by Raghavarao [1971].

For the purpose of this study, the use and benefits of using a Hadamard matrix could be explained as follows. If the regression model is expressed as:

$$E(y) = \mathbf{X}b \qquad \ldots.12$$

where the elements of y are values determined in the experiments, such as specific filter resistance, iron removal efficiency and the degree of agglomeration in this case, and the columns of **X** are the values of the chosen operating parameters, then:

$$b = (\mathbf{X'X})^{-1}\,\mathbf{X'}y \qquad \ldots.13$$

The number of experiments could now be limited if only two points, a minimum and maximum value for example, for each parameter (covariate) is used; covariates are referred to as parameters and *b* is called the vector of parameters. These covariates are then included in the regression model as +1 and –1, the maximum and minimum values respectively. This causes the size of the regression coefficient to be half of the total possible influence of a covariate on y. Therefore, the +1 and –1 choice of covariates give a 2^n - factorial model, with observations only made at specific points, e.g. for 6 parameters, 8 observations or experiments are required instead of $2^6 = 64$ observations or experiments. Therefore, the number of experiments could be limited to a minimum without much influence on the statistical accuracy of the data, if a Hadamard matrix is used to determine the relative influence of parameters. In this study the relative influence of six parameters on agglomeration was determined. The

parameters and their values are summarised in Table 21. Most of the boundaries chosen for the different parameters are typical of the Zincor iron removal process and other industrial environments where iron is precipitated in the form of ferrihydrite and schwertmannite.

Table 21. Parameters and their values used to determine their relative influence on the agglomeration of metastable iron phases.

Parameter	Minimum value	Maximum value
pH	2.6	3.2
Temperature	45°C	65°C
Stirring rate	400 rpm	600 rpm
Hot iron solution iron concentration, C_{Fe}	5 g/L	15 g/L
Mass of seed	10 g/L	100 g/L
Hot iron solution Zn concentration, C_{Zn}	0 g/L	80 g/L

For six parameters/covariates, the Hadamard matrix in the +1, –1 notation is presented in Table 22.

Table 22. Hadamard matrix of the parameters evaluated.

Experiment	pH	Temperature	Stirring rate	C_{Fe}	Seed mass	C_{Zn}
1	–	–	–	+	+	+
2	+	–	–	–	–	+
3	–	+	+	–	+	–
4	+	+	+	+	–	–
5	–	–	–	+	–	–
6	+	–	–	–	+	–
7	–	+	+	–	–	+
8	+	+	+	+	+	+

In Table 22 the (+) symbol corresponded to maximum values listed for each parameter in Table 21 and the (−) symbol was associated with the lower limit as mentioned earlier. The results, e.g. the specific filter resistance values K to R, obtained from the eight experiments were then used to solve equation 14 for each parameter as follows:

$$b_{pH} = (-K + L - M + N - O + P - Q + R)/8 \quad \ldots.14$$

The values obtained for the different parameters were then compared with each other and ranked, i.e. the parameters are viewed as objects that are weighted. The value with the highest weight then indicated which parameter had the biggest influence on the agglomeration process for the specific product quality parameter, such as the filter resistance, iron removal efficiency or degree of agglomeration, evaluated.

In terms of the filterability of the precipitates, the specific filter resistance of the solids produced was again calculated using equation 9.

The degree of agglomeration for each experiment, as indicated by the relative reduction in the number of particles present, was calculated from the particle number density data obtained from the Malvern particle analyses (refer to Appendix 3). The number density was calculated at t_0 (N_0) and t_{1hr} (N_{1hr}). The degree of agglomeration was then calculated as follows:

$$\text{Degree of agglomeration} = [1 - (N_{1hr}/N_0)] \times 100 \quad \ldots.15$$

5.2.3 Influence of seed mass and seed size

The influence of changes in the initial seed mass and mean seed size on agglomeration was investigated with all the other parameters fixed at pre-determined values. The experimental conditions used to study the influence of seed mass and size on the agglomeration degree, final particle size, specific filter resistance and solid purity are summarised in Tables 23 and 24, respectively. Enough seed material was

prepared to perform the experiments in triplicate. The seed material was produced using the experimental setup shown in Figure 6 and the procedure described in section 3.2.3. The pH and temperature during the experiment were maintained at 3.0 and 60°C, respectively (refer to section 3 for chemical composition of the seed).The seed material was dried, milled and properly mixed. The mean particle size of the seed was 5.04 μm, as determined using the Malvern Mastersizer. The full particle size distribution of the seed is shown in Appendix 1.

Table 23. Experimental conditions used to evaluate changes in the initial seed mass on precipitate product quality.

No.	pH	Temperature (°C)	Stirring rate (rpm)	C_{Fe} (g/L)	Seed mass (g/L)	C_{Zn} (g/L)
1	3.2	65	600	10	10	0
2	3.2	65	600	10	25	0
3	3.2	65	600	10	50	0
4	3.2	65	600	10	100	0
5	3.2	65	600	10	150	0

Table 24. Experimental conditions used to evaluate changes in the initial seed size on precipitate product quality.

No.	pH	Temperature (°C)	Stirring rate (rpm)	C_{Fe} (g/L)	Seed size (μm)	C_{Zn} (g/L)
1	3.2	65	600	10	2.2	80
2	3.2	65	600	10	5.3	80
3	3.2	65	600	10	6.8	80
4	3.2	65	600	10	12.4	80

The seed particles used to evaluate the effect of the seed size were prepared by milling four parts of a batch of seed, separately for different times, to give the mean seed sizes indicated in Table 24. An initial seed concentration of 50g/L was used in each experiment.

5.3 Results and discussion

The results obtained from the experimental trials using the conditions listed in Table 21 together with their Hadamard arrangement are summarised in Table 25.

Table 25. Precipitate characteristics obtained for the operating variables indicated.

No.	pH	Temp. (°C)	Stirring rate (rpm)	C_{Fe} (g/L)	Seed mass (μm)	Zn conc. (g/L)	Filter resistance ($Pa.s.m^{-2}$)	Fe removal efficiency (%)	Degree of agglomeration (%)
1	2.6	45	400	15	100	80	4.80×10^{11}	92.81	60.9
2	3.2	45	400	5	10	80	4.09×10^{11}	99.77	-69.9
3	2.6	65	400	5	100	0	5.04×10^{10}	98.71	62.1
4	3.2	65	400	15	10	0	5.34×10^{10}	99.98	-40.9
5	2.6	45	600	15	10	0	2.47×10^{11}	95.82	-137.4
6	3.2	45	600	5	100	0	6.46×10^{10}	99.87	37.6
7	2.6	65	600	5	10	80	1.20×10^{12}	93.32	-6.7
8	3.2	65	600	15	100	80	5.67×10^{10}	99.98	67.5

The vector (b) of each variable was calculated from the results shown in Table 25 according to equation 11 and ranked. The outcome of this exercise is presented in Table 26.

Table 26. Relative importance of the different operating parameters evaluated.

Parameter	Specific filter resistance		Fe removal efficiency		Degree of agglomeration	
	b-value	Order of importance	b-value	Order of importance	b-value	Order of importance
pH	-1.74×10^{11}	1	1.34	1	1.92	4
Temperature	1.97×10^{10}	4	-0.30	3	23.85	2
Stirring rate	7.16×10^{10}	5	-48.62	6	-6.41	5
Hot iron solution iron concentration	-1.11×10^{11}	3	0.33	2	-9.13	6
Mass of seed	-1.57×10^{11}	2	-1.34	4	60.38	1

Precipitation processes are generally only used in industrial processes if the liquid-solid separation step(s) can be performed economically. Furthermore, precipitation is utilised as a purification or concentration step and the efficiency of such an operation is of utmost importance. Specific attention is therefore given to the specific filter resistance and iron removal efficiency in the discussions that follows. Since the degree of agglomeration strongly influences the filterability of iron residues, the factors that impact on this process are also discussed. Emphasis is put on the relative influence of the operating parameters on the precipitation of metastable iron phases.

From Table 26 it is evident that pH, seed concentration, iron solution iron concentration and temperature have the biggest effect on filterability and iron removal efficiency. In terms of the degree of agglomeration the seed concentration, temperature and pH together with a significant change in solution viscosity (change in solution zinc concentration) need to be considered to optimise the agglomeration step. Overall, pH is the most important parameter, followed by the seed concentration, temperature and iron solution iron concentration. This outcome implies that:

- Every effort needs to be made to improve pH control in iron precipitation processes. The impact of pH on iron precipitate quality should also be seen in light of the relative small pH window of 2.6 to 3.2 that was evaluated, i.e. a small change in pH in this range could have a significant effect on agglomeration, iron removal efficiency, the filterability and purity of the precipitate.
- Seed addition is essential to ensure good quality iron precipitates. However, it is often not considered or neglected in industrial processes. In this study, special attention is given to the utilisation of seed to improve iron precipitate quality.
- Adequate dilution is required in iron precipitation processes to improve the efficiency of the step.
- Changes in the physico-chemical parameters were of greater importance than changes in the hydrodynamic environment for the range of each operating parameter explored.

The fundamental reasons why these variables influence agglomeration, filterability of the precipitate and the iron removal efficiency are discussed in the following paragraphs.

5.3.1 Influence of the operating pH, temperature and solution iron concentration

The influence of pH and temperature on the degree of agglomeration is shown in Figures 34 and 35, respectively, indicating that agglomeration is optimum at a pH around 3.0 and increases significantly up to temperatures around 60°C. These results are in good agreement with earlier work [Claassen *et al.*, 2003(a)], which showed the same trends for the filterability of iron precipitates.

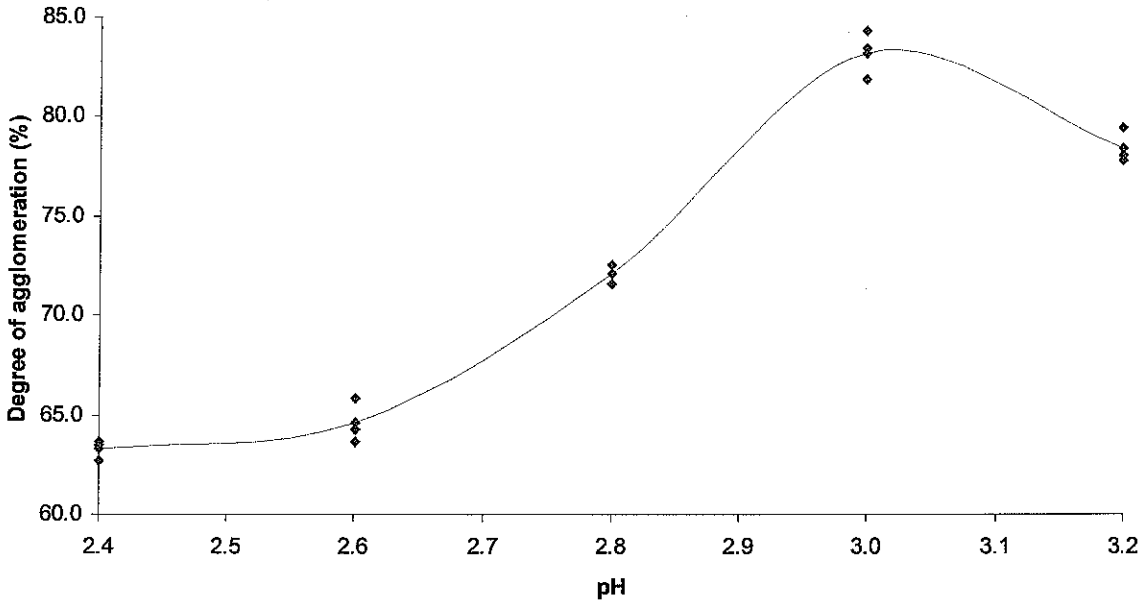

Figure 34. Influence of pH on the degree of agglomeration for the precipitation of metastable iron phases at 60°C and stirring rate of 600 rpm from an iron solution containing 10 g/L Fe, added as $Fe_2(SO_4)_3$, and 5 g/L H_2SO_4. A 2.5% ZnO slurry was used as neutralizing agent.

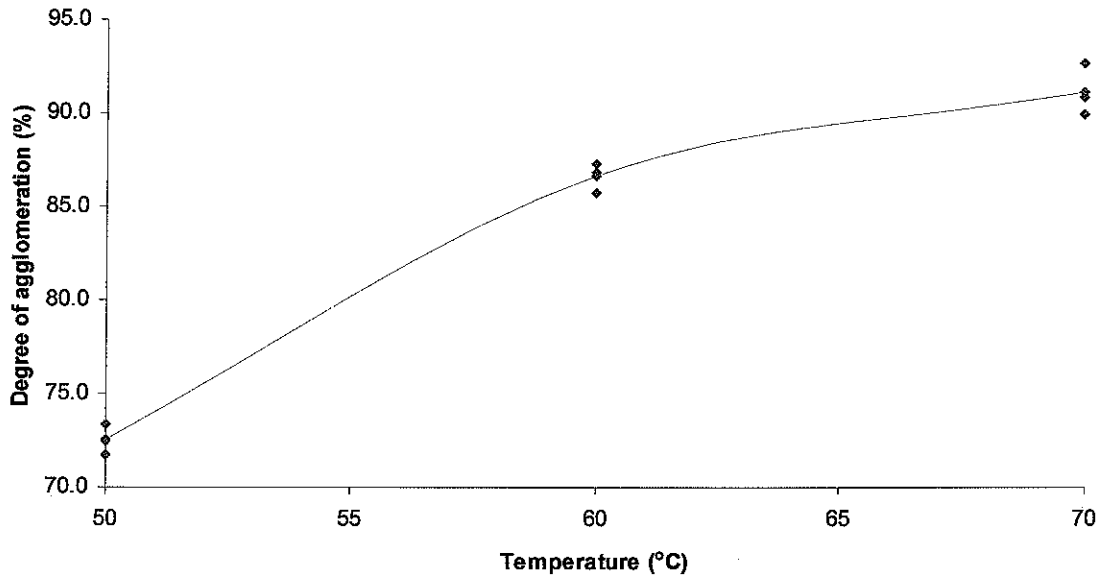

Figure 35. Influence of temperature on the degree of agglomeration for the precipitation of metastable iron phases at a pH of 3.0 and stirring rate of 600 rpm from an iron solution containing 10 g/L Fe, added as $Fe_2(SO_4)_3$, and 5 g/L H_2SO_4. A 2.5% ZnO slurry was used as neutralizing agent.

pH, temperature and iron solution iron concentration influence agglomeration in several ways. It is known that these variables influence the supersaturation level, which is the driving force for precipitation. Supersaturation in turn influences the final particle size, size distribution and morphology of the precipitates and therefore its filterability amongst other things. It is well known that small, low-density particles are formed at high supersaturation levels [Gösele *et al.*, 1990], which occur at low temperatures, high pH values and high initial solute concentrations. It was shown earlier that the relative supersaturation present during iron precipitation varies between about 1,000 and 30,000 at pH values between 1.85 and 3.5 and temperatures ranging from 50°C to 90°C, i.e. at a pH of about 1.85 and a temperature of 90°C, the relative supersaturation was estimated at 1,000, but at a pH of 3.5 and a temperature of 50°C, it increased to about 30,000. Therefore, an increase in pH causes supersaturation to increase as the solubility of iron decreases. The results summarised in Figure 4 indicate an increase in the degree of agglomeration up to a pH of about 3.0, whereafter it decreases. It is proposed that the solution iron concentration available only supports agglomeration up to a pH of about 3.0, whereafter the increase in the population density outweighs the agglomeration rate. On the other hand, an increase in temperature at a fixed pH results in a reduction in the solute concentration (refer to Figures 7 to 9), which is required to produce better quality iron precipitates as indicated in Figure 5.

Furthermore, it was proposed [Sakamoto *et al.*, 1976; Yamada, 1980; Veesler *et al.*, 1994; Ilievski and White, 1994; Johnston and Cresswell, 1996] that diffusion of growth species across a particle surface is faster at higher temperatures, providing a higher probability of cementation of particles. If supersaturation is controlled below the point where 2-line ferrihydrite is formed (pH below about 2.95 and temperature greater than about 75°C according to Figure 14), higher pH values and solute concentrations should also promote agglomeration as it supplies the material that cements particles together. Since all tests were conducted at constant supersaturation, agglomeration took place for the duration of each experiment. This is not the case for batch processes where a depletion of the solute concentration with time has a detrimental effect on agglomeration and the economics of downstream processes.

In terms of iron precipitation, an increase in pH causes supersaturation to increase as the solubility of iron decreases due to the formation of a variety of iron species. However, it appears from Figure 34 as though the increase in supersaturation only supports agglomeration up to a pH of about 3.0, where after the supersaturation is consumed by an increase in the nucleation rate. On the other hand, the effect of temperature on supersaturation is probably a result of the increased surface diffusion rates of iron molecules at higher temperatures, which support the formation of particle bridges required for agglomeration.

In terms of the three steps of the agglomeration process discussed earlier, it appeared therefore as if pH, temperature and the initial iron concentration impacted on phase 3, namely, the phase of consolidation.

5.3.2 Influence of mixing, seed addition and solution viscosity

Even though it was shown that, for the range of stirring rates evaluated, the mixing intensity did not have a significant impact on the variables used, the role of mixing in precipitation processes should not be underestimated, as it impacts on the range and distribution of the supersaturation [Franke and Mersmann, 1995; Van Leeuwen *et al.*, 1996 (a); Van Leeuwen *et al.*, 1996 (b); Baldyga and Orciuch, 2001]. It is known that the supersaturation influences the rate of nucleation, which determines the final particle size and size distribution as discussed in the previous paragraph. The relationship between the quality of the precipitate and mixing is not simple, and increased mixing may either increase or decrease the filterability of a precipitate as shown earlier.

Furthermore, changes in the hydrodynamic environment could impact on agglomeration and the specific filter resistance if the probability of particle collisions and the formation of interparticle bridges are influenced [Seyssiecq *et al*, 1998]. These steps are influenced by the amount of energy dissipated (stirring rate) in a precipitation system, since a change in the stirring rate not only changes the collision frequency of particulates, but could also result in particles either bouncing off each other, or keeping out of range of inter-particle forces due to a change in its kinetic

energy. Increased collision rates generally cause disagglomeration. Low agglomeration rates are therefore expected at both low and high stirring rates, and will result in smaller particles and increased filter resistance. Other variables that influence agglomeration include the particle population density, expressed in terms of the initial seed mass, the initial seed size and the viscosity of the solution.

Figure 36 indicates that the degree of agglomeration is optimal at solids concentrations between about 15 g/L and 35 g/L (Zone B). Agglomeration is limited by the probability of particle collisions at values below about 15 g/L (Zone A) and dissagglomeration starts to dominate at levels above of about 35 g/L (Zone C).

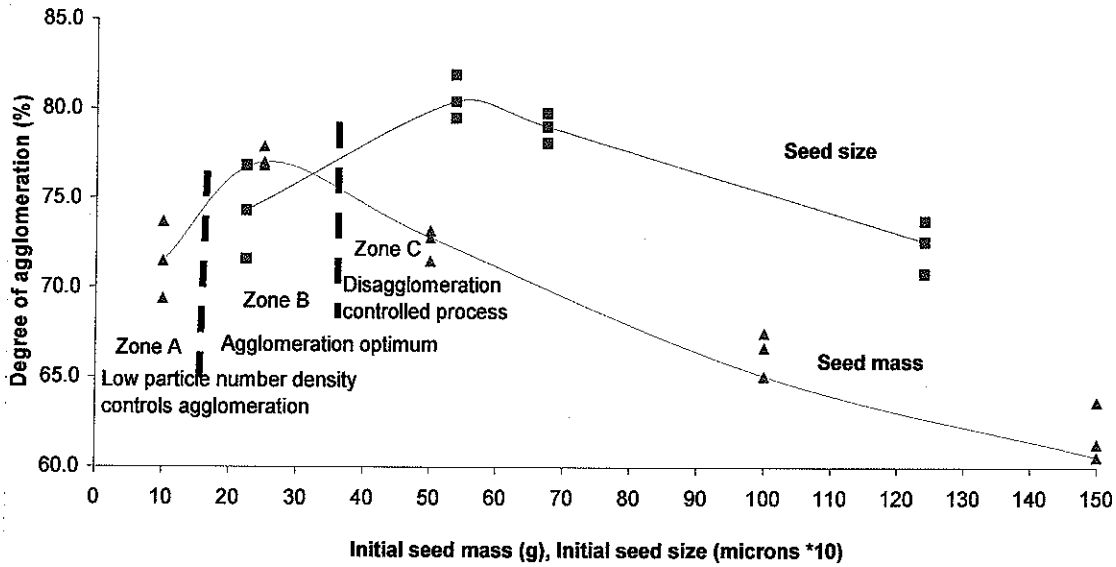

Figure 36. Influence of the initial seed size and seed mass on the degree of agglomeration for the precipitation of metastable iron phases at a pH of 3.2, 65°C and stirring rate of 600 rpm from an iron solution containing 10 g/L Fe, added as $Fe_2(SO_4)_3$, and 5 g/L H_2SO_4. A 2.5% ZnO slurry was used as neutralizing agent.

The change in the final mean particle size of the precipitate produced as a function of the initial seed mass followed the same trend than the degree of agglomeration, as indicated in Figure 37.

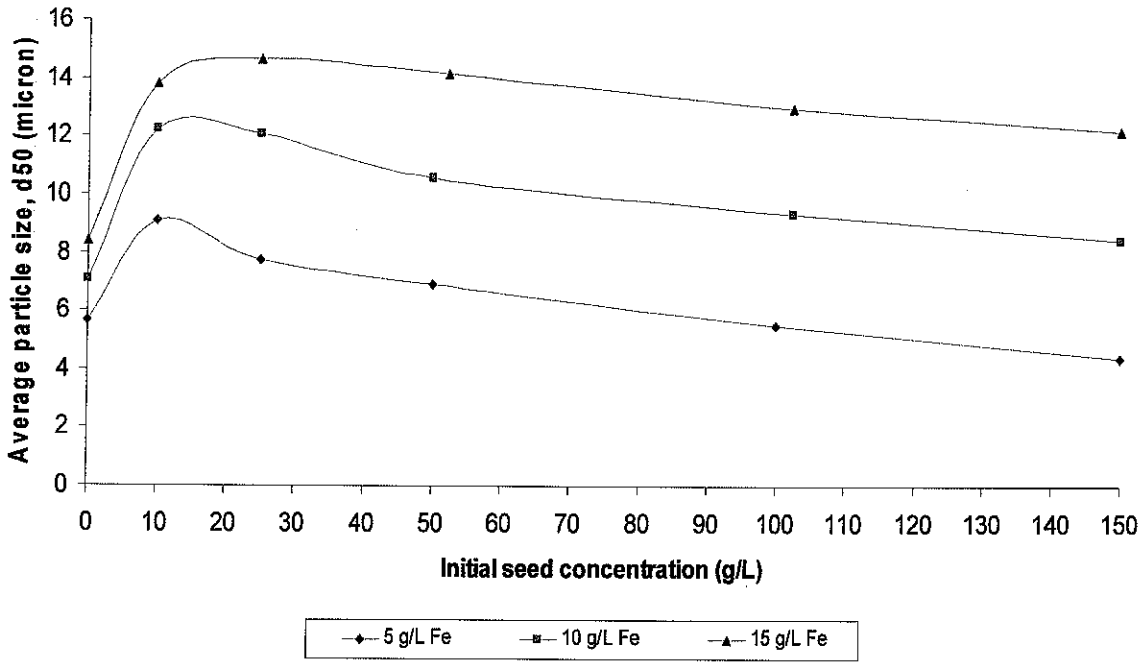

Figure 37. Influence of the initial seed mass on the final mean particle size for the precipitation of metastable iron phases at a pH of 3.2, 65°C and stirring rate of 600 rpm from an iron solution containing 5, 10 and 15 g/L Fe, added as $Fe_2(SO_4)_3$, and 5 g/L H_2SO_4. A 2.5% ZnO slurry was used as neutralizing agent.

Figure 37 shows that particle growth was stimulated by an increase in the initial seed concentration up to levels of 10 - 30 g/L seed, depending on the initial hot iron solution iron concentration. It also shows that the initial iron concentration had a significant impact on the final particle size of the precipitate as alluded to earlier. The increase in the final particle size probably indicates that iron precipitated on the surface of the seed material, and so reduces the particle number density by stimulating growth through agglomeration. Therefore, an increase in the initial iron concentration could result in the formation of bigger particles, as it supplies the cement that is required to form the interparticle bridges, as was mentioned earlier. Higher initial iron concentrations also support the addition of more seed material, which could improve the purity of the iron precipitates formed, by reducing the zinc and sulphate contents, as shown later.

The influence of the initial seed size on the degree of agglomeration is also shown in Figure 36. It is clear from the experimental data that agglomeration is optimal at initial seed sizes around 6.0μm. This size more or less corresponds to the point where the process changes from orthokinetic to perikinetic agglomeration under the conditions used. Orthokinetic agglomeration takes place between particles at least an order of magnitude smaller than the smallest eddies in a well-mixed environment [Saffman and Turner, 1956]. At these eddy sizes, also called the Kolmogoroff or turbulence microscale, the particles move within the eddies and the movement of the particles are strongly influenced by the viscosity of the solution. No exchange of particles between eddies take place, which inhibits agglomeration growth. On the other hand, when larger particles contained in large eddies are mixed, the eddies exchange particles which then agglomerate. For the experimental setup and conditions used in this study, the Kolmogoroff microscale was calculated to give an eddy size of about 58μm, which indicates that particles between 5.5μm and 6.0μm are no longer contained in micro-eddies as discussed earlier. The Kolmogoroff microscale (λ_0) was determined with the following equation [Seyssiecq *et al*, 1998]:

$$\lambda_0 = [\nu^3/\varepsilon]^{0.25} \qquad \ldots.16$$

where the kinematic viscosity (ν) of the fluid was calculated as 4.23×10^{-7} m^2/s (from $\rho_{solution}$ = 1.326 g/cm^3 and viscosity = 5.512×10^{-4} $N.s/m^2$ measured separately) and the energy dissipation (ε) was calculated as 0.007 W/kg (energy dissipated = 0.038 $kg.m^2/s$ and the slurry mass = 5.30 kg) with 80 g/L Zn in solution. The data in Figure 36 therefore indicates that agglomeration was influenced by viscosity effects up to a particle size of about 6μm, after which it was limited by a reduction in the number density of particulates as a result of agglomeration growth. For a solution containing 0 g/L Zn (used in the Hadamard matrix as minimum value), the value of λ_0 calculated was about 40μm (from $\rho_{solution}$ = 1.042 g/cm^3, viscosity = 3.800×10^{-4} $N.s/m^2$, energy dissipated = 0.038 $kg.m^2/s$ and the slurry mass = 4.17kg measured separately). The critical particle size where agglomeration changes from an orthokinetic to a perikinetic process is therefore estimated at 4μm. Since the experiments included in the Hadamard matrix were performed with seed with an

initial mean size of about 5.0µm, it probably initially followed an orthokinetic mechanism when the solutions contained 80 g/L zinc and a perikinetic mechanism for solutions with no zinc. This relative big change in zinc concentration is not expected to occur in industrial processes, but it illustrates the important role that solution viscosity could play in agglomeration processes. Furthermore, agglomeration in precipitation processes should be controlled to ensure that a change from an orthokinetic to a perikinetic dominated process takes place to support growth.

Seed addition was found not only to promote agglomeration, but it also improved the precipitate purity. Figures 38 and 39 show how the zinc and sulphate content of the iron precipitates changed with a change in the initial seed concentration.

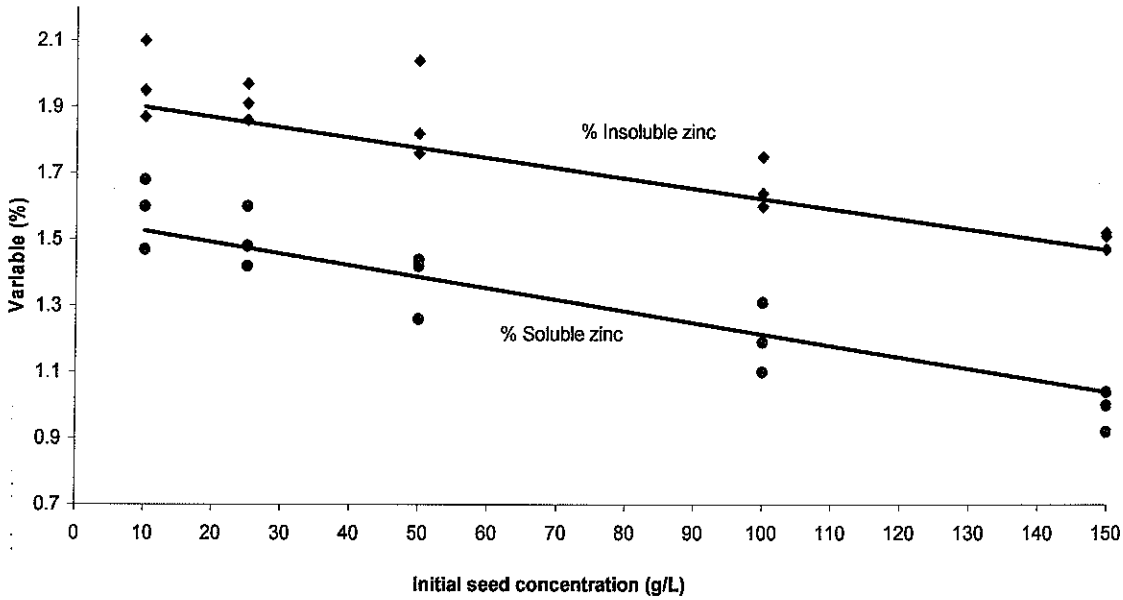

Figure 38. Influence of the initial seed concentration on precipitate zinc content for metastable iron phases formed at a pH of 3.2, 65°C and stirring rate of 600 rpm from an iron solution containing 10 g/L Fe, added as $Fe_2(SO_4)_3$, and 5 g/L H_2SO_4. A 2.5% ZnO slurry was used as neutralizing agent.

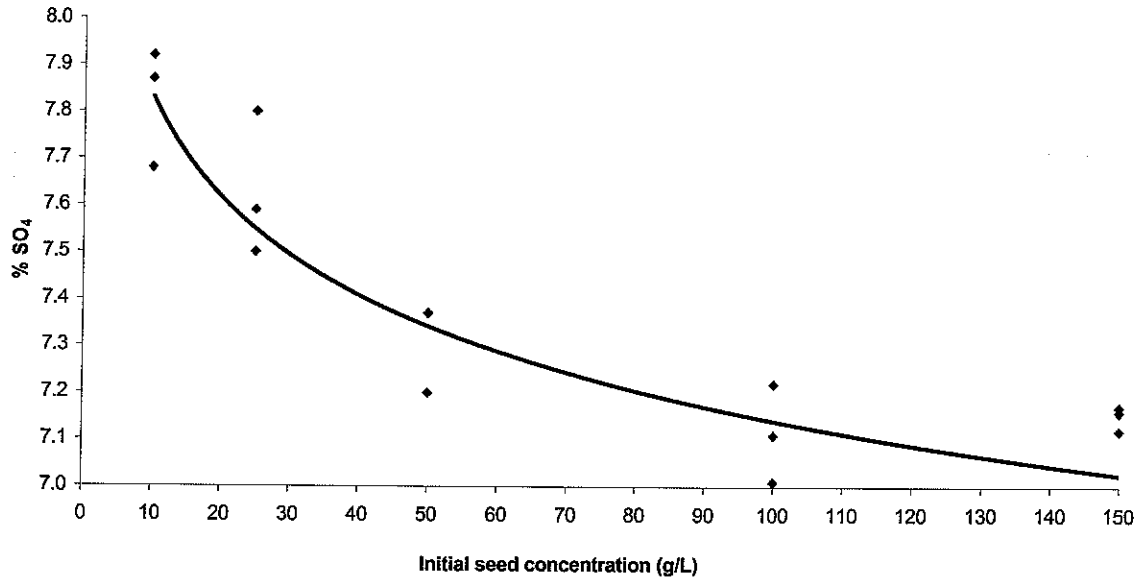

Figure 39. Influence of the initial seed concentration on precipitate sulphate content for metastable iron phases formed at a pH of 3.2, 65°C and stirring rate of 600 rpm from an iron solution containing 10 g/L Fe, added as $Fe_2(SO_4)_3$, and 5 g/L H_2SO_4. A 2.5% ZnO slurry was used as neutralizing agent.

In Figure 38, insoluble- and soluble zinc refer to acid- and water soluble zinc, respectively. The acid soluble zinc portion reflects the amount of unleached ZnO and encapsulated $ZnSO_4$ solution present in the precipitate, whereas the water soluble zinc present is an indication of the adsorbed solution and thus of the relative surface area of the agglomerates. As expected, less iron was precipitated on the surface of ZnO particles and more on the surfaces of seed particles as the seed concentration increased. In the presence of seed particles, the formation of new nuclei is expected to be limited, and it can be expected that the relative surface area of the final product will be lower with commensurate lower soluble zinc losses. This reduction in the relative surface area probably also contributed towards lowering the sulphate content, in the form of adsorbed sulphate complexes, on the precipitates, as shown in Figure 39.

In industrial zinc circuits, where an iron residue is often produced, the filterability (washability) of the precipitate determines the loss of zinc as water-soluble zinc and is of utmost importance. Figure 40 indicates how the addition of a relative small amount of seed material (up to about 50 g/L) could improve the filterability of iron precipitates by about 80%. The increased filterability is probably a result of a reduction in the particle population density and the formation of bigger particles, as indicated in Figure 37.

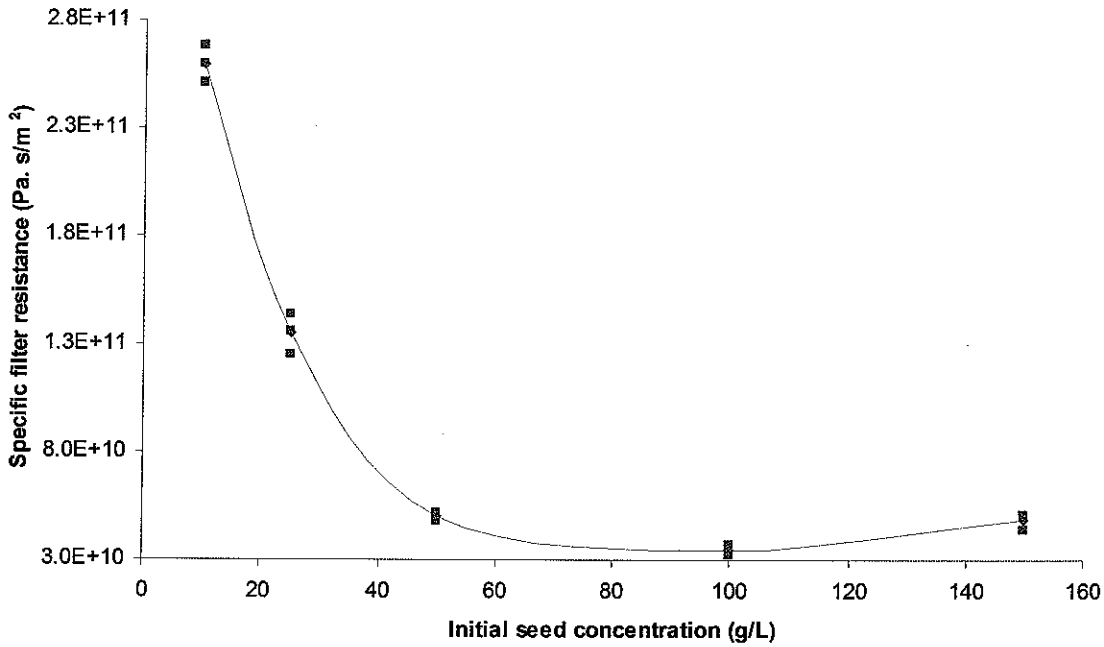

Figure 40. Influence of the initial seed concentration on the specific filter resistance of metastable iron phases formed at a pH of 3.2, 65°C and stirring rate of 600 rpm from an iron solution containing 10 g/L Fe, added as $Fe_2(SO_4)_3$, and 5 g/L H_2SO_4. A 2.5% ZnO slurry was used as neutralizing agent.

5.4 Conclusions

In crystallization processes, the nucleation- and growth steps determine the final product quality, i.e. the final particle size, particle size distribution and purity. These qualities in turn influence the down stream processing potential of the material. In order to improve the quality of metastable iron phases, such as ferrihydrite and schwertmannite, very often encountered in industrial environments, the factors that influence the growth process were considered. Since agglomeration is the dominant growth process in iron precipitation, specific attention was given to the operating parameters that influence the three stages of the agglomeration process. An algorithm, the so-called Hadamard matrix, was used to indicate the relative importance of these operating variables with respect to the degree of agglomeration, iron removal efficiency and the filterability of the product. This could assist the process engineer to focus on the more important parameters.

In terms of the relative importance of the operating variables, the study has shown that seed addition, temperature, pH and solution zinc content, which effects viscosity, had the biggest influence on the degree of agglomeration. It was shown that initial seed concentrations between 15 g/L and 35 g/L gave the optimum degree of agglomeration, probably due to the higher collision frequency achieved. The final product particle size was found to follow the same trend as the degree of agglomeration when the initial seed concentration was changed. Initial seed concentrations of up to 50 g/L were used to improve the specific filter resistance by about 80%. Seed additions also resulted in an improvement in the precipitate purity by reducing the zinc and sulphate contents of the final product.

Furthermore, temperature and pH influenced the consolidation of agglomerates through its influence on the supersaturation. It was shown elsewhere [Claassen *et al.*, 2003] that agglomeration growth is optimal at pH values around 3 and temperatures above 60°C. The influence of the solution zinc content or solution viscosity on the agglomeration process, stems from the effect that it has on the collision frequency of particles an order of magnitude smaller than the Kolmogoroff microscale. Optimum agglomeration was achieved with seed particles in the size range 5μm to 6μm.

The relative importance of operating variables with regards to the filterability of the precipitate and the iron removal efficiency, as iron is mostly removed as an impurity from hydrometallurgical circuits, was also determined. It was shown that pH, temperature, the hot iron solution iron concentration and seed addition had the biggest impact. The hot iron solution iron concentration influenced the final particle size as it impacted on the consolidation stage of the agglomeration process. The results have shown that higher hot iron solution iron concentrations supported agglomeration growth at higher seed concentration to give a coarser final product.

The study also indicated that, according to the outcome of the Hadamard matrix for the range of each operating parameter explored, the physico-chemical parameters were of greater importance than changes in the hydrodynamic environment. However, the mixing intensity could adversely affect the precipitation process through its influence on the first two stages of the agglomeration process, namely the probability of collisions and time allowed for particles to stay together, and the range and distribution of supersaturation and should therefore always be considered when an attempt is made to improve precipitate quality.

6. SUMMARY

The quality of precipitated products produced in hydrometallurgical refining circuits, is of utmost importance as it greatly influences plant efficiency and the cost of the operation. However, product quality in precipitation systems hasn't received the same amount of attention as the quality of crystalline products. This probably stems from the fact that precipitation processes and their products are more complex than crystallization systems. This is specifically true for the precipitation of poorly crystalline iron phases from hot ferric sulphate media in the pH range 1.5 to 3.5.

In order to address the general lack of knowledge with regards to the production of good quality iron precipitates under the conditions listed here, an industrial iron removal process, the Zincor Process and its residues were studied. This was followed by a more detailed study into the role that supersaturation, the driving force for precipitation, plays during the formation of poorly crystalline phases as well as the factors that influence the nucleation and growth processes. The aim of this detailed study was, firstly, to determine typical supersaturation levels present during the precipitation of iron and its influence on the morphology of the final product, secondly, to determine the impact of changes in the mixing environment on product quality as it influences supersaturation and the rate of nucleation (precipitation systems are mostly mixing controlled) and, thirdly, to define the conditions required for optimal growth of the precipitated nuclei and primary particles as growth through agglomeration is required to improve the downstream handling properties of the iron precipitate.

The findings from the study of the Zincor iron removal process formed the basis of this document and are therefore briefly discussed. Results obtained from the detailed study into the factors that influence iron precipitate product quality, indicated that the type of phase(s) produced and its stability, the supersaturation present during its formation, changes in the mixing environment and particle growth, specifically agglomeration growth, had a significant impact on the quality of these precipitates. The results were therefore summarized in three chapters, namely, metastability in iron precipitation, mixing and precipitation and agglomeration.

The following paragraphs give a summary of the most important findings of the work performed on means to improve the product quality of poorly crystalline iron phases.

6.1 Metastability in iron precipitation

The understanding and control of the hydrolysis of ferric iron at elevated temperatures and a pH range between about 1.5 and 3.5 plays a critical role in the production of the desired quality iron precipitate. Firstly, it is known that the critical nuclei of phases such as ferrihydrite and schwertmannite are more stable than that of goethite. Ferrihydrite and schwertmannite are therefore mostly formed under the above-mentioned conditions and are metastable towards goethite, the most stable iron phase. The (meta)stability of schwertmannite, however, is not well-defined in industrial environments. Furthermore, the existence of schwertmannite as a mineral entity is questionable, i.e. it could be argued that it is ferrihydrite with a higher sulphate content as the crystal structure of this phase has not been determined yet. In this study the relative stability of schwertmannite and ferrihydrite as well as the typical supersaturation levels prevailing during their formation, was determined. It was shown that:

- A definite phase transition line was identified between the (meta)stability regions of ferrihydrite and schwertmannite for a series of pH and temperature values studied. It therefore appears as though schwertmannite does exist as a phase in its own right and that it could play an important role in industrial iron removal processes.
- Both schwertmannite and ferrihydrite contains variable amounts of sulphate. In fact, schwertmannite produced at a relatively low supersaturation, contains lower sulphate values than ferrihydrite produced at high relative supersaturation. This is discussed in more detail in the following paragraphs.
- Ferrihydrite is the more stable phase at pH values above about 2.70 at 50°C and its stability increases with an increase in temperature at a fixed pH. At pH values above about 3.0 and temperatures below approximately 70°C, two-line ferrihydrite was found to be the dominant phase. A small amount of schwertmannite was found to be present in this region.

Furthermore, it is also known that poor quality precipitates, i.e. fine, voluminous precipitates with high relative surface area and impurity values, are formed when the critical supersaturation is exceeded. The critical supersaturation level is indicated by the so-called metastability limit. This is the point where a sudden decrease in the iron concentration occurs. In this study, the metastability limit and metastability region, which is the region between the metastability limit and the solubility limit, were determined for the case where metastable iron phases such as ferrihydrite and schwertmannite are formed from hot dilute ferric iron solution. The relative supersaturation present during the precipitation of these phases and its influence on the quality of the final product was also studied. It was shown that:

- The metastability ranges between a pH of about 2.0 at 50°C and 1.6 at 90°C.
- Therefore, most industrial processes where iron is precipitated from ferric iron solutions, operates well above the metastability limit in the region where rapid nucleation occurs and poor quality precipitates are produced.
- The width of the metastable zone was reduced to between 0.2 and 0.3 pH units, mainly by the presence of seed material and intensive mixing. In crystallization processes operation within the metastable zone is encouraged as it promotes growth rather than nucleation. Low molecular growth rates at low solute concentration make this approach less attractive for iron precipitation. Nonetheless, it was found that precipitating iron in a stagewise fashion even above the metastability limit improved the quality of the final product significantly.
- Ferrihydrite and schwertmannite precipitated over a range of relative supersaturation levels between pH values of about 1.65 and 3.5 and temperatures between 50°C and 90°C, but the quality of ferrihydrite and schwertmannite produced were dependent on the supersaturation level.
- Two-line ferrihydrite was precipitated at relative supersaturation levels between approximately 10,000 and 30,000.
- Six-line ferrihydrite was precipitated at relative supersaturation levels between approximately 2,500 and 25,000.
- Schwertmannite was precipitated at relative supersaturation levels between approximately 1,000 and 20,000.

- Relative supersaturation levels lower than about 1,000 are required for the production of goethite. It is known that goethite precipitation is achieved when the ferric iron concentration is controlled at very low levels by the slow rate of ferrous iron oxidation at elevated temperatures and low pH values as a result of the poor solubility of oxygen under these conditions.
- Schwertmannite could be produced at lower supersaturation levels than ferrihydrite and therefore is of a better quality. The sulphate content of schwertmannite varied between about 14% at a pH of about 2.20 and a temperature of 50°C to approximately 7% at a pH of about 2.45 and a temperature of 90°C. For ferrihydrite, the sulphate content varied between about 10% and 6.5% at pH and temperatures values of 2.7 at 50°C and 3.05 at 90°C, respectively.
- Low supersaturation levels effective at higher temperatures and lower pH values, generally support the production of precipitates with lower impurity levels (moisture, sulphate and zinc content). Exceptions to this are the increase in the zinc content of the precipitates, with an increase in temperature, and an increase in moisture and sulphate values in precipitates formed at low pH values. At low pH values fine precipitates were produced, with a higher relative surface area, resulting in higher sulphate and moisture levels. It was proposed that the increase in temperature results in increased surface diffusion rates and rates of precipitation of iron species, which could entrain unleached ZnO or $ZnSO_4$ solution.

6.2 Mixing and precipitation

It is known that high supersaturation levels are present during ferric iron precipitation with the result that the timescales of the chemical reactions and nucleation are much lower than the timescales of macro, meso and micromixing. Ferric iron precipitation processes are therefore mixing controlled, and any change in the rate-limiting step is therefore expected to influence the quality of the precipitates. The study into the influence of changes to the mixing environment on the quality of iron precipitates, indicated the following:

- The three-zone model approach was used effectively to indicate that the quality of iron precipitates, expressed in terms of its filterability and purity, is sensitive to changes in the macro and micromixing environments.
- The filterability of the precipitates is more sensitive to changes in cation/ferric mass transfer, in the region of the inlet points, than mass transfer of the neutralizing agent. An increase in dilution of the hot iron solution had a significant impact on product quality.
- The specific filter resistance of the solids was reduced by about 50% by using the three-zone model approach to precipitate poorly crystalline iron phases. Furthermore, the water and acid soluble zinc values in the precipitate were reduced by 14% and 75%, respectively.
- The reactivity, expressed in terms of particle size, of the neutralising agent had a significant influence on the weak acid soluble zinc values associated with the precipitate. The use of a coarser neutralising agent resulted in increased zinc losses.
- The pumping capacity of an impeller should be selected in such a manner that mixing times below about 5 minutes are avoided.
- In iron precipitation systems, agitators are generally running at lower speeds and high mixing times, i.e. precipitation is macromixing controlled. In such systems the macrofluid is poorly mixed whereas the microfluid is well mixed. When this is the case, it is known that the reactor geometry and position of the feed points could influence product quality.
- The controlling mixing environment, i.e. macro or micromixing controlled, generally indicates where feed points should be placed. In a well-mixed

macrofluid, as in a DTB reactor, feed points should be placed far away from the agitator. In a CSTR, where the macrofluid is less homogeneous, feed points need to be placed close to the agitator.

- Feed points, the hot iron solution and neutralising agent in this case, should be placed on opposite sides of the reactor to increase mixing time.
- An optimized DTB reactor should give precipitates with superior quality compared to the traditional CSTR.
- When precipitation is either micromixing or macromixing controlled, a precipitate with poor filterability is produced. A balance between the agitator speed and agitator pumping capacity for a specific type of reactor therefore needs to be found.
- Any change to the mixing environment in a precipitation system needs to be carefully considered before implementation, as it could have a significant influence on the final product quality, especially the filterability of the precipitate.

6.3 Agglomeration

Supersaturation, the driving force for precipitation, not only influences the nucleation process but also particle growth. It is known that particle growth in precipitation systems typically takes place in the form of agglomeration. Particle growth is required to ensure that down stream processes, such as thickening and filtration, are viable. However, if the agglomeration process is not well controlled, it could lead to the formation of particles with high relative surface areas and increased impurity levels. It is therefore necessary to determine the influence as well as the relative importance of typical operating variables on product quality parameters such as the filterability, particle size and purity of the precipitates formed. In this part of the study it was found that:

- A Hadamard matrix could be used to indicate that the degree of agglomeration is influenced by, in order of importance, seed addition, temperature, solution viscosity and pH. In the same way, it was shown that the filterability of iron precipitates is sensitive to pH, seed addition, hot iron solution iron concentration and temperature. When the impact of the variables on iron removal efficiency was evaluated, it was found that pH, hot iron solution iron concentration, temperature and seed addition were most important. Overall, pH is the most important parameter, followed by seed addition, temperature and iron solution iron concentration.
- Every effort needs to be made to optimize pH control in iron precipitation processes. The impact of pH on iron precipitate quality should also be seen in light of the relative small pH window of 2.6 to 3.2 that was evaluated, i.e. a small change in pH in this range could have a significant effect on agglomeration, iron removal efficiency, the filterability and purity of the precipitate through its influence on supersaturation.
- Seed addition is essential to ensure good quality iron precipitates. However, it is often not considered, or even neglected in industrial processes. It was found that seed addition supported agglomeration, and that up to initial seed concentrations of about 25g/L, it resulted in lower sulphate and zinc levels and stabilized the process.

- Higher seed concentrations require higher solute concentrations to ensure that growth takes place.
- Agglomeration was found to be optimum for initial seed sizes between 5 and 6μm.
- Agglomeration should be controlled to ensure that the change from orthokinetic to perikinetic agglomeration takes place.
- Higher solute concentrations support growth at higher seed concentrations, which gives a coarser final product.
- Changes in the physico-chemical parameters were of greater importance than changes in the hydrodynamic environment, for the range of each operating parameter explored.

APPENDICES

Appendix 1: Ferric iron nucleation and solubility curves

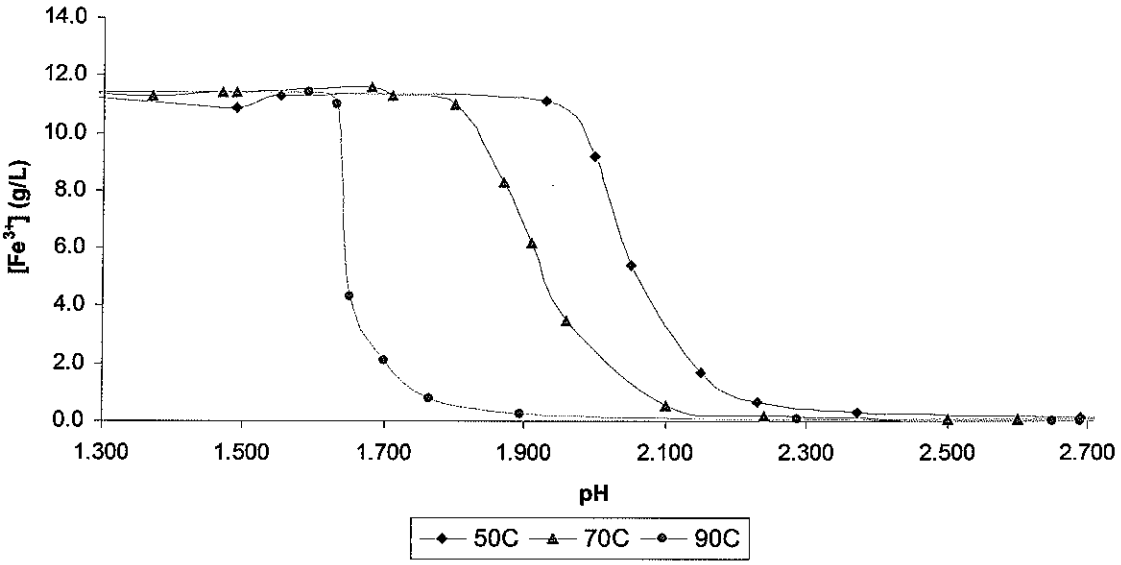

Figure A1.1. Nucleation data for ferric iron determined at 50, 70 and 90°C. The pH was changed stepwise in increments of 0.5 pH units every 20 minutes. The pH was controlled by adding $Ca(OH)_2$, ZnO powder and 98% H_2SO_4.

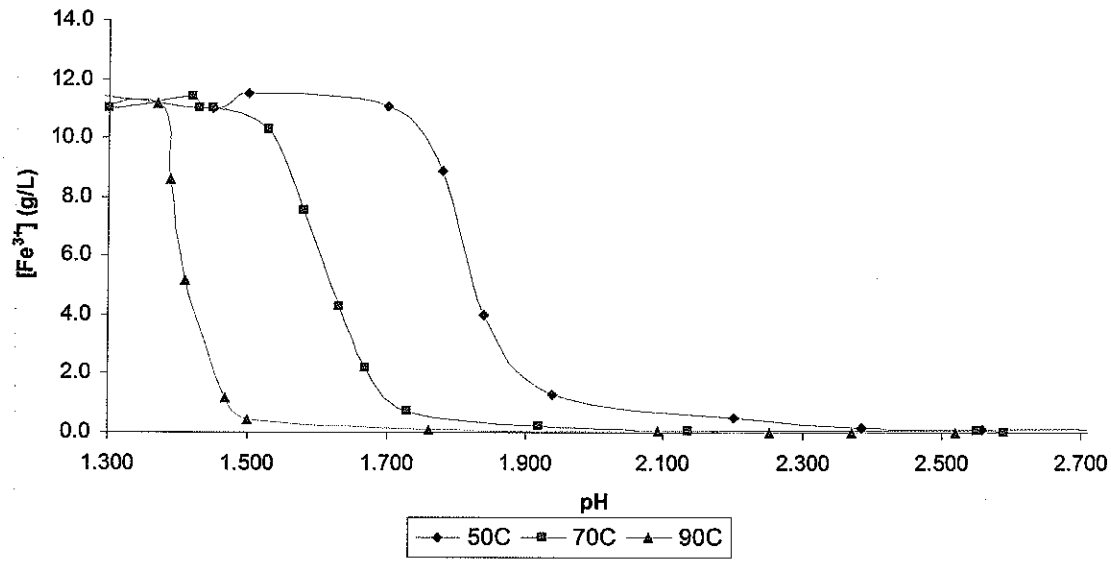

Figure A1.2. Solubilization data for ferric iron determined at 50, 70 and 90°C. The pH was changed stepwise in increments of 0.5 pH units every 20 minutes. The pH was controlled by adding $Ca(OH)_2$, ZnO powder and 98% H_2SO_4.

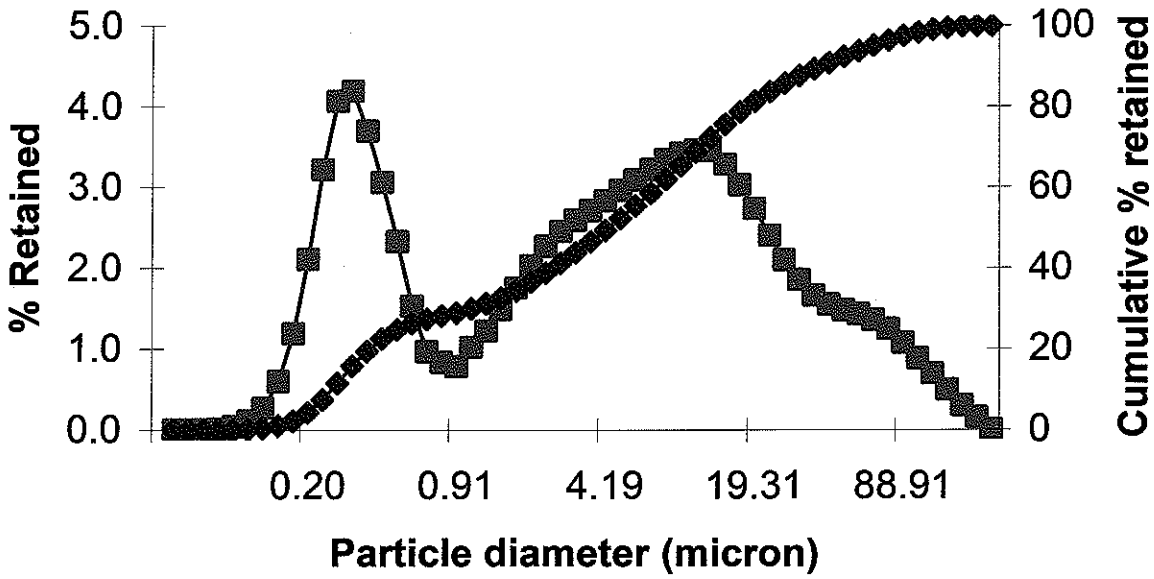

Figure A1.3. Particle size distribution of the seed material used to determine the influence of seed mass on agglomeration as determined by a Malvern Mastersizer.

Appendix 2: Ferric iron equilibrium solubility data as calculated by STABCAL™

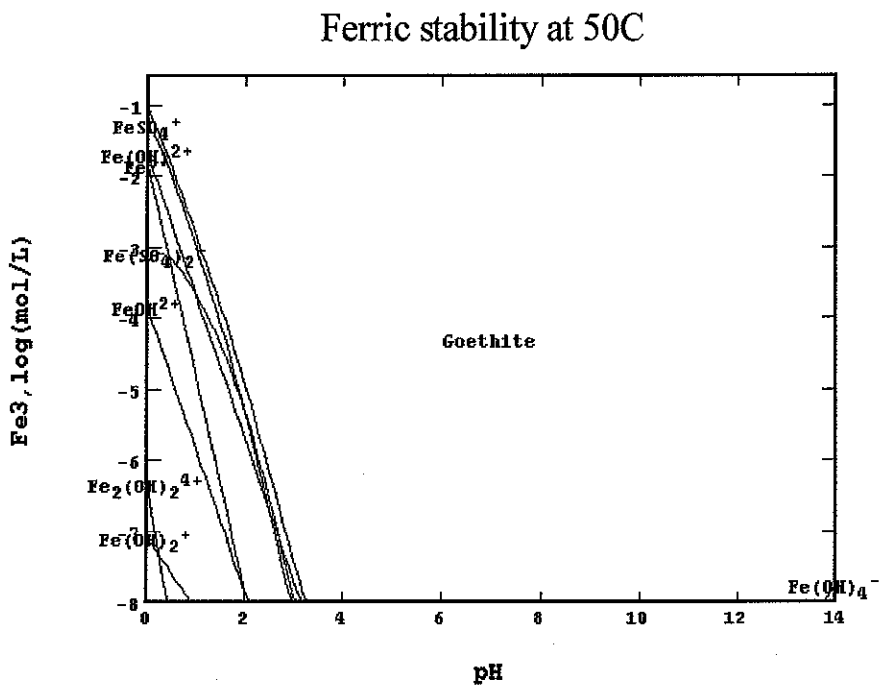

Figure A2.1. Ferric ion stability diagram determined with the STABCAL™ NBS-database at 50°C.

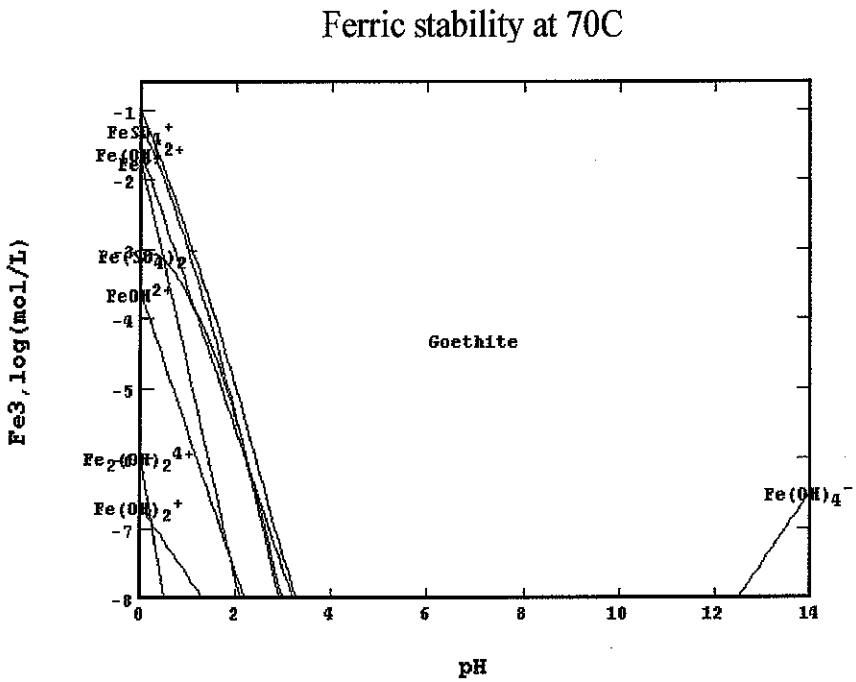

Figure A2.2. Ferric ion stability diagram determined with the STABCAL™ NBS-database at 70°C.

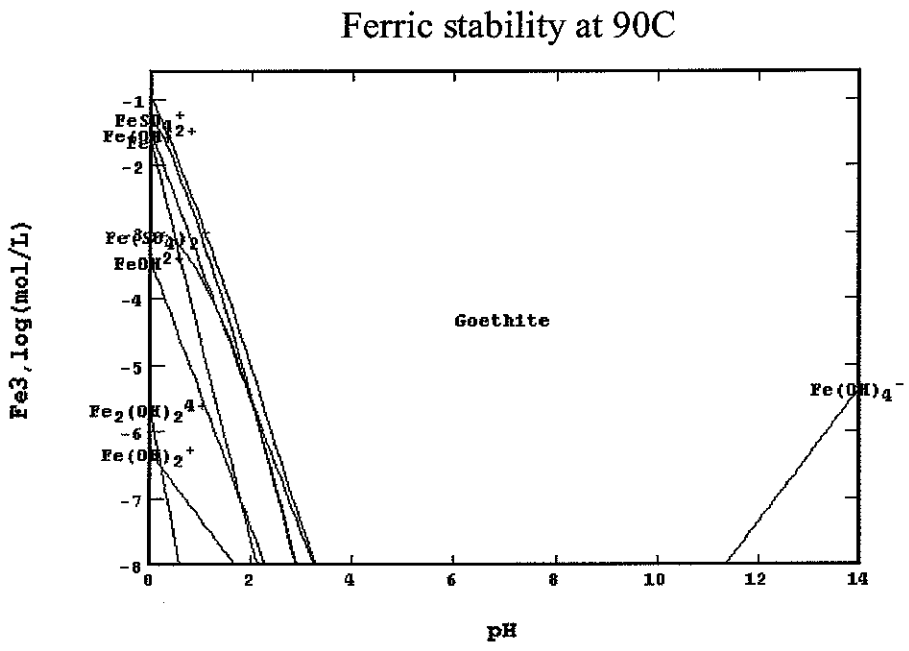

Figure A2.3. Ferric ion stability diagram determined with the STABCAL™ NBS-database at 90°C.

Appendix 3:

Table A3.1. Spreadsheet used to calculate particle population density from Malvern particle analysis data.

total solid mass (g)	5.00E+01	measured from the total mass of sample or calculated from a process mass balance				
rho solid (kg/m3)	3232					
vol ppted (m3)	1.55E-05					
*SIZES*um	Vol %	Delta L (m)	Lbar (m)	N (1/m3)	n(L) (1/m4) =N/Delta L	n(L) * Lbar (1/m3)
0.05	0.00					
0.06	0.00041	1.00E-08	6.50E-08	2.83E+12	2.83E+20	1.84E+13
0.07	0.00126	1.00E-08	7.50E-08	2.87E+11	2.87E+19	2.15E+12
0.08	0.00326	1.00E-08	8.50E-08	6.06E+11	6.06E+19	5.15E+12
0.09	0.00836	1.00E-08	9.50E-08	1.12E+12	1.12E+20	1.07E+13
0.11	0.02145	2.00E-08	1.20E-07	1.43E+12	7.15E+19	8.58E+12
0.13	0.05364	1.50E-08	1.33E-07	2.72E+12	1.82E+20	2.41E+13
0.15	0.12592	2.06E-08	1.56E-07	4.18E+12	2.03E+20	3.17E+13
41.43	0.56831	5.87E-06	4.44E-05	2.42E+06	4.13E+11	1.83E+07
48.27	0.39668	6.84E-06	5.17E-05	1.22E+06	1.78E+11	9.20E+06
56.23	0.21086	7.96E-06	6.02E-05	5.37E+05	6.74E+10	4.06E+06
65.51	0.05121	9.28E-06	7.01E-05	1.81E+05	1.95E+10	1.36E+06
76.32	0.00937	1.08E-05	8.17E-05	2.77E+04	2.57E+09	2.10E+05
88.91	0.00258	1.26E-05	9.52E-05	3.21E+03	2.55E+08	2.43E+04
103.58	0.00051	1.47E-05	1.11E-04	5.59E+02	3.81E+07	4.22E+03
120.67	0.00007	1.71E-05	1.29E-04	6.98E+01	4.09E+06	5.28E+02
140.58	0	1.99E-05	1.51E-04	6.06E+00	3.05E+05	4.58E+01
163.77	0.00764	2.32E-05	1.75E-04	0.00E+00	0.00E+00	0.00E+00
190.80	0.50994	2.70E-05	2.04E-04	2.65E+02	9.80E+06	2.00E+03
222.28	1.92305	3.15E-05	2.38E-04	1.12E+04	3.55E+08	8.45E+04
258.95	3.96071	3.67E-05	2.77E-04	2.66E+04	7.27E+08	2.01E+05
301.68	4.71965	4.27E-05	3.23E-04	3.47E+04	8.12E+08	2.62E+05
351.46	3.57416	4.98E-05	3.76E-04	2.62E+04	5.26E+08	1.98E+05
409.45	1.78791	5.80E-05	4.38E-04	1.25E+04	2.16E+08	9.47E+04
477.01	0.46826	6.76E-05	5.11E-04	3.96E+03	5.87E+07	3.00E+04
555.71	0	7.87E-05	5.95E-04	6.57E+02	8.34E+06	4.96E+03
647.41	0	9.17E-05	6.93E-04	0.00E+00	0.00E+00	0.00E+00
			m0	**8.19E+13**		
			m1	**8.89E+06**		
			m2	**3.77E+00**		
			m3	**8.98E-06**		
			m4	**1.34E-10**		
			lbar1,0	**1.09E-07**		

LIST OF FIGURES

LIST OF TABLES

REFERENCE LIST

Arregui, V., Gordon, A.R., and Steinveit, G., 1980. The Jarosite Process – Past, Present and Future. Lead-Zinc-Tin '80. Proceedings of the 109th Annual Meeting, Las Vegas, Nevada, February *24-28*, 97-123.

Ashurst, K.G. and Hancock, R.D., 1977. The thermodynamics of the formation of sulphate complexes of iron(III), cobalt(II), iron(II), manganese(II) and copper(II) in perchlorate medium. NIM Report No. 1914, Randburg, South Africa.

Babcan, J., 1971. Synthesis of Jarosite - $KFe_3(SO_4)_2(OH)_6$. Geol. Zb., 22 (*2*), 299-304.

Baldyga, J. and Orciuch, W., 2001. Some hydrodynamic aspects of precipitation. Powder Technology, 121, 9-19.

Bigham, J. M., Carlson, L. and Murad, E., 1994. Schwertmannite, a new iron oxyhydroxy-sulphate from Pyhasalmi, Finland, and other localities. Min. Mag., 58, 641-648.

Bigham, J.M., Schwertmann, U., Carlson, L. and Murad, E, 1990. A poorly crystallized oxyhydroxysulfate of iron formed by bacterial oxidation of Fe(II) in acid mine waters. Geochim. Cosmochim. Acta, 54, 2743 – 2758.

Bigham, J.M., Schwertmann, U., Traina, S.J., Winland, R.L. and Wolf, M., 1996. Schwertmannite and the chemical modeling of iron in acid surface waters. Geochim. Cosmochim. Acta, 60, 2111 – 2121.

Claassen, J.O., 2002. Characterization and optimization of the Zincor iron removal process. M. Eng. Thesis. University of Pretoria, Pretoria, South Africa, 149p.

Claassen, J.O., Meyer, E.H.O., Rennie, J. and Sandenbergh, R.F., 2002. Iron removal from zinc-rich process solutions: Defining the Zincor Process. Hydrometallurgy, 67, 87-108.

Claassen, J.O., Meyer, E.H.O., Rennie, J. and Sandenbergh, R.F., 2003(a). Iron precipitation from zinc-rich process solutions: Optimizing the Zincor Process, J. SAIMM, May 2003, 253 - 263.

Claassen, J.O., Rennie, J., Van Niekerk W.H., Meyer, E.H.O. and Sandenbergh, R.F., 2003(b). Recent developments in iron removal and control at the Zinc Corporation of South Africa. Hydrometallurgy 2003, 5th International Symposium Proceedings. C. Young, A. Alfantazi, C. Anderson, A. James, D. Dreisinger, B. Harris, (Eds.). TMS, Canada, 1675 – 1690.

Chen, T.T. and Cabri, L.J., 1986. Mineralogical overview of iron control in hydrometallurgical processing. Proceedings of the First International Symposium on Iron Control in Hydrometallurgy, J.E. Dutrizac and A.J. Monhemius, (Eds.), Ellis Horwood, England, 19 – 55.

Cornell, R.M. and Schwertmann, U., 1996. The Iron Oxides - Structure, Properties, Reactions, Occurrence and Uses. Weinheim, New York, 573p.

Cubeddu, F., Piasentin, M. and Reilly, F., 1996. The para-goethite process at the Enirisorse-Porto Vesme plant. Proceedings of the Second International Symposium on Iron Control in Hydrometallurgy, J.E. Dutrizac and G.B. Harris, (Eds.), The Canadian Institute of Mining, Metallurgy and Petroleum, Ottawa, Canada, 147 – 162.

David, R. and Klein, J., 2001. Reaction Crystallization. Crystallization Technology Handbook, Mersmann, A. (Ed.), New York, Marcel Dekker Inc., 832p.

Demopoulos, G., 1993. Precipitation in aqueous processing of inorganic materials: A unified colloid-crystallization approach to the production of powders with controlled properties. First International Conference on Processing Materials for Properties, H. Henein and T. Oki, (Eds.), The Minerals, Metals and Materials Society, 537 – 540.

Demopoulos, G. P., 2003. Short Course: Aqueous precipitation and crystallization for the production of particulate solids with desired properties. Hydrometallurgy 2003, 5th International Symposium Proceedings, Vancouver, Canada.

Dirksen, J. A. and Ring, T. A., 1991. Fundamentals of crystallization: kinetic effects on particle size distribution and morphology. Chem. Eng. Sci., 46 (10), 2389-2427.

Dutrizac, J.E., 1985. Jarosite type compounds and their application in the metallurgical industry. Hydrometallurgy, Research, Developments and Plant Practice. Proc. 112th AIME Annual Meeting, K. Osseo-Asare and J.D. Miller, (Eds.), TMS-AIME, Atlanta, Georgia, 6-10 March 1985, 531 – 551.

Dutrizac, J.E., 1999. Determination of schwertmannite in hydrometallurgical leach residues. Part 1 – The Nature of Schwertmannite. Part 2 – Examination of Hydrometallurgical Leach Residues, Department of Public Works and Government Services Canada, Contract 028SQ.23440-7-1012, unpublished.

Fogler, H.S., 1999. Elements of Chemical Reaction Engineering, 3rd Edition, N.R. Amundson, (Ed.), Prentice Hall, New Jersey, 967p.

Franke, J. and Mersmann, A., 1995. The influence of the operational conditions on the precipitation process. Chem Eng. Sci., 50 (11), 1737-1753.

Garside, J., Gaska, J. and Mullin, J. W., 1972. J. Crystal Growth, 13/14, 510.

Garside, J., 1977. Kinetics of crystallization from solutions. Crystal growth and Materials, Kaldis, E. and Scheel, H. J. (Eds.), North-Holland, Amsterdam, 484p.

Gordon, A.R. and Pickering, R.W., 1975. Improved leaching technologies in the electrolytic zinc industry. Metal. Trans., 6B, 43-53.

Gösele, W., Egel-Hess, W., Wintermantel, K., Faulhaber, F. R. and Mersmann, A., 1990. Feststoffbildung durch Fällung. Chem. Inge. Tech., 62, 544-552.

Gösele, W. and Kind, M., 1991. Study on the influence of mixing on the quality of continuous precipitating products. Chem. Ing. Tech., 63, 59 - 62.

Habashi, F., 1999. Textbook of Hydrometallurgy. Metallurgie Extractive, Quebec, Canada, 739p.

Ilievski, D. and White, E.T., 1994. Agglomeration mechanisms in $Al(OH)_3$ crystallization from caustic aluminate solutions. Proceedings of the First International Technology Forum, Denver, Co, AIChE, New York, 305 – 310.

Jambor, J.L. and Dutrizac, J. E., 1998. Occurrence and constitution of natural and synthetic ferrihydrite, a widespread iron oxy-hydroxide. Chemical Reviews, 98 (7), 2549 – 2585.

Johnston, J.R.R. and Cresswell, P.J., 1996. Modelling alumina precipitation: dynamic solution of the population balance equation. Fourth International Alumina Quality Workshop, Darwin, June 1996, 281 – 290.

Kind, M., 2002. Colloidal aspects of precipitation processes. Chem. Eng. Sci., 57, 4287-4293.

Loan, M., Parkinson, G., Newman, M. and Farrow, J., 2001. Iron oxy-hydroxide crystallization in a hydrometallurgical residue. J. of Crystal Growth, 235, 482-488.

McCristal, T.G. and Manning, J., 1998. Conversion of the Pasminco Hobart Smelter to para-goethite. Zinc and Lead Processing. J. E. Dutrizac, J. A. Gonzales, G.L. Bolton and P. Hancock, (Eds.), The Metallurgical Society of CIM, 439 – 453.

Mersmann, A., 2001. Fundamentals of crystallization. Crystallization technology handbook, 2nd Edition, Mersmann, A. (Ed.), New York, Marcel Dekker, 832p.

Meyer, E.H.O., Howard, G., Heagele, R. and Beck, R.D., 1996. Iron control and removal at the Zinc Corporation of South Africa. Proceedings of the Second International Symposium on Iron Control in Hydrometallurgy, J.E. Dutrizac and G.B. Harris, (Eds.), The Canadian Institute of Mining, Metallurgy and Petroleum. Ottawa, Canada, 163 – 182.

Mullin, J. W., (Ed.), 1972. Crystallization, 2nd Edition, Butterworths, London, 480p.

Mullin, J. W., (Ed.), 1976. Industrial Crystallization, Plenum Press, New York.

Mullin, J. W. and Ang, N. M. 1976. Disc. Faraday Soc., 61, 141.

Nielsen, A.E., (Ed.), 1964. Kinetics of precipitation, Pergamon Press, New York.

Nielsen, A.E., 1967. Crystal Growth, Peiser H.S. (Ed.), Pergamon Press, New York, 419p.

Nyvlt, J., (Ed.), 1971. Industrial crystallization from solutions, Butterworths, London.

Nyvlt, J., (Ed.), 1982. Industrial Crystallization: the state of the art. 2nd Edition, Verlag Chemie, Weinheim, 182p.

Nyvlt, J., Söhnel, O., Matuchova, M. and Broul, M., 1985. The Kinetics of Industrial Crystallization, Chemical Engineering Monograph Series, 19, Elsevier, Amsterdam, 350p.

Onozaki, A., Sato, K. and Kuramochi, S., 1986. Effect of some impurities on iron precipitation at the Iijima Zinc Refinery. Proceedings of the First International Symposium on Iron Control in Hydrometallurgy, J.E. Dutrizac and A.J. Monhemius, (Eds.), Ellis Horwood, England, 742 - 752.

Pammenter, R.V., Kershaw, M.G. and Horsham, T.R., 1986. The Low-contaminant Jarosite Process – Further developments and the implementation of the process. Proceedings of the First International Symposium on Iron Control in Hydrometallurgy, J.E. Dutrizac and A.J. Monhemius, (Eds.), Ellis Horwood, England, 603 - 617.

Pamplin, B.R., (Ed.), 1975. Crystal Growth. International series of monographs in the science of the solid state, Volume 6, 672p.

Patent, 1964, Asturiana de Zinc S. A., Spanish Patent No. 304,601, Application lodged October 1964. Equivalent U.S. Patent No. 3,434,798 granted March 25, 1969.

Patent, 1965(a), Det Norske Zinkkompani A/S Norwegian Patent NO. 108,047, Application lodged April 30, 1965. Equivalent U.S. Patent No. 3,434,947 granted March 25, 1969.

Patent, 1965(b), Electrolytic Zinc Company of Australasia Limited, Australian Patent No. 401,724. Application lodged 31st March, 1965. Equivalent U.S. Patent No. 3,493,365 granted 3rd February, 1970.

Patent, 1966, "Procédé de préparation d'oxydes de fer hydraté", Belgian Patent, No. 676.970,24, February 1966.

Patent, 1972, Societe de la Vieille Montagne, Belgian Patent No. 724,214. Application lodged November 20, 1968, Equivalent U.S. Patent No. 3,652,264, granted March 28, 1972.

Patrizi, A., Persia, G. and Pescetelli, A., 1985. The new electrolytic zinc plant at Porto Vesme, Italy. Zinc '85: International Symposium on Extractive Metallurgy of Zinc, K. Tozawa, (Ed.), The Mining and Metallurgical Institute of Japan. Tokyo, 413 – 434.

Raghavarao, D., 1971. Constructions and Combinatorial Problems in Design of Experiments, Wiley, New York, 274p.

Rosmalen Van, G. M. and Kramer, H. J. M., 1998. Crystallization and Precipitation. Workshop held in Gauteng, South Africa in cooperation with the University of Cape Town, 10-12 June 1998.

Saffman, P.G. and Turner, J.S., *1956.* On the collision of drops in turbulent clouds. J. Fluid. Mech., 1, 16.

Sakamoto, K., Kanahara, M. and Matsushita, K., 1976. Agglomeration of crystalline particles of gibbsite during the precipitation in sodium aluminate solutions. Light Metals, 2, 149 – 162.

Söhnel, O. and Garside, J., 1992. Precipitation, Butterworths, London.

Seyssiecq, I., Veesler, S., Boistelle, R. and Lamerant, J.M., 1998. Agglomeration of gibbsite $Al(OH)_3$ crystals in Bayer liquors. Influence of the process parameters. Chem. Eng. Sci., 53 (12), 2177-2185.

Tainton, U.C. and Leyson, L.T., 1924. Electrolytic zinc from complex ores. Trans. AIME, (LXX), 486 – 522.

Tsunoda, S., Maeshiro, I., Ewi, M. and Sekine, K., 1973. The construction and operation of the Iijima Electrolytic Zinc Plant. AIME T.M.S. Paper No. A73 – 65, Chicago.

Uusipaavalniemi, E., and Karlman, S.G., 1996. Handling of iron at the zinc plant in Kokkola. Proceedings of the Second International Symposium on Iron Control in Hydrometallurgy, J.E. Dutrizac and G.B. Harris, (Eds.). The Canadian Institute of Mining, Metallurgy and Petroleum, Ottawa, Canada, 101 – 115.

Van Leeuwen, M.L.J., Bruinsma, O.S.L. and Van Rosmalen, G.M., 1996(a). Influence of mixing on the product quality in precipitation. Chem. Eng. Sc., 51 (11), 2595 - 2600.

Van Leeuwen, M.L.J., Bruinsma, O.S.L. and Van Rosmalen, G.M., 1996(b). Three-zone approach for precipitation of barium sulphate. J. of Crystal Growth, 166, 1004 - 1008.

Veesler, S., Roure, S. and Boistelle, R., 1994. General concept of hydrargillite $Al(OH)_3$ agglomeration. J. of Crystal Growth, *135, 505 – 512.*

Vicum, L., Mazzotti, M. and Baldyga, J., 2004. Modelling of stirred tank mixing-precipitation processes. Proceedings of the Swiss Symposium on Crystallization and Precipitation, Switzerland, March 2004.

Walton, A.G., 1967. The formation and properties of precipitates. Monographs on Analytical Chemistry and its Applications, Volume 23. Elving P.J. and Kolthoff, I.M. (Eds.), Interscience, New York, 232p.

Walton, A.G., 1969. Nucleation. Zettlemoyer A. C. (Ed.). New York, Marcel Dekker Inc., 225p.

Yakovlev, Y.B., Kul'ba, F.Y., Pus'ko, A.G. and Gerchikova, M.N., 1977. Hydrolysis of iron(III) sulphate in zinc sulphate solutions at 25, 50 and 80°C. Russ. J. Inorg. Chem., 22 (1), 27 – 29.

Yamada, K., 1980. Nucleation and aggregation during crystallization of aluminium tri-oxide in sodium aluminate solution. J. Japanese Inst. Light Metals, 32 (12), 720-726.